

Spectral Alignment of Networks

Soheil Feizi¹, Gerald Quon², Mariana Recamonde-Mendoza³, Muriel Médard¹,
Manolis Kellis¹ and Ali Jadbabaie⁴

December 5, 2021

Abstract

Network alignment refers to the problem of finding a bijective mapping across vertices of two graphs to maximize the number of overlapping edges and/or to minimize the number of mismatched interactions across networks. This problem arises in many fields such as computational biology, social sciences and computer vision and is often cast as an expensive quadratic assignment problem (QAP). Although spectral methods have received significant attention in different network science problems such as network clustering, the use of spectral techniques in the network alignment problem has been limited partially owing to the lack of principled connections between spectral methods and relaxations of the network alignment optimization. In this paper, we propose a network alignment framework that uses an orthogonal relaxation of the underlying QAP in a maximum weight bipartite matching optimization. Our method takes into account the ellipsoidal level sets of the quadratic objective function by exploiting eigenvalues and eigenvectors of (transformations of) adjacency graphs. Our framework not only can be employed to provide a theoretical justification for existing heuristic spectral network alignment methods, but it also leads to a new scalable network alignment algorithm which outperforms existing ones over various synthetic and real networks. Moreover, we generalize the objective function of the network alignment problem to consider both matched and mismatched interactions in a standard QAP formulation. This can be critical in applications where networks have low similarity and therefore we expect more mismatches than matches. We assess the effectiveness of our proposed method theoretically for certain classes of networks, through simulations over various synthetic network models, and in two real-data applications; in comparative analysis of gene regulatory networks across human, fly and worm, and in user de-anonymization over twitter follower subgraphs.

1 Introduction

The term *network alignment* encompasses several distinct but related problem variants [1]. In general, network alignment aims to find a bijective mapping across two (or more) networks so that if two nodes are connected in one network, their images are also connected in the other network(s). If such an errorless alignment scheme exists, network alignment can be simplified to the problem of graph isomorphism [2]. However, in general, an errorless alignment scheme may not be feasible

¹ Massachusetts Institute of Technology (MIT), Cambridge, US.

² University of California, Davis.

³ Instituto de Informática, Universidade Federal do Rio Grande do Sul, Porto Alegre, RS, Brazil.

⁴ MIT Institute for Data Systems and Society, and Department of Electrical and Systems Engineering, University of Pennsylvania.

An earlier version of this paper is available on MIT DSpace: <http://hdl.handle.net/1721.1/94606>

across two networks. In that case, network alignment aims to find a mapping with the minimum error and/or the maximum overlap.

Network alignment has a broad range of applications in systems biology, social sciences, computer vision, and linguistics. For instance, network alignment has been used frequently as a comparative analysis tool in studying protein-protein interaction networks across different species [3–8]. In computer vision, network alignment has been used in image recognition by matching similar images [9, 10]. It has also been applied in ontology alignment to find relationships among different representations of a database [11, 12], and in user de-anonymization to infer user/sample identifications using similarity between datasets [13].

A network alignment optimization seeks an assignment of nodes and edges across multiple networks to maximize (or alternatively minimize) a cost function with quadratic terms. This problem is closely related to the quadratic assignment problem (QAP) [14] which is computationally challenging to solve exactly. Reference [15] shows that approximating a solution of maximum quadratic assignment problem within a factor better than $2^{\log^{1-\epsilon} n}$ is not feasible in polynomial time in general. However, owing to numerous applications of quadratic assignment problems in different areas, several algorithms have been designed to solve it approximately: some methods use exact search approaches based on branch-and-bound [16] and cutting plane [17]. These methods can only be applied to very small problem instances owing to their high computational complexity. Some methods attempt to solve the underlying QAP by linearizing the quadratic term and transforming the optimization into a mixed integer linear program (MILP) [18–21]. In practice, the very large number of introduced variables and constraints in linearization of the QAP objective function poses an obstacle for solving the resulting MILP efficiently. Some methods use convex relaxations of the QAP to compute a bound on its optimal value [22–26]. The provided solution by these methods may not be a feasible solution for the original quadratic assignment problem. Other methods to solve the network alignment optimization include semidefinite [26, 27] or non-convex [28] relaxations, Bayesian inference [29], message passing [30] or other heuristics [3, 4, 6, 31–35]. We will review these methods in Section 2.2. For more details on these methods, we refer readers to references [14, 36].

Spectral inference methods have received significant attention in various network science problems such as network clustering and low dimensional embedding problems [37–41]. However, the use of spectral techniques in the network alignment problem has been limited [3, 4, 31, 32] partially owing to the lack of principled connections between existing spectral network alignment methods and relaxations of the underlying QAP. In fact, the performance of existing spectral network alignment methods have been assessed mostly through limited simulations and/or validations with real data where an analytical performance characterization is lacked even in simple cases.

In this paper, we propose a network alignment framework that uses an orthogonal relaxation of the underlying QAP in a maximum weight bipartite matching optimization. Our method simplifies, in a principled way, the network alignment optimization to simultaneous alignment of eigenvectors of (transformations of) adjacency graphs scaled by corresponding eigenvalues. We show that our framework not only can be employed to provide a theoretical justification for existing heuristic spectral network alignment methods, but it also leads to a new scalable network alignment algorithm which outperforms existing ones over various synthetic and real networks. We prove that our solution is asymptotically exact with high probability for Erdős-Rényi graphs [42], under some general conditions. Proofs are based on a characterization of eigenvectors of Erdős-Rényi graphs, along with some spectral perturbation analysis. For an analytical performance characterization of our proposed method, we consider asymptotically large Erdős-Rényi graphs owing to their tractable

spectral characterization. Note that finding an isomorphic mapping across asymptotically large Erdős-Rényi graphs is a well studied problem and can be solved efficiently through canonical labeling [43]¹. However, note that in the network alignment problem graphs can be non-isomorphic as well. Also note that in our optimality analysis we only consider finite and asymptotically large graphs. For arguments on infinite graphs, see Section 2.3.

Moreover, we generalize the objective function of the network alignment problem to consider both matched and mismatched interactions in a standard QAP formulation. In general, existing scalable network alignment methods only consider maximizing the number of overlapping edges (matches) across two networks and ignore the number of resulting mismatches (interactions that exist only in one of the networks). This limitation can be critical particularly in applications where networks have different sizes and low similarity. Through analytical performance characterization, simulations on synthetic networks, and real-data analysis, we show that the combination of both algorithmic and qualitative aspects of our network alignment framework leads to improved performance of our proposed algorithm compared to existing network alignment methods. On simple examples, we isolate multiple aspects of the proposed algorithm and show that each aspect is critical in the performance of the method. The proposed algorithmic and qualitative improvements can also be adapted to existing network alignment packages.

Some network alignment formulations aim to align paths [7] or subgraphs [8, 44] across two (or multiple) networks. The objective of these methods is different from our network alignment optimization where a bijective mapping across nodes of two networks is desired according to a quadratic assignment problem. Solutions of these different methods may be related. For instance, a bijective mapping across nodes of two networks can provide information about conserved pathways and/or subgraphs across networks, and vice versa.

Many networks have modular structures in which groups of nodes tend to interact with each other more strongly compared to the rest of the network [45, 46]. One can take advantage of such modular structure to split a large network alignment optimization into small subproblems and use semidefinite programming (SDP) over each subproblem, which yields a more accurate approximation to the underlying QAP at the expense of more computation [22–27]. Here, we consider a special class of modular networks and propose an extension of the spectral network alignment algorithm where spectral information is used to split a large QAP into smaller ones over which a SDP-based optimization [27] is performed. This hybrid method has high performance similar to SDP, while enjoying significantly less computational complexity.

We illustrate the effectiveness of our spectral network alignment algorithm against some existing network alignment methods over various synthetic network models including Erdős-Rényi, power law, regular, and stochastic block structures, under different noise models. Having illustrated the efficiency of our algorithm both theoretically and through simulations, we apply it to two real-data applications: We use network alignment to compare gene regulatory networks across human, fly and worm species which we infer by integrating genome-wide functional and physical genomics datasets from ENCODE and modENCODE consortia. We show that our network alignment method infers conserved regulatory interactions across these species despite long evolutionary distances separating these organisms. Moreover, we find strong conservation of centrally-connected genes and biological pathways, especially for human-fly comparisons. In a second application, we show that our spectral network alignment algorithm improves our ability to de-anonymize small subgraphs of the Twitter

¹Laszlo Babai has recently outlined his proof that the computational complexity of the general graph isomorphism problem is Quasipolynomial time.

follower network sampled in years 2008 and 2009, where we de-anonymize user IDs in 2009 using user IDs in 2008. This application illustrates the extent of personal information that can be retrieved from network structures, and raises additional considerations that need to be addressed in different privacy-related applications.

The rest of the paper is organized as follows. In Section 2, we present the network alignment problem and review existent network alignment techniques. In Section 3, we introduce our proposed algorithm and discuss its relationship with the underlying quadratic assignment problem. Moreover, we present the optimality of our method over random graphs, under some general conditions. In Section 4, we consider the trace formulation of the network alignment optimization and introduce a network alignment algorithm which uses higher-order eigenvectors of adjacency graphs to align network structures. In Section 5, we consider the network alignment problem of modular networks and introduce an algorithm which solves it efficiently. In Section 6, we compare performance of our method with existent network alignment methods over different synthetic network structures. In Section 7, we introduce our network inference framework to construct integrative gene regulatory networks in different species used in the network alignment application. In Section 8, we illustrate applications of our method in comparative analysis of regulatory networks across species. In Section 9, we explain an application of network alignment in user de-anonymization over twitter follower subgraphs. In Section 10, we present proofs for the main results of the paper.

2 Network Alignment Problem Setup

2.1 Problem Formulation and Notation

In this section, we introduce the network alignment problem formulation. Let $G_1 = (V_1, E_1)$ and $G_2 = (V_2, E_2)$ be two graphs (networks) where V_a and E_a represent set of nodes and edges of graph $a = 1, 2$, respectively. By abuse of notation, let G_1 and G_2 be their matrix representations as well where $G_a(i, j) = 1$ iff $(i, j) \in E_a$, for $a = 1, 2$. Suppose network a has n_a nodes, i.e., $|V_a| = n_a$. We assume that networks are un-weighted (binary), and possibly directed. The proposed framework can be extended to the case of weighted graphs as well.

Let X be an $n_1 \times n_2$ binary matrix where $x(i, j') = 1$ means that node i in network 1 is mapped to node j' in network 2. The pair (i, j') is called a mapping edge across two networks. In the network alignment setup, each node in one network can be mapped to at most one node in the other network, i.e., $\sum_i x(i, j') \leq 1$ for all j' , and similarly, $\sum_{j'} x(i, j') \leq 1$ for all i .

Let \mathbf{y} be a vectorized version of X . That is, \mathbf{y} is a vector of length $n_1 n_2$ where, $y(i + (j' - 1)n_1) = x(i, j')$. To simplify notation, define $y_{i,j'} \triangleq x(i, j')$. Two mappings (i, j') and (r, s') can be matches which cause overlaps, can be mismatches which cause errors, or can be neutrals (Figure 1-a).

Definition 1 Suppose $G_1 = (V_1, E_1)$ and $G_2 = (V_2, E_2)$ are undirected graphs. Let $\{i, r\} \subseteq V_1$ and $\{j', s'\} \subseteq V_2$ where $x(i, j') = 1$ and $x(r, s') = 1$. Then,

- (i, j') and (r, s') are matches if $(i, r) \in E_1$ and $(j', s') \in E_2$.
- (i, j') and (r, s') are mismatches if only one of the edges (i, r) and (j', s') exists.
- (i, j') and (r, s') are neutrals if none of the edges (i, r) and (j', s') exists.

Definition 1 can be extended to the case where G_1 and G_2 are directed graphs. In this case, mappings (i, j') and (r, s') are matches/mismatches if they are matches/mismatches in one of the

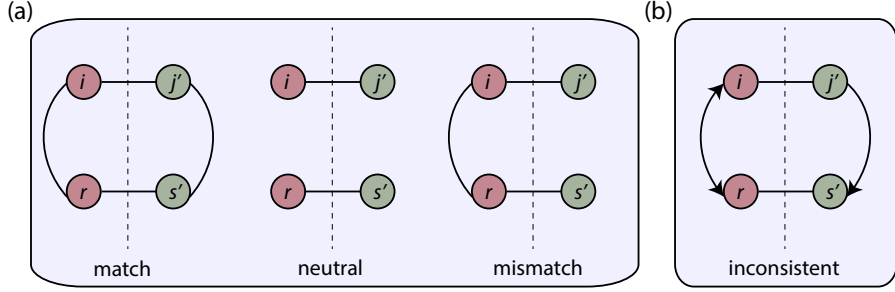


Figure 1: (a) An illustration of matched, mismatched, and neutral mappings, for undirected graphs. (b) An illustration of inconsistent mappings, for directed graphs, where they are matches in one direction, and mismatches in the other direction.

possible directions. However, it is possible to have these mappings be matches in one direction, while they are mismatches in the other direction (Figure 1-b). These mappings are denoted as *inconsistent mappings*, defined as follows:

Definition 2 Let $G_1 = (V_1, E_1)$ and $G_2 = (V_2, E_2)$ be two directed graphs and $\{i, r\} \subseteq V_1$ and $\{j', s'\} \subseteq V_2$ where $x(i, j') = 1$ and $x(r, s') = 1$. If edges $i \rightarrow r$, $r \rightarrow i$, and $j' \rightarrow s'$ exist, however, $s' \rightarrow j'$ does not exist, then mappings (i, j') and (r, s') are inconsistent.

Existing network alignment formulations aim to find a mapping matrix X which maximizes the number of matches between networks. However, these formulations can lead to mappings which cause numerous mismatches, especially if networks have different sizes and low similarity. In this paper, we propose a more general formulation for the network alignment problem which considers both matches and mismatches simultaneously.

For a given alignment matrix X across networks G_1 and G_2 , we assign an *alignment score* by considering the number of matches, mismatches and neutrals caused by X :

$$\text{Alignment Score (X)} = s_1(\# \text{ of matches}) + s_2(\# \text{ of neutrals}) + s_3(\# \text{ of mismatches}), \quad (2.1)$$

where s_1 , s_2 , and s_3 are scores assigned to matches, neutrals, and mismatches, respectively. Note that existing alignment methods ignore effects of mismatches and neutrals by assuming $s_2 = s_3 = 0$ which is restrictive particularly in aligning graphs with different number of nodes and low similarity. In the following, we re-write (2.1) as a quadratic assignment formulation.

Consider two undirected graphs $G_1 = (V_1, E_1)$ and $G_2 = (V_2, E_2)$. We form an *alignment network* represented by adjacency matrix A in which nodes are mapping edges across the original networks, and the edges capture whether the pair of mapping edges induce matches, mismatches or neutrals (Figure 2).

Definition 3 Let $\{i, r\} \subseteq V_1$ and $\{j', s'\} \subseteq V_2$, where $x(i, j') = 1$ and $x(r, s') = 1$.

$$A[(i, j'), (r, s')] = \begin{cases} s_1, & \text{if } (i, j') \text{ and } (r, s') \text{ are matches,} \\ s_2, & \text{if } (i, j') \text{ and } (r, s') \text{ are neutrals,} \\ s_3, & \text{if } (i, j') \text{ and } (r, s') \text{ are mismatches,} \end{cases} \quad (2.2)$$

where s_1 , s_2 , and s_3 are scores assigned to matches, neutrals, and mismatches, respectively.

We can re-write (2.2) as follows:

$$A[(i, j'), (r, s')] = (s_1 + s_2 - 2s_3)G_1(i, r)G_2(j', s') + (s_3 - s_2)(G_1(i, r) + G_2(j', s')) + s_2. \quad (2.3)$$

We can summarize (2.2) and (2.3) as follows:

$$A = (s_1 + s_2 - 2s_3)(G_1 \otimes G_2) + (s_3 - s_2)(G_1 \otimes \mathbb{1}_{n_2}) + (s_3 - s_2)(\mathbb{1}_{n_1} \otimes G_2) + s_2(\mathbb{1}_{n_1} \otimes \mathbb{1}_{n_2}), \quad (2.4)$$

where \otimes represents matrix Kronecker product, and $\mathbb{1}_n$ is an $n \times n$ matrix whose elements are all ones.

A similar scoring scheme can be used for directed graphs. When graphs are directed, some mappings can be inconsistent according to Definition 2, i.e., they are matches in one direction and mismatches in another. Scores of inconsistent mappings can be assigned randomly to matched/mismatched scores, or to an average score of matches and mismatches (i.e., $(s_1 + s_3)/2$). For random graphs, inconsistent mappings are rare events. For example, suppose network edges are distributed according to a Bernoulli distribution with parameter p . Then, the probability of having an inconsistent mapping for a particular pair of paired nodes across networks is equal to $4p^3(1-p)$. Therefore, their effect in network alignment is negligible particularly for large sparse networks. Throughout the paper, for directed graphs, we assume inconsistent mappings have negligible effect unless it is mentioned explicitly.

Alignment scores s_1 , s_2 and s_3 of (2.2) can be arbitrary in general. However, in this paper we consider the case where $s_1 > s_2 > s_3 > 0$ with the following rationale: Suppose a mapping matrix X has a total of κ non-zero edges. For example, if networks have $n_1 = n_2 = n$ nodes and there is no unmapped nodes across two networks, $\kappa = n$. The total number of matches, mismatches and neutrals caused by this mapping is equal to $\binom{\kappa}{2}$. Thus, for mapping matrices with the same number of mapping edges, without loss of generality, one can assume that, alignment scores are strictly positive $s_1, s_2, s_3 > 0$ (otherwise, a constant can be added to the right-hand side of (2.2)). In general, mappings with high alignment scores might have slightly different number of mapping edges owing to unmapped nodes across the networks which has a negligible effect in practice. Moreover, in the alignment scheme, we wish to encourage matches and penalize mismatches. Thus, throughout this paper, we assume $s_1 > s_2 > s_3 > 0$.

In practice, some mappings across two networks may not be possible owing to additional side information. The set of possible mappings across two networks is denoted by $\mathcal{R} = \{(i, j') : i \in V_1, j' \in V_2\}$. If $\mathcal{R} = V_1 \times V_2$, the problem of network alignment is called *unrestricted*. However, if some mappings across two networks are prevented (i.e., $y_{i,j'} = 0$, for $(i, j') \notin \mathcal{R}$), then the problem of network alignment is called *restricted*.

In the following, we present the network alignment optimization which we consider in this paper:

Definition 4 (Network Alignment Problem Setup) *Let $G_1 = (V_1, E_1)$ and $G_2 = (V_2, E_2)$ be*

two binary networks. Network alignment aims to solve the following optimization:

$$\begin{aligned}
\max_{\mathbf{y}} \quad & \mathbf{y}^T A \mathbf{y}, \\
\sum_i y_{i,j'} \leq 1, \quad & \forall i \in V_1, \\
\sum_{j'} y_{i,j'} \leq 1, \quad & \forall j' \in V_2, \\
y_{i,j'} \in \{0, 1\}, \quad & \forall (i, j') \in V_1 \times V_2, \\
y_{i,j'} = 0, \quad & \forall (i, j') \notin \mathcal{R},
\end{aligned} \tag{2.5}$$

where A is defined according to (2.3), and $\mathcal{R} \subseteq V_1 \times V_2$ is the set of possible mappings across two networks.

In the following, we re-write (2.5) using the trace formulation of a standard QAP. Here, we consider undirected networks $G_1 = (V_1, E_1)$ and $G_2 = (V_2, E_2)$ with n_1 and n_2 nodes, respectively. Without loss of generality, we assume $n_1 \leq n_2$. Moreover, we assume that all nodes of the network G_1 are mapped to nodes of the network G_2 (i.e., there are no un-aligned nodes in G_1).

Define $\xi_1 \triangleq s_1 + s_2 - 2s_3$, $\xi_2 \triangleq s_3 - s_2$ and $\xi_3 \triangleq s_2$. We can rewrite the objective function of Optimization (2.5) using (2.4) as follows:

$$\begin{aligned}
\mathbf{y}^T A \mathbf{y} &= \xi_1 \mathbf{y}^T (G_1 \otimes G_2) \mathbf{y} + \xi_2 \mathbf{y}^T (G_1 \otimes \mathbf{1}_{n_2}) \mathbf{y} + \xi_2 \mathbf{y}^T (\mathbf{1}_{n_1} \otimes G_2) \mathbf{y} + \xi_3 \mathbf{y}^T (\mathbf{1}_{n_1} \otimes \mathbf{1}_{n_2}) \mathbf{y} \\
&= \xi_1 \text{Tr}(G_1 X G_2 X^T) + \xi_2 \text{Tr}(G_1 X \mathbf{1}_{n_2} X^T) + \xi_2 \text{Tr}(\mathbf{1}_{n_1} X G_2 X^T) + \xi_3 \text{Tr}(\mathbf{1}_{n_1} X \mathbf{1}_{n_2} X^T) \\
&= \text{Tr}\left((G_1 + \frac{\xi_2}{\xi_1})X(\xi_1 G_2 + \xi_2)X^T\right) + (\xi_3 - \frac{\xi_2^2}{\xi_1})\text{Tr}(\mathbf{1}_{n_1} X \mathbf{1}_{n_2} X^T) \\
&= \text{Tr}(G'_1 X G'_2 X^T) + (\xi_3 - \frac{\xi_2^2}{\xi_1})(\min(n_1, n_2))^2 \\
&= \text{Tr}(G'_1 X G'_2 X^T) + \text{constant},
\end{aligned}$$

where

$$\begin{aligned}
G'_1 &\triangleq G_1 + \frac{\xi_2}{\xi_1} = G_1 + \frac{s_3 - s_2}{s_1 + s_2 - 2s_3}, \\
G'_2 &\triangleq \xi_1 G_2 + \xi_2 = (s_1 + s_2 - 2s_3)G_2 + (s_3 - s_2).
\end{aligned}$$

Thus, the network alignment optimization (2.5) can be reformulated as follows:

$$\begin{aligned}
\max_X \quad & \text{Tr}(G'_1 X G'_2 X^T), \\
\sum_i x_{i,j'} \leq 1, \quad & \forall i \in V_1, \\
\sum_{j'} x_{i,j'} \leq 1, \quad & \forall j' \in V_2, \\
x_{i,j'} \in \{0, 1\}, \quad & \forall (i, j') \in V_1 \times V_2, \\
x_{i,j'} = 0, \quad & \forall (i, j') \notin \mathcal{R}.
\end{aligned} \tag{2.6}$$

2.2 Prior Work

Network alignment problem (2.5) is an example of a quadratic assignment problem (QAP) [14]. Reference [15] shows that approximating a solution of maximum quadratic assignment problem within a factor better than $2^{\log^{1-\epsilon} n}$ is not feasible in polynomial time in general. However, owing to various applications of QAP in different areas, many methods exist for approximate solutions. In the following, we briefly summarize previous works by categorizing them into four groups and explain advantages and shortcomings of each. For more details on these methods, we refer readers to references [14, 36].

- **Exact search methods:** These methods provide a global optimal solution for the quadratic assignment problem. However, owing to their high computational complexity, they can only be applied to very small problem instances. Examples of exact algorithms include methods based on branch-and-bound [16] and cutting plane [17].
- **Linearizations:** These methods attempt to solve QAP by eliminating the quadratic term in the objective function of Optimization (2.5), transforming it into a mixed integer linear program (MILP). An existing MILP solver is applied to find a solution for the relaxed problem. Examples of these methods are Lawlers linearization [18], Kaufmann and Broeckx linearization [19], Frieze and Yadegar linearization [20], and Adams and Johnson linearization [21]. These linearizations can provide bounds on the optimal value of the underlying QAP [15]. In general, linearization of the QAP objective function is achieved by introducing many new variables and new linear constraints. In practice, the very large number of introduced variables and constraints poses an obstacle for solving the resulting MILP efficiently.
- **Semidefinite/convex relaxations and bounds:** These methods aim to compute a bound on the optimal value of the network alignment optimization, by considering the alignment matrix in the intersection of the sets of orthogonal and stochastic matrices. The provided solution by these methods may not be a feasible solution of the original quadratic assignment problem. Examples of these methods include orthogonal relaxations [22], projected eigenvalue bounds [23], convex relaxations [24–26], and matrix splittings [27]. In the computer vision literature, [31, 32] use spectral techniques to approximately solve QAP by inferring a cluster of assignments over the feature network. Then, they use a greedy approach to reject assignments with low associations.

In particular, [27] introduces a convex relaxation of the underlying network alignment optimization based on matrix splitting which provides bounds on the optimal value of the underlying QAP. The proposed SDP method provides a bound on the optimal value and additional steps are required to derive a feasible solution. Moreover, owing to its computational complexity, it can only be used to align small networks, limiting its applicability to alignment of large real networks ². In Section 5, we address these issues and introduce a hybrid method based on our proposed scheme in Section 3, and the semidefinite relaxation of [27] to align large modular network structures with low computational complexity.

- **Other methods:** There are several other techniques to approximately solve network alignment optimization. Some methods use a Lagrangian relaxation [47], Bayesian framework [29],

²In our simulations, networks should have approximately less than 70 nodes to be able to run it on an ordinary laptop.

or message passing [30], or some other heuristics [3, 4, 6]. In Section 6, we assess the performance of some of these network alignment techniques through simulations.

2.3 Network Alignment and Graph Isomorphism

Network alignment optimization (2.5) is closely related to the problem of *graph isomorphism*, defined as follows:

Definition 5 (Graph Isomorphism) *Let $G_1 = (V_1, E_1)$ and $G_2 = (V_2, E_2)$ be two binary networks. G_1 and G_2 are isomorphic if there exists a permutation matrix P such that $G_1 = PG_2P^T$.*

The computational problem of determining whether two finite graphs are isomorphic is called the *graph isomorphism problem*. Moreover, given two isomorphic networks G_1 and G_2 , the problem of graph isomorphism aims to find the permutation matrix P such that $G_1 = PG_2P^T$. The computational complexity of this problem is unknown [48].

Network alignment and graph isomorphism problems are related to each other. Loosely speaking, network alignment aims to minimize the distance between premuted versions of two networks (or, alternatively to maximize their overlap). Therefore, if the underlying networks are isomorphic, an optimal solution of the network alignment optimization should be the same (or close) to the underlying permutation matrix P , where $G_1 = PG_2P^T$. In the following lemma, we formalize such a connection between the network alignment optimization and the classical graph isomorphism problem:

Lemma 1 *Let G_1 and G_2 be two isomorphic Erdős-Rényi graphs [42] such that $\Pr[G_1(i, j) = 1] = p$ and $G_2 = PG_1P^T$, where P is a permutation matrix. Let $p \neq 0, 1$. Then, for any selection of scores $s_1 > s_2 > s_3 > 0$, P maximizes the expected network alignment objective function of Optimization (2.5).*

Proof The proof is presented in Section 10.1. ■

The result of Lemma 1 can be extended to the case where edges of graphs are flipped through a random noise matrix:

Lemma 2 *Let G_1 be an Erdős-Rényi graphs such that $\Pr[G_1(i, j) = 1] = p$. Let \tilde{G}_1 be a graph resulting from flipping edges of G_1 independently and randomly with probability q . Suppose $G_2 = P\tilde{G}_1P^T$ where P is a permutation matrix. Let $0 < p < 1/2$ and $0 \leq q < 1/2$. Then, for any selection of scores $s_1 > s_2 > s_3 > 0$, P maximizes the expected network alignment objective function of Optimization (2.5).*

Proof The proof is presented in Section 10.1. ■

Finding an isomorphic mapping across sufficiently large Erdős-Rényi graphs can be done efficiently with high probability (w.h.p.) through canonical labeling [43]. Canonical labeling of a network consists of assigning a unique label to each vertex such that labels are invariant under isomorphism. The graph isomorphism problem can then be solved efficiently by mappings nodes with the same canonical labels to each other [49]. One example of canonical labeling is the degree neighborhood of a vertex defined as a sorted list of neighborhood degrees of vertices [43]. Note that, network alignment formulation is more general than the one of graph isomorphism; network alignment aims to find an optimal mappings across two networks which are not necessarily isomorphic.

Remark 1 In [50], Babai, Erdős, and Selkow derive an interesting and perhaps a counter-intuitive result on random graph isomorphism. Based on their result, *any two infinite random graphs are isomorphic with probability one*. For instance, consider two infinite Erdős-Rényi graphs G_1 and G_2 where $\Pr[G_1(i, j) = 1] = p_1$ and $\Pr[G_2(i, j) = 1] = p_2$ and $p_1, p_2 \neq 0, 1$. The result of [50] indicates that, G_1 and G_2 are isomorphic even if $p_1 \neq p_2$. This may seem counter-intuitive as two networks may seem to have different densities. However, this result is only true for *infinite graphs*, not asymptotically large ones. The difference may seem subtle but significant. In infinite graphs, notions of graph size, graph density, etc. are different than the ones for finite graphs. Throughout this paper, we only consider finite or asymptotically large graphs, not infinite ones. In the following, we give some intuition on the results of [50] about infinite graphs.

The proof of the result in [50] is based on a notion for infinite graphs called *the extension property* which roughly states that, an infinite graph G has the extension property if for any two disjoint finite subsets of nodes V_1 and V_2 , there exists a vertex $v \in V - V_1 - V_2$ such that v is connected to all vertices in V_1 and to no vertices in V_2 . If two infinite graphs have extension properties, they are isomorphic with probability one. One way to prove this is to construct an infinite sequences of mappings by considering disjoint subsets of nodes V_1 and V_2 , and adding a node v according to the extension property.

Finally, it is straightforward to show that an infinite Erdős-Rényi graph with parameter $p \neq 0, 1$ has the extension property with probability one. This is analogous to the monkey-text book problem: if a monkey randomly types infinite letters, with probability one, he will type any given text book. This is because the number of letters in a text book is finite and therefore, the probability that the letter sequence of a given text book does not appear in a random infinite letter sequence is zero. Now consider two finite disjoint subsets V_1 and V_2 over an infinite graph. Note that being finite is key here. Similarly, the probability that a vertex v exists such that it is connected to all vertices in V_1 and to no vertices in V_2 is one because its complement set has zero probability (or it has zero Lebesgue measure if we map binary sequences to numbers in $[0, 1]$).

3 EigenAlign Algorithm

We now introduce *EigenAlign*, an algorithm which solves a relaxation of the network alignment optimization (2.5) leveraging spectral properties of networks. Unlike other alignment methods, EigenAlign considers both matches and mismatches in the alignment scheme. Moreover, we prove its optimality (in an asymptotic sense) in aligning Erdős-Rényi graphs under some technical conditions. In the following, we describe the EigenAlign algorithm:

Algorithm 1 (EigenAlign Algorithm) *Let $G_1 = (V_1, E_1)$ and $G_2 = (V_2, E_2)$ be two binary networks whose corresponding alignment network is denoted by A according to (2.3). EigenAlign algorithm solves the network alignment optimization (2.5) in two steps:*

- **Eigenvector Computation Step:** *In this step, we compute \mathbf{v} , an eigenvector of the alignment network A with the maximum eigenvalue.*
- **Linear Assignment Step:** *In this step, we solve the following maximum weight bipartite*

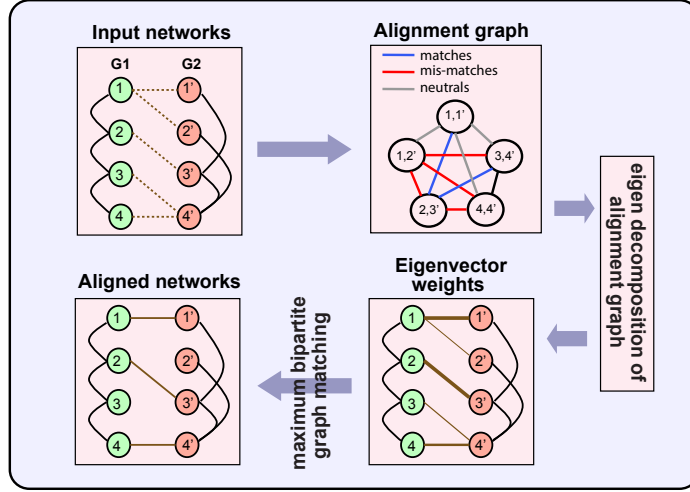


Figure 2: Framework of EigenAlign algorithm 1.

matching optimization:

$$\begin{aligned}
 \max_{\mathbf{y}} \quad & \mathbf{v}^T \mathbf{y}, \\
 \sum_{j'} y_{i,j'} \leq 1, \quad & \forall i \in V_1, \\
 \sum_i y_{i,j'} \leq 1, \quad & \forall j' \in V_2, \\
 y_{i,j'} \in \{0, 1\}, \quad & \forall (i, j') \in V_1 \times V_2, \\
 y_{i,j'} = 0, \quad & \forall (i, j') \notin \mathcal{R}.
 \end{aligned} \tag{3.1}$$

This framework is depicted in Figure 2. In the rest of this section, we provide intuition on different steps of the EigenAlign algorithm through both quadratic assignment relaxation argument as well as a fixed point analysis. In Section 3.3, we discuss optimality of EigenAlign over random graphs. In Section 4, we will introduce an extension of the EigenAlign algorithm which uses higher-order eigenvectors of adjacency graphs to align network structures.

3.1 EigenAlign as a Relaxation of Quadratic Assignment

In this section, we explain EigenAlign as a relaxation of the underlying quadratic assignment optimization (2.5). For simplicity, we assume all mappings across networks are possible (i.e., $\mathcal{R} = \{(i, j') : \forall i \in V_1, \forall j' \in V_2\}$). In the restricted network alignment setup, without loss of generality, one can eliminate rows and columns of the alignment matrix corresponding to mappings that are not allowed.

In the eigen decomposition step of EigenAlign, we ignore bijective constraints (i.e., constraints $\sum_i y_{i,j'} \leq 1$ and $\sum_{j'} y_{i,j'} \leq 1$) because they will be satisfied in the second step of the algorithm through a linear optimization. By these assumptions, Optimization (2.5) can be simplified to the

following optimization:

$$\begin{aligned} \max_{\mathbf{y}} \quad & \mathbf{y}^T A \mathbf{y}, \\ & y_{i,j'} \in \{0, 1\}, \quad \forall (i, j') \in V_1 \times V_2. \end{aligned} \quad (3.2)$$

To approximate a solution of this optimization, we relax integer constraints to constraints over a hyper-sphere restricted by hyper-planes (i.e., $\|\mathbf{y}\|_2 \leq 1$ and $\mathbf{y} \geq 0$). Using this relaxation, Optimization (3.2) is simplified to the following optimization:

$$\begin{aligned} \max_{\mathbf{y}} \quad & \mathbf{y}^T A \mathbf{y}, \\ & \|\mathbf{y}\|_2 \leq 1, \\ & \mathbf{y} \geq 0. \end{aligned} \quad (3.3)$$

In the following, we show that \mathbf{v} , the leading eigenvector of the alignment matrix A is an optimal solution of Optimization (3.3). Suppose \mathbf{y}_1 is an optimal solution of Optimization (3.3). Let \mathbf{y}_2 be a solution of the following optimization which ignores non-negativity constraints:

$$\begin{aligned} \max_{\mathbf{y}} \quad & \mathbf{y}^T A \mathbf{y}, \\ & \|\mathbf{y}\|_2 \leq 1. \end{aligned} \quad (3.4)$$

Following the Rayleigh – Ritz formula, the leading eigenvector of the alignment matrix is an optimal solution of Optimization (3.4) (i.e., $\mathbf{y}_2 = \mathbf{v}$). Now we use the following theorem to show that in fact $\mathbf{y}_1 = \mathbf{v}_1$:

Theorem 1 (Perron–Frobenius Theorem [2]) *Suppose A is a matrix whose elements are strictly positive. Let \mathbf{v} be an eigenvector of A corresponding to the largest eigenvalue. Then, $\forall i, v_i > 0$. Moreover, all other eigenvectors must have at least one negative, or non-real component.*

Since \mathbf{y}_2 is a solution of a relaxed version of Optimization (3.4), we have $\mathbf{y}_2^T A \mathbf{y}_2 \geq \mathbf{y}_1^T A \mathbf{y}_1$. Using this inequality along with Perron-Frobenius Theorem lead to $\mathbf{y}_1 = \mathbf{v}$, as the unique solution of optimization (3.3).

The solution of the eigen decomposition step assigns weights to all possible mappings across networks ignoring bijective constraints. However, in the network alignment setup, each node in one network can be mapped to at most one node in the other network. To satisfy these constraints, we use eigenvector weights in a linear optimization framework of maximum weight bipartite matching setup of Optimization (3.1) [51].

Remark 2 Many existing network alignment techniques are based on iterative algorithms [3,4,30]. The EigenAlign relaxation of the underlying quadratic assignment problem can be viewed as the following fixed point solution using a linear mapping function which can be solved iteratively:

$$y(t_1) = \frac{1}{\lambda} \sum_{t_2} A(t_1, t_2) y(t_2), \quad (3.5)$$

where λ is a constant and t_i represents a node in the alignment network A . Note that, this mapping function is not necessarily a contraction. Instead of using an iterative approach, EigenAlign solves

this relaxation in a closed form using the leading eigenvector of the alignment network. In particular, (3.5) can be re-written as,

$$A\mathbf{y} = \lambda\mathbf{y}, \quad (3.6)$$

where \mathbf{y} is the vector of mapping weights whose elements represent a measure of centrality of nodes in the alignment network. If A is diagonalizable, eigenvectors of matrix A provide solutions for this equation, where λ is the eigenvalue corresponding to eigenvector \mathbf{y} . However, eigenvectors of matrix A can have negative components which are not allowed in the mapping function since $y_{i,j'} \geq 0$. Since components of matrix A are all positive, similarly to discussions of (3.3), according to Perron-Frobenius Theorem 1, all components of the eigenvector associated with the maximum positive eigenvalue are positive. This result holds for non-negative matrices as well if they are strongly connected. Therefore, the leading eigenvector of matrix A satisfies desired conditions for the mapping function and provides alignment scores for the nodes in the alignment network.

Remark 3 Suppose G_1 and G_2 are two undirected graphs with n_1 and n_2 nodes, respectively. IsoRank [3] is a network alignment method which aligns networks using neighborhood similarities of nodes. Let I be the identity matrix of size $n_1 \times n_1$. Suppose D_1 and D_2 are diagonal matrices of sizes $n_1 \times n_1$ and $n_2 \times n_2$ whose diagonal elements are node degrees of networks G_1 and G_2 , respectively. The first step of the IsoRank algorithm solves the following fixed point equation:

$$\mathbf{y} = (I \otimes D_1^{-1})A(I \otimes D_2^{-1})\mathbf{y}, \quad (3.7)$$

where \otimes represents matrix Kronecker product, and $s_2 = s_3 = 0$ in (2.3). IsoRank solves (3.7) using a power iteration method. The IsoRank algorithm has several differences with EigenAlign in both algorithmic and qualitative aspects. From a qualitative aspect, IsoRank ignores effects of mismatches across networks by assuming $s_2 = s_3 = 0$. IsoRank uses a stationary centrality measure in the alignment network, having a degree scaling step which is based on the assumption of uniformly random distribution of alignment scores over potential mappings. Moreover, it uses a greedy method to select bijective mappings across networks, instead of the linear optimization framework used in the EigenAlign algorithm. In Sections 6 and 8, over both synthetic and real networks, we show that, the EigenAlign solution has significantly better performance compared to the one of IsoRank. Moreover, in Section 6, we isolate multiple aspects of the EigenAlign algorithm on some toy examples, and evaluate their individual contributions in its performance. We note that, existent network alignment methods such as IsoRank may be improved by borrowing algorithmic and/or qualitative ideas of the proposed EigenAlign method. However, these extensions are beyond the scope of this paper.

3.2 Computational Complexity of EigenAlign

In this part, we analyze computational complexity of the EigenAlign Algorithm 1. Suppose the number of nodes of networks G_1 and G_2 are $\mathcal{O}(n)$. Let $k = \mathcal{O}(|\mathcal{R}|)$ be the number of possible mappings across two networks. In an unrestricted network alignment setup, we have $k = \mathcal{O}(n^2)$. However, in a restricted network alignment, k may be significantly smaller than n^2 . EigenAlign has three steps:

- (i) The alignment network A should be formed which has a computational complexity of $\mathcal{O}(k^2)$ because all pairs of possible mappings should be considered.

- (ii) In the eigen decomposition step, we need to compute the leading eigenvector of the alignment network. This operation can be performed in almost linear time in k using QR algorithms and/or power methods [52]. Therefore, the worst case computational complexity of this part is $\mathcal{O}(k)$.
- (iii) Finally, we use eigenvector weights in a maximum weight bipartite matching algorithm which can be solved efficiently using linear programming or Hungarian algorithm [51]. The worst case computational complexity of this step is $\mathcal{O}(n^3)$. If the set \mathcal{R} has a specific structure (e.g., small subsets of nodes in one network are allowed to be mapped to small subsets of nodes in the other network), this cost can be reduced significantly. In Section 8, we see this structure in aligning regulatory networks across species as genes are allowed to be aligned to homologous genes within their gene families.

Proposition 1 *The worst case computational complexity of the EigenAlign Algorithm is $\mathcal{O}(k^2 + n^3)$.*

Remark 4 For large networks, to reduce the overall computational complexity, the linear assignment optimization may be replaced by a greedy bipartite matching algorithm. In the greedy matching approach, at each step, the heaviest possible mapping is added to the current matching until no further mappings can be added. It is straightforward to show that this greedy algorithm finds a bipartite matching whose weight is at least half the optimum. The computational complexity of this greedy algorithm is $\mathcal{O}(k \log(k) + nk)$.

3.3 Performance Characterization of EigenAlign Over Erdős-Rényi Graphs

In this section, we analyze optimality of the EigenAlign algorithm over Erdős-Rényi graphs, for both isomorphic and non-isomorphic cases, and under two different noise models. While real networks often have different structures than Erdős-Rényi graphs, the analytical tractability and the spectral characterization of these graphs makes it possible to actually prove that the proposed relaxations are asymptotically tight, at least in special cases, providing a rigorous foundation for the proposed EigenAlign algorithm. In this section, we only consider finite and asymptotically large graphs. For arguments on infinite graphs, see Section 2.3.

Suppose $G_1 = (V_1, E_1)$ is an undirected Erdős-Rényi graph with n nodes where $\Pr[G_1(i, j) = 1] = p$. Self-loops are allowed as well. Suppose \tilde{G} is a noisy version of the graph G_1 . We consider two different noise models in this section:

- Noise Model I: In this model, we have,

$$\tilde{G}_1 = G_1 \odot (1 - Q) + (1 - G_1) \odot Q, \quad (3.8)$$

where \odot represents the Hadamard product, and Q is a binary random matrix whose edges are drawn i.i.d. from a Bernoulli distribution with $\Pr[Q(i, j) = 1] = p_e$. In words, the operation $G_1 \odot (1 - Q) + (1 - G_1) \odot Q$ flips edges of G_1 independently randomly with probability p_e .

- Noise Model II: In this model, we have,

$$\tilde{G}_1 = G_1 \odot (1 - Q) + (1 - G_1) \odot Q', \quad (3.9)$$

where Q and Q' are binary random matrices whose edges are drawn i.i.d. from a Bernoulli distribution with $\Pr[Q(i, j) = 1] = p_e$ and $\Pr[Q'(i, j) = 1] = p_{e_2}$. Under this model, edges of G_1 flip independently randomly with probability p_e , while non-connecting tuples in G_1 will be connected in \tilde{G}_1 with probability p_{e_2} . Because G_1 is an Erdős-Rényi graph with parameter p , choosing

$$p_{e_2} = \frac{pp_e}{1-p}, \quad (3.10)$$

leads to the expected density of networks G_1 and G_2 be p .

We define G_2 as follows:

$$G_2 = P\tilde{G}_1P^T, \quad (3.11)$$

where P is a permutation matrix. Throughout this section, we assume that we are in the restricted network alignment regime: we desire to choose n mappings $i \leftrightarrow j'$ across two networks among $|\mathcal{R}| = kn$ possible mappings where $i \in V_1$, $j' \in V_2$, and $k > 1$. n true mappings ($i \leftrightarrow i'$ if $P = I$) are included in \mathcal{R} , while the remaining $(k-1)n$ mappings are selected independently randomly. Moreover, we choose scores assigned to matches, neutrals and mismatches as $s_1 = \alpha + \epsilon$, $s_2 = 1 + \epsilon$ and $s_3 = \epsilon$, respectively, where $\alpha > 1$ and $0 < \epsilon \ll 1$. These selections satisfy score conditions $s_1 > s_2 > s_3 > 0$.

Theorem 2 (EigenAlign over Erdős-Rényi graphs) *Let \tilde{P} be the solution of the EigenAlign Algorithm 1. Then, under both noise models (3.8) and (3.9), if $0 < p < 1/2$, and $0 \leq p_e < 1/2$, then as $n \rightarrow \infty$, the error probability goes to zero:*

$$\Pr\left[\frac{1}{n}\|\tilde{P} - P\|\right] \rightarrow 0.$$

Theorem 2 states that, the EigenAlign algorithm is able to recover the underlying permutation matrix which relates networks G_1 and G_2 to each other according to (3.11). On the other hand, according to Lemma 2, this permutation matrix is in fact optimizes the expected network alignment score.

Proposition 2 *Under conditions of Theorem 2, the permutation matrix inferred by EigenAlign maximizes the expected network alignment objective function defined according to Optimization (2.5).*

In noise models (3.8) and (3.9), if we put $p_e = 0$, then G_2 is isomorphic with G_1 because there exists a permutation matrix P such that $G_2 = PG_1P^T$. For this case, we have the following Corollary:

Corollary 1 (EigenAlign on Isomorphic Erdős-Rényi graphs) *Let G_1 and G_2 be two isomorphic Erdős-Rényi graphs with n nodes such that $G_1 = PG_2P^T$, where P is a permutation matrix. Under conditions of Theorem 2, as $n \rightarrow \infty$, the error probability of EigenAlign solution goes to zero.*

We present proofs of Theorem 2 and Corollary 1 in Sections 10.2 and 10.3. In the following, we sketch main ideas of their proofs: Since input networks G_1 and G_2 are random graphs, the

alignment network formed according to (2.3) will be a random graph as well. The first part of the proof is to characterize the leading eigenvector of this random alignment network. To do this, we first characterize the leading eigenvector of the expected alignment network which in fact is a deterministic graph. In particular, we prove that eigenvector scores assigned to true mappings is strictly larger than the ones assigned to false mappings. To prove this, we characterize top eigenvalues and eigenvectors of the expected alignment network algebraically. The restricted alignment condition (i.e., $|\mathcal{R}| = kn$) is necessary to have this bound. Then, we use Wedin Sin Theorem [53] from perturbation theory, Gershgorian circle Theorem [54] from spectral matrix theory, and Chernoff bound to characterize the leading eigenvector of the random alignment network for sufficiently large n . Finally, we use Chebyshev's inequality to show that the error probability of the EigenAlign algorithm is asymptotically zero w.h.p.

Note that finding an isomorphic mapping across asymptotically large Erdős-Rényi graphs (Corollary 1) is a well studied problem and can be solved efficiently through canonical labeling [43]. However, those techniques do not address a more general network alignment problem similar to the setup considered in Theorem 2. For more details, see Section 2.3.

Theorem 2 and Corollary 1 consider a restricted network alignment case where $|\mathcal{R}| = kn$. As explained briefly in the proof sketch and with more details in Lemma 3, this technical condition is necessary to show that, expected eigenvector scores of true mappings are strictly larger than the ones of false mappings as $n \rightarrow \infty$. In Section 6 and through simulations, we show that error of the EigenAlign algorithm is empirically small even in an unrestricted network alignment setup.

4 Low Rank Alignment of Networks

The EigenAlign algorithm introduced in Section 3 uses the leading eigenvector of the alignment graph to align graph structures. EigenAlign can be viewed as the rank-one approximation of the linearization of the underlying quadratic assignment problem. In this section, we introduce an extension of EigenAlign which uses higher-order eigenvector of adjacency graphs to align network structures. We refer to this extension as *LowRank Align*. LowRank Align can be useful specially in cases where leading eigenvectors of graphs are not informative. This case occurs for instance in the alignment of regular graph structures. Moreover, LowRank Align does not require an explicit formation of the alignment graph which can be costly for large networks if all mappings across networks are possible.

Suppose G_1 and G_2 are input networks with n_1 and n_2 nodes. For simplicity, in this section we assume that they are symmetric. Recall that X represents the mapping matrix whose size is $n_1 \times n_2$. In this section, we use the trace formulation of the quadratic assignment problem.

The maximum overlap network alignment optimization can be written as follows:

$$\begin{aligned} \max \quad & \text{Tr}(G_1 X G_2 X^T), \\ \text{subject to} \quad & \sum_{i=1}^{n_1} x_{i,j} \leq 1, \quad \forall 1 \leq j \leq n_2, \\ & \sum_{j=1}^{n_2} x_{i,j} \leq 1, \quad \forall 1 \leq i \leq n_1, \\ & x_{i,j} \in \{0, 1\}, \quad \forall 1 \leq i \leq n_1, \forall 1 \leq j \leq n_2. \end{aligned} \tag{4.1}$$

Optimization (4.1) finds a mapping matrix X that maximizes the number of overlapping edges

(matches) across two graphs. However, such a mapping can cause numerous mismatches. We discuss a balanced network alignment optimization later in this section.

For simplicity, we assume $n_1 = n_2 = n$. All discussions can be extended to the case where $n_1 \neq n_2$. Let \square be the set of all permutation matrices of size $n \times n$. Thus, optimization (4.1) can be written as follows:

$$\begin{aligned} \max_{X \in \square} \quad & \text{Tr}(G_1 X G_2 X^T), \end{aligned} \quad (4.2)$$

Let X^* be an optimal solution of optimization (4.2). Finding an optimal solution of this optimization is known to be NP-hard [15].

If $X \in \square$, we have,

$$\text{Tr}(G_1 X G_2 X^T) = \text{Tr}((G_1 + \delta_1 I)X(G_2 + \delta_2 I)X^T) + \text{constant}. \quad (4.3)$$

In other words, we can add and subtract multiples of identity to make the resulting symmetric matrices positive definite, without changing the structure of the problem. Thus, without loss of generality, we assume that matrices G_1 and G_2 are positive semi-definite.

Several algorithms have considered relaxations/approximations of this optimization as follows:

$$\begin{aligned} \max_{X \in \Gamma} \quad & \text{Tr}(G_1 X G_2 X^T), \end{aligned} \quad (4.4)$$

Suppose X_0 is a solution of optimization (4.4) such that $\|X^* - X_0\|_2 \leq \epsilon$ (i.e., its distance from the optimal solution is bounded by ϵ). X_0 may not be a valid permutation matrix. One way to find a permutation matrix using X_0 is to project X_0 over the space of permutation matrices \square :

$$\begin{aligned} \max_{X \in \square} \quad & \text{Tr}(X X_0^T), \end{aligned} \quad (4.5)$$

However, it has been shown that an optimal solution of optimization (4.5) has a poor perform in practice [55]. In the following, we propose an alternative algorithm to efficiently infer a permutation matrix using X_0 with a certain performance guarantee:

Consider the following optimization:

$$\begin{aligned} \max_{X \in \square} \quad & \text{Tr}(G_1 X_0 G_2 X^T), \end{aligned} \quad (4.6)$$

This is a maximum weight bipartite matching optimization which can be solved exactly using linear programming. Let X_{lin}^* be an optimal solution of optimization (4.6). Define

$$\begin{aligned} f(X) &\triangleq \text{Tr}(G_1 X G_2 X^T), \\ \tilde{f}(X) &\triangleq \text{Tr}(G_1 X_0 G_2 X_0^T) + 2\text{Tr}(G_1 X_0 G_2 (X - X_0)^T). \end{aligned} \quad (4.7)$$

Theorem 3 Let X^* and X_{lin}^* be optimal solutions of optimizations (4.1) and (4.6), respectively. We have,

$$|f(X^*) - \tilde{f}(X_{lin}^*)| \leq \epsilon^2 \sum_{i=1}^n \sigma_i(G_1) \sigma_i(G_2), \quad (4.8)$$

where ϵ is a bound on the relaxation gap ($\|X^* - X_0\|_2 \leq \epsilon$), and $\sigma_i(G_a)$ represents the i -th largest singular value of matrix G_a , for $a = 1, 2$.

Proof See Section 10.4. ■

If Γ is assumed to be the set of orthogonal matrices (i.e., $\Gamma = \mathcal{O}$), an optimal solution of optimization (4.4) can be found using eigen decomposition of matrices G_1 and G_2 as follows:

Theorem 4 Suppose v_i and u_i are eigenvectors of symmetric matrices G_1 and G_2 corresponding to the i -th largest eigenvalues $\sigma_i(G_1)$ and $\sigma_i(G_2)$, respectively. Let V and U be eigenvector matrices whose i -th columns are v_i and u_i , respectively. Then,

$$X_0 = VU^T = \sum_{i=1}^n v_i u_i^T, \quad (4.9)$$

is an optimal solution of optimization (4.4) over orthogonal matrices (i.e., $\Gamma = \mathcal{O}$).

Proof See reference [22]. ■

Remark 5 Theorem 4 characterizes an optimal solution of the orthogonal relaxation of the network alignment optimization. However, for any v_i , $-v_i$ is also an eigenvector of the matrix G_1 . A similar argument can be mentioned for eigenvectors of the matrix G_2 . Let

$$\mathcal{X}_0 \triangleq \left\{ X_0 : X_0 = \sum_{i=1}^n s_i v_i u_i^T, \mathbf{s} \in \{-1, 1\}^n \right\}, \quad (4.10)$$

where s_i is the i -th component of the vector \mathbf{s} . The set \mathcal{X}_0 represents multiple optimal solutions of optimization (4.4) when $\Gamma = \mathcal{O}$. \mathcal{X}_0 can have at most 2^n distinct members.

Suppose $X_0 \in \mathcal{X}_0$. Then, optimization (4.6) can be simplified to the following optimization which finds a valid permutation matrix using the orthogonal relaxation of the network alignment optimization:

$$\begin{aligned} \max \quad & \text{Tr}\left(\left(\sum_{i=1}^n \sigma_i(G_1) \sigma_i(G_2) v_i u_i^T\right) X^T\right), \\ & X \in \square. \end{aligned} \quad (4.11)$$

This optimization can be solved efficiently using linear programming.

Remark 6 A projection of $X_0 \in \mathcal{X}_0$ over permutation matrices according to optimization (4.5) leads to the following optimization:

$$\begin{aligned} \max \quad & \text{Tr}\left(\left(\sum_{i=1}^n v_i u_i^T\right) X^T\right), \\ & X \in \square. \end{aligned} \quad (4.12)$$

Unlike optimization (4.12), the objective function of (4.11) takes into account eigenvalues of matrices G_1 and G_2 as well. In other words, eigenvectors with largest eigenvalues contribute more to the objective function compared to the ones with small eigenvalues. To this end, the objective function of optimization (4.11) simplifies the network alignment problem to the simultaneous alignment of eigenvectors whose contributions in the overall alignment score are weighed by their corresponding eigenvalues.

One efficient way to approximate a solution for the original network alignment optimization (4.2) would be to obtain a solution X_0 for its orthogonal relaxation using eigen decomposition of input matrices (Theorem 4), and then to use optimization (4.11) to obtain a feasible solution with bounded error (Theorem 3). However, as we discussed above, there are possibly exponentially many optimal solutions for optimization (4.11) and obtaining their resulting permutation matrices would be computationally infeasible. However, because contributions of eigenvectors with small eigenvalues to the objective function of optimization (4.11) is small, one can instead solve the following optimization based on the low rank approximation of the objective function:

$$\begin{aligned} \max \quad & \text{Tr}\left(\left(\sum_{i=1}^k \sigma_i(G_1) \sigma_i(G_2) v_i u_i^T\right) X^T\right), \\ X \in \sqcap, \end{aligned} \quad (4.13)$$

where objective function considers only top k eigenvectors of input matrices (i.e., its affinity matrix is low rank). The following optimization summarizes the *LowRank Align algorithm*:

$$\begin{aligned} \max \quad & \text{Tr}\left(\left(\sum_{i=1}^k s_i \sigma_i(G_1) \sigma_i(G_2) v_i u_i^T\right) X^T\right), \\ X \in \sqcap, \\ s_i \in \{-1, 1\}, \quad & \forall 1 \leq i \leq k. \end{aligned} \quad (4.14)$$

where k is a constant that determines the rank of the affinity matrix.

In the restricted network alignment setup, some mapping pairs may not be allowed. In that case, one can set the affinity weights of such pairs in optimization (4.14) to be $-\infty$.

Remark 7 Unlike EigenAlign, LowRank Align does not require an explicit formation of the alignment graph which can be costly for large networks if all mappings across them are possible. Moreover, in such cases, the linear assignment step can be performed using a greedy method described in Remark 4 to reduce the overall computational complexity of the alignment method.

Optimization (4.1) finds a mapping across two graphs G_1 and G_2 to maximize the number of overlapping edges (matches) across them. However, the resulting mapping matrix can cause numerous mismatches, particularly for graphs with different sizes, because the objective function of optimization (4.1) does not penalize the number of mismatches. The number of mismatches caused by a mapping matrix X across two graphs G_1 and G_2 is equal to:

$$\begin{aligned} \text{number of mismatches} &= \text{Tr}\left(G_1 X (1 - G_2) X^T + G_1 X (1 - G_2) X^T\right) \\ &= -2 \text{Tr}(G_1 X G_2 X^T) + \text{Tr}(G_1 X \mathbb{1} X^T) + \text{Tr}(\mathbb{1} X G_2 X^T), \end{aligned} \quad (4.15)$$

where $\mathbb{1}$ represents a matrix of all ones. The following optimization considers both matches and mismatches caused by a mapping matrix X :

$$\max_{X \in \sqcap} (\beta_1 + 2\beta_2) \text{Tr}(G_1 X G_2 X^T) - \beta_2 \text{Tr}(G_1 X \mathbb{1} \mathbb{1}^T + \mathbb{1} X G_2 X^T), \quad (4.16)$$

where \sqcap is the set of all permutation matrices of size $n \times n$. β_1 and β_2 are match and mismatch contribution weights in the objective function of optimization (4.16). This optimization is similar to an alignment optimization where the number of mismatches is bounded. Moreover, the objective function of Optimization (4.16) is equivalent to the one introduced in (2.1) for some choices of s_1 , s_2 and s_3 . One can simply this optimization to the following optimization:

$$\max_{X \in \sqcap} \text{Tr}((G_1 - \alpha) X (G_2 - \alpha) X^T), \quad (4.17)$$

where

$$\alpha = \frac{\beta_2}{\beta_1 + \beta_2} = \frac{1}{2 + \beta_1/\beta_2} = \frac{1}{2 + R}. \quad (4.18)$$

To obtain optimization (4.17), we ignore the term $\text{Tr}(\mathbb{1} X \mathbb{1} X^T)$ since it is a constant term over permutation matrices $X \in \sqcap$. This is also true even when the size of two graphs are not equal (i.e., $n_1 \neq n_2$) if all nodes of the smaller graph are mapped to some nodes in the larger graph. To solve optimization (4.17), one needs to choose α (or equivalently $R = \beta_1/\beta_2$). This parameter tunes contributions of matches and mismatches in the network alignment objective function. Choosing $\alpha \rightarrow 0$ ($R \rightarrow \infty$) results in merely maximizing the number of matches across two graphs, while $\alpha = 1/2$ only considers minimizing the number of mismatches across two networks. To have balance between maximizing matches and minimizing mismatches across two networks, one can choose,

$$R = \frac{\beta_1}{\beta_2} = \frac{\text{number of mismatches}}{\text{number of matches}}. \quad (4.19)$$

5 Alignment of Modular Networks

Many networks have modular structures in which groups of nodes tend to interact with each other more strongly compared to the rest of the network [45, 46]. One can take advantage of such modular structure to split the large network alignment optimization into small subproblems and use a computationally expensive, but tight, semidefinite programming (SDP) [27] over each subproblem.

As we discuss in Section 3.1, EigenAlign provides a simple relaxation of the QAP in (2.5), based on the eigenvector centrality of the alignment graph. This can be thought of as a linearization of the quadratic assignment cost along the direction of the eigenvector centrality. EigenAlign relaxes integer constraints to constraints over a hyper-sphere restricted by hyper-planes. This relaxation leads to an efficient method to align large networks. There are several methods based on convex relaxations of the underlying QAP that seek solutions in the intersection of orthogonal and stochastic matrices [22–27]. In general, these relaxations are tighter (hence better) than the one used in the EigenAlign algorithm and lead to a better approximation of the optimal solution. However,

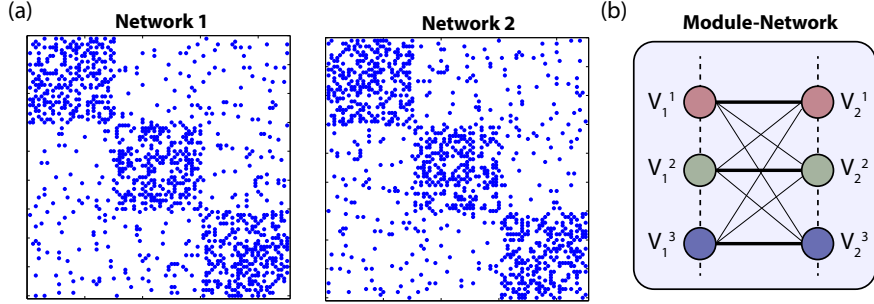


Figure 3: (a) Example modular network structures of Definition 6. (b) An illustration of the module-network bipartite graph whose nodes correspond to modules in the original networks.

these methods have high computational complexity, which limits their applicability in aligning large networks. For instance, as reported in [27] and also according to our experiments, to be able to run the SDP-based method proposed in [27] on an ordinary laptop, networks should not have more than around 70 nodes. Although this threshold can be improved by a better implementation of the method, this SDP-based method is not scalable for large networks. Moreover, distributed first-order methods to solve large SDPs [56] based on low-rank factorization [57], block coordinate descent methods [58], spectral bundle methods [59], and eigenvalue saddle point transformations [60] can be enhanced by splitting a large optimization into smaller ones, particularly for modular network structures.

Here, we propose a method, which we term *EigenAlign+SDP*, that uses the EigenAlign algorithm along with an SDP-based relaxation of the underlying QAP over modular network structures. The proposed algorithm uses the EigenAlign solution to identify small subgraphs (modules, or blocks) across two networks which are likely to be aligned to each other. Then, it uses a more computationally expensive SDP-based method to solve multiple small-size network alignment problems, in parallel. The proposed method is based on this key insight that, the EigenAlign solution provides a robust mapping of modules across networks, which enables the use of more expensive and accurate optimization methods over small sub-problems.

In this section, we consider stochastic block network structures:

Definition 6 Let $G_1 = (V_1, E_1)$ be an undirected graph. Suppose there is a partition of nodes $\{V_1^1, V_1^2, \dots, V_1^m\}$, where nodes in the same partition are connected to each other independently randomly with probability p , while nodes across partitions are connected to each other independently randomly with probability q .

Let \tilde{G}_1 be a noisy version of G_1 . Here, we consider the noise model II (3.9) as it is more general, while all arguments can be extended to the noise model I (3.8). We assume G_2 is a permuted version of \tilde{G}_1 according to (3.11), i.e., $G_2 = P\tilde{G}_1P^T$. Figure 3-a demonstrates example networks according to this model.

In the following, we present the *EigenAlign+SDP* method which aims to infer an optimal alignment across G_1 and G_2 .

Algorithm 2 (EigenAlign+SDP Algorithm) Let $G_1 = (V_1, E_1)$ be a stochastic block matrix of Definition 6, and $G_2 = (V_2, E_2)$ is defined according to (3.11). The *EigenAlign+SDP* algorithm

solves the network alignment optimization (2.5) in the following steps:

- **EigenAlign Step:** In this step, we compute the EigenAlign solution across G_1 and G_2 .
- **Spectral Partitioning Step:** In this step, we use a spectral partitioning method [37] to partition each network to m blocks.
- **Module Alignment Step:** In this step, we use the EigenAlign solution in a maximum weight bipartite matching optimization to compute an optimal alignment of modules across G_1 and G_2 .
- **SDP-based Alignment Step:** In this step, we use an SDP-based relaxation of the underlying QAP [27] followed by a maximum weight bipartite matching step, to compute node alignments in each module pairs.

In the following, we explain the above steps in more detail. In the EigenAlign step, we use EigenAlign algorithm 1 to find a mapping across networks G_1 and G_2 , denoted by X^* . In the spectral partitioning step, we use the algorithm proposed in [37] to find m blocks (modules) in each network. These modules are denoted by $\{V_1^1, V_1^2, \dots, V_1^m\}$ and $\{V_2^1, V_2^2, \dots, V_2^m\}$, in networks G_1 and G_2 , respectively. Note that other network clustering methods can be used in this step alternatively. Moreover, here we assume that, the number of clusters (blocks) m is known. Otherwise, it can be learned using Bayesian [61] or Monte Carlo [62] techniques. In the module alignment step, we use the EigenAlign solution X^* to infer a mapping across inferred modules. To do this, we form a bipartite module-network whose nodes in the first and second layers correspond to $\{V_1^1, V_1^2, \dots, V_1^m\}$, and $\{V_2^1, V_2^2, \dots, V_2^m\}$, respectively (Figure 3-b). The edge weight connecting node i in the first layer of this graph to node j' in the second layer (i.e., $w(i, j')$) is computed as follows:

$$w(i, j') = \sum_{\substack{a \in V_1^i \\ b \in V_2^{j'}}} X^*(a, b). \quad (5.1)$$

We use these weights in a maximum bipartite matching optimization to infer a one-to-one mapping across modules of two networks. Other methods based on random walks over aggregation of Markov chains [63] can be used in this step to find module mappings. In the last step, we use an SDP-based relaxation of the underlying QAP [27] along with a linear programming step of maximum weight bipartite matching to compute node alignments in each module-pair. In this step, other methods based on convex/semidefinite relaxations of the underlying QAP can be used as well.

In the following, we prove that the EigenAlign solution provides a robust module-level mapping across networks even in the high-noise regime.

Define,

$$\begin{aligned} \mathcal{M}_{in} &\triangleq \{(i, j') : i \in V_1^a, j' \in V_2^a, 1 \leq a \leq m\} \\ \mathcal{M}_{across} &\triangleq \{(i, j') : i \in V_1^a, j' \in V_2^b, 1 \leq a, b \leq m, a \neq b\}, \end{aligned} \quad (5.2)$$

where \mathcal{M}_{in} and \mathcal{M}_{across} represent mappings within and across modules in two networks, respectively. We wish to show that eigenvector centrality scores assigned to \mathcal{M}_{in} mappings in the EigenAlign algorithm are strictly larger than the ones assigned to \mathcal{M}_{across} mappings. Suppose G_1 and G_2 have m blocks, each with size n . Thus, the total number of nodes in each network is mn .

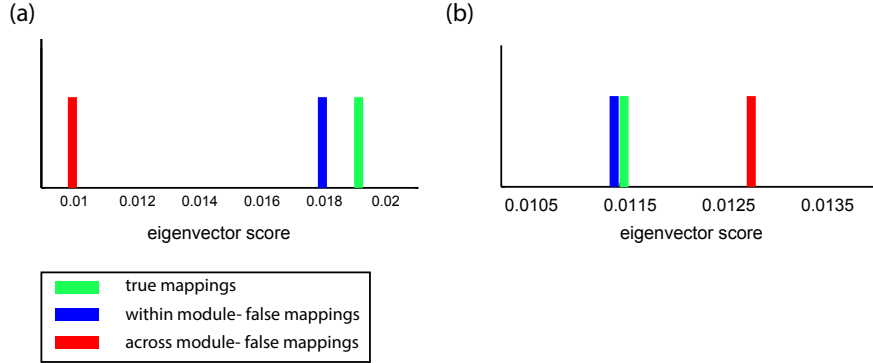


Figure 4: Eigenvector scores of within and across module mappings of the expected alignment network with parameters $n = 20$, $m = 4$, $p = 0.3$, $q = 0.01$, and (a) $\alpha = 100$, (b) $\alpha = 10$. Parameters of panel (a) satisfy conditions of Theorem 5.

Let A represent the alignment network across G_1 and G_2 , according to (2.3). This network has m^2n^2 number of nodes, out of which mn^2 are within module mappings (i.e., $|\mathcal{M}_{in}| = mn^2$), and the rest are across module mappings (i.e., $|\mathcal{M}_{across}| = (m^2 - m)n^2$). Let \bar{A} be the expected alignment matrix, where $\bar{A}(t_1, t_2) = \mathbb{E}[A(t_1, t_2)]$. To highlight key optimality conditions, in this section, we focus on the eigenvector analysis of the matrix \bar{A} . Similarly to Section 3.3, these properties can be extended to the alignment network A by using perturbation analysis of random matrices.

We choose scores assigned to matches, neutrals and mismatches as $s_1 = \alpha + \epsilon$, $s_2 = 1 + \epsilon$ and $s_3 = \epsilon$, respectively, where $\alpha > 1$ and $0 < \epsilon \ll 1$. To simplify notation, we assume ϵ is sufficiently small so that its effect is negligible. Let v correspond to the leading eigenvector of the expected alignment matrix \bar{A} .

Theorem 5 *For the noiseless case ($p_e = 0$), if $p > q$, $\alpha > 1/q - 1$, and $m > 2$, then,*

$$v(i) > v(j), \quad \forall i \in \mathcal{M}_{in}, \forall j \in \mathcal{M}_{across}. \quad (5.3)$$

Proof A proof is presented in Section 10.5. ■

The condition $p > q$ implies that the connectivity density of nodes in modules are larger than the one across modules. This condition is also essential in the spectral partitioning step of the EigenAlign+SDP algorithm to infer modules reliably. The condition $m > 2$ is a technical condition required in the proof of the strict inequality of (5.3). In Section 6.3, through simulations, we show that this condition is not essential for the algorithm. The condition $\alpha > 1/q - 1$ guarantees that the expected alignment score of two mapping pairs where one belongs to \mathcal{M}_{in} and the other one belongs to \mathcal{M}_{across} is strictly larger than the one where both mappings belong to \mathcal{M}_{across} . More details on these optimality conditions can be found in Section 10.5.

Now, we consider the case when G_2 is related to a noisy version of G_1 :

Theorem 6 *Suppose $0 \leq p_e^2 \ll 1$ and $0 \leq p_{e_2}^2 \ll 1$. Let $p > q$, $m > 2$ and $\alpha \gg 1/q$.*

- If $q \leq \frac{1}{4}$ and $p < \frac{1}{1+p_e}$,
- or, if $q > \frac{1}{4}$ and $p < \min\left(\frac{1}{1+p_e}, \frac{6q - \sqrt{4q(4q-1)(1-q)}}{2(1+2q)}\right)$,

then,

$$v(i) > v(j), \quad \forall i \in \mathcal{M}_{in}, \forall j \in \mathcal{M}_{across}. \quad (5.4)$$

Proof A proof is presented in Section 10.6. \blacksquare

If $p_e = 0$, the condition $p < \frac{1}{1+p_e}$ is simplified to $p < 1$. For higher noise level, this condition guarantees that correct within module mappings are assigned to higher scores than incorrect within-module ones. The additional constraint $p < \frac{6q - \sqrt{4q(4q-1)(1-q)}}{2(1+2q)}$ is required to guarantee that, the expected alignment score of two mapping pairs, one in \mathcal{M}_{in} and the other one in \mathcal{M}_{across} , is strictly larger than the one where both mappings belong to \mathcal{M}_{across} . We illustrate Theorems 5 and 6 in Figure 4. More details on these sufficient optimality conditions can be found in Section 10.6.

Theorems 5 and 6 indicate that eigenvector scores of within module mappings are strictly larger than the ones of across module mappings, in the expected alignment network. However, definitions of \mathcal{M}_{in} and \mathcal{M}_{across} are based on the permutation matrix P which relates networks G_1 and G_2 according to (3.11). In general, P may not be necessarily the optimal solution of the network alignment optimization (2.5). In the following, we provide conditions where the permutation matrix P in fact maximizes the expected objective function of the network alignment optimization (2.5).

Theorem 7 *Under the conditions of Theorem 5, if*

$$p \leq \frac{1 + \sqrt{1 + (\alpha^2 - 1)q}}{1 + \alpha}, \quad (5.5)$$

then, the permutation matrix P maximizes the expected objective function of the network alignment optimization (2.5).

Proof A proof is presented in Section 10.7. \blacksquare

For instance, setting $\alpha = 1/q$ and $q \ll 1$, the condition of Theorem 7 results to the condition $p^2 \leq q$.

Theorem 8 *Under the conditions of Theorem 6, if*

$$p^2 \leq \frac{q(1 - p_e)}{1 + p_e^2}, \quad (5.6)$$

then, the permutation matrix P maximizes the expected objective function of the network alignment optimization (2.5).

Proof A proof is presented in Section 10.8. \blacksquare

Conditions of Theorems 7 and 8 are based on an upper bound on the parameter p . To explain this condition intuitively, suppose the permutation matrix P maps modules V_1^a in network G_1 to modules V_2^a in network G_2 , where $1 \leq a \leq m$. In the case of large number of modules, the expected alignment score of the permutation matrix P is dominated by mapping-pairs (V_1^a, V_2^a) and (V_1^b, V_2^b) , where $a \neq b$. These scores depend on the connectivity density across modules, namely q . On the other hand, consider an incorrect permutation matrix \tilde{P} where $\frac{1}{nm} \|P - \tilde{P}\| > 0$. The alignment score of \tilde{P} is upper bounded by scores of incorrect within module mappings which depend on p . To have a sufficient optimality condition, we wish the expected alignment score of P to be larger than the

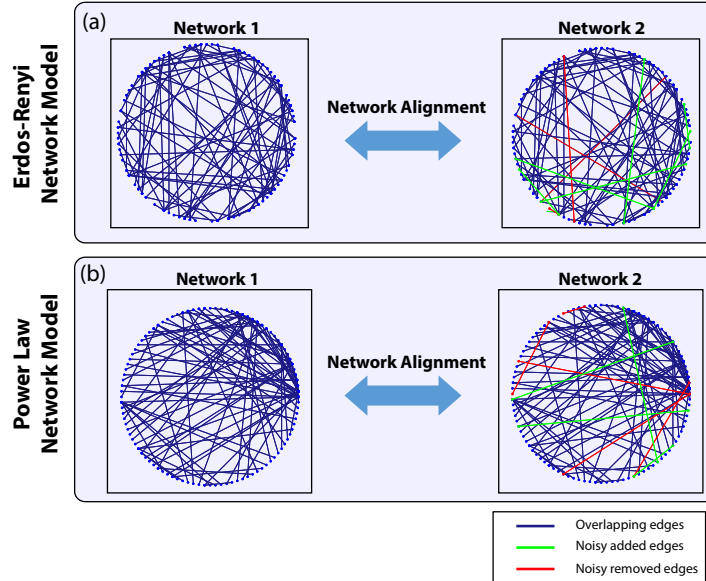


Figure 5: Examples of (a) Erdős-Rényi, and (b) power law networks used in Section 6.1.

upper bound of the expected alignment score of \tilde{P} . More details on these optimality conditions are presented in Sections 10.7 and 10.8.

In the EigenAlign+SDP algorithm 2, errors can also happen in other steps of the algorithm including the network partitioning and semidefinite relaxation steps. In Section 6.3, we empirically analyze the performance of the proposed algorithm. Our results suggest that the proposed method significantly outperforms existent network alignment techniques in aligning modular networks, while it has significantly lower computational complexity compared to standard convex-relaxation methods.

6 Performance Evaluation Over Synthetic Networks

We now compare the performance of the EigenAlign algorithm against other network alignment methods including IsoRank [3], NetAlign [30], Klau linearization [47] as well as an SDP-based method [27] through simulations. IsoRank is a global network alignment method which uses an iterative approach to align nodes across two networks based on their neighborhood similarities. NetAlign formulates the alignment problem in a quadratic optimization framework and uses message passing to approximately solve it. Klau linearization uses Lagrange multipliers to relax the underlying quadratic assignment problem. The SDP-based method [27] uses a convex relaxation of the underlying QAP based on matrix splitting. In our simulations, we use default parameters of these methods.

6.1 Erdős-Rényi and Power-Law graphs

Here, we test alignment methods over two types of input networks:

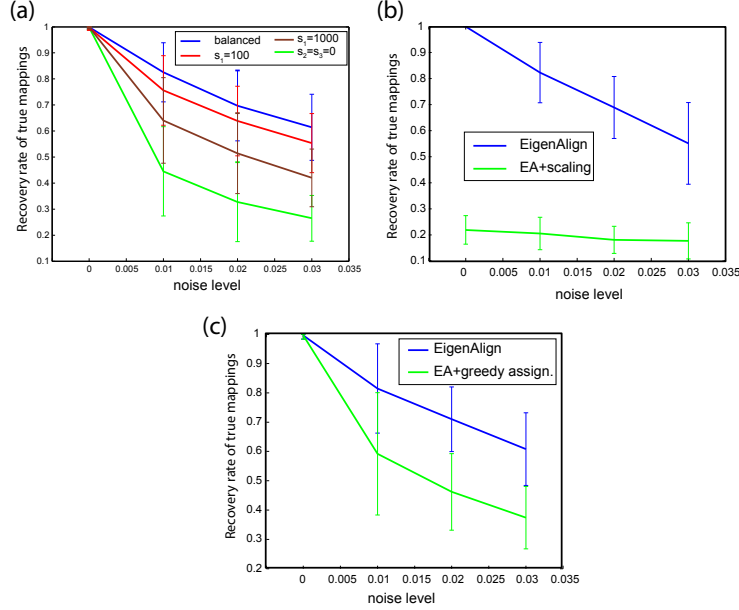


Figure 6: EigenAlign (EA) performance over power law graphs (a) with different alignment scores, (b) with alignment network scaling, and (c) with the greedy assignment method. At each point, simulations have been repeated 20 times.

- *Erdős-Rényi graphs* [42]: In this case, G_1 is a symmetric random graph where, $\Pr[(i, j) = 1] = p$ (see an example in Figure 5-a).
- *Power law graphs* [64]: We construct G_1 as follows; we start with a random subgraph with 5 nodes. At each iteration, a node is added to the network connecting to θ existent nodes with probabilities proportional to their degrees. This process is repeated till the number of nodes in the network is equal to n (see an example in Figure 5-b).

G_2 is then formed according to (3.11). In our experiments, we consider two noise models (3.8) and (3.9). In the case of the power law network model, we use the density of G_1 as parameter p in the noise model II of (3.9). We denote p_e as the *noise level* in both models.

In (3.11), P can be an arbitrary permutation matrix. In our simulations, we choose P such that, $P(i, n - i + 1) = 1$, for all $1 \leq i \leq n$, where n is the number of nodes in the network. Let \tilde{P} represent the solution of a network alignment method in aligning networks G_1 and G_2 . The recovery rate of true mappings is defined as,

$$1 - \frac{1}{2n} \|P - \tilde{P}\|. \quad (6.1)$$

As we explain in Proposition 2, this recovery rate is directly related to the number of inferred matches and mismatches in the network alignment optimization (2.5). Thus, we illustrate performance evaluations using this metric, noting that using other metrics such as the number of inferred matches/mismatches results in similar performance trends and conclusions. Moreover, in our simulations, all mappings across networks are considered to be possible (i.e., an unrestricted network alignment case).

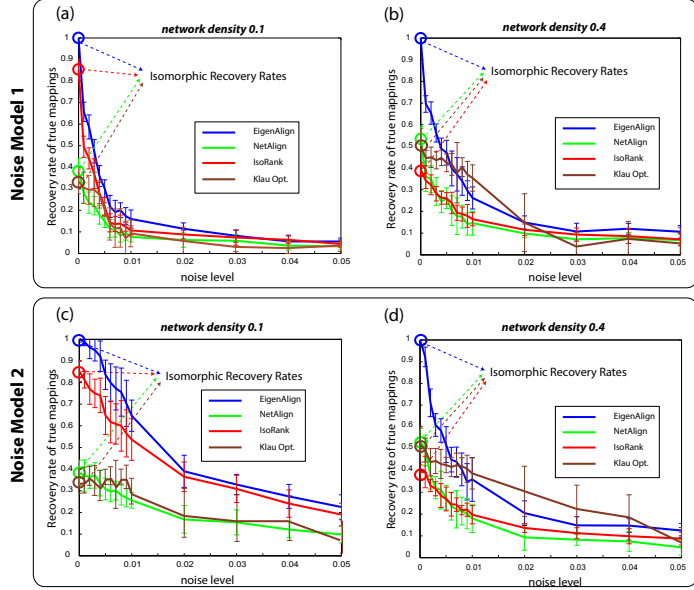


Figure 7: Performance evaluation of alignment methods over Erdős-Rényi graphs. EigenAlign outperforms IsoRank, NetAlign and Klau optimization in low and high network densities, in all considered noise levels, in both noise models. At each point, simulations have been repeated 10 times.

Figure 6 illustrates individual contributions of different components of the EigenAlign algorithm by isolating multiple aspects of the algorithm. In these experiments, we use the power-law network structure with 50 nodes, $\theta = 3$, and noise model II. Performance trends and conclusions are similar for other cases as well. In EigenAlign Algorithm 1, we use $s_1 = \alpha + \epsilon$, $s_2 = 1 + \epsilon$, and $s_3 = \epsilon$, where $\epsilon = 0.001$ and,

$$\alpha = 1 + \frac{\# \text{ of mismatches}}{\# \text{ of matches}}. \quad (6.2)$$

This choice of α satisfies the required condition $\alpha > 1$. Moreover, by this selection of α , we have,

$$|s_1 - 1 - \epsilon|(\# \text{ of matches}) = |s_3 - 1 - \epsilon|(\# \text{ of mismatches}), \quad (6.3)$$

which makes a balance between matched and mismatched interaction scores across networks and leads to an improved performance of the method (Figure 6-a). Note that, ignoring mismatches ($s_2 = s_3 = 0$) leads to a significant decrease in the EigenAlign performance. Choosing other values of α can provide a way to adjust relative importance of matching and non-matching interactions in different applications. In general, this parameter can be tuned in different applications using standard machine learning techniques such as cross validations [65]. Moreover, Figure 6-b illustrates the performance of the EigenAlign algorithm if we scale the alignment network by its node degrees (we replace $A_{i,j}$ by $A_{i,j}/d_i d_j$, where d_i is the degree of node i). As illustrated in this figure, this scaling removes our global match-mismatch score assignments and leads to a significant decrease in the performance. It is worth noting that, other scaling/scoring methods may be deployed leading to high network alignment performance in different applications. Finally, Figure 6-c illustrates

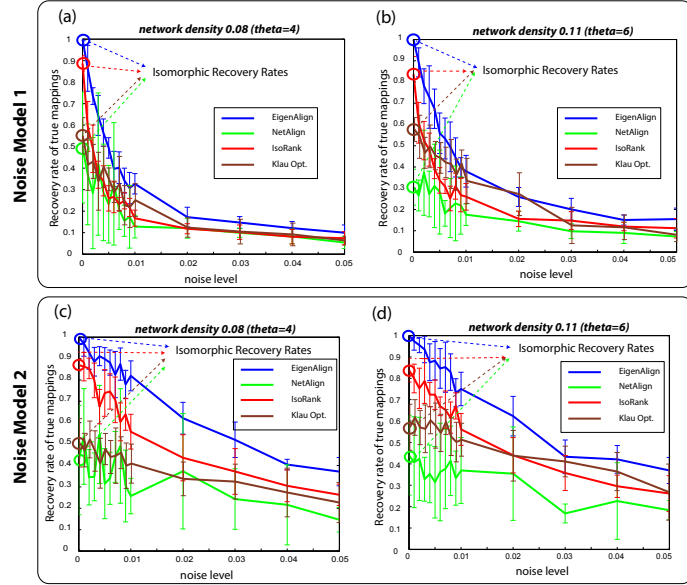


Figure 8: Performance evaluation of alignment methods over power law graphs. EigenAlign outperforms IsoRank, NetAlign, and Klau optimization in low and high network densities, in all considered noise levels, in both noise models. At each point, simulations have been repeated 10 times.

the performance of the EigenAlign algorithm if we replace the linear optimization of maximum weight bipartite matching with the greedy approach of Remark 4. As illustrated in this figure, this variation of the EigenAlign method decreases the performance, although it also decreases the computational complexity.

Next, we compare the performance of the EigenAlign method with the one of other network alignment methods over synthetic networks with $n = 100$ nodes. For large networks, the SDP-based method of [27] has high computational complexity, thus we excluded it from these experiments. Later, we will investigate the performance of the SDP-based method over small networks ($n \leq 50$).

Figure 7 shows the recovery rate of true mappings obtained by EigenAlign, IsoRank, NetAlign and Klau relaxation, over Erdős-Rényi graphs, and for both noise models. In the noiseless case (i.e., $p_e = 0$), the network alignment problem is simplified to the problem of graph isomorphism as explained in Section 3.3. In this case, the EigenAlign algorithm finds true mappings without error in both low and high network densities (i.e., the recovery rate of (6.1) is one.). In noisy cases and in both low and high network densities, EigenAlign shows consistently high performance compared to other methods.

Figure 8 shows the recovery rate of true mappings obtained by three considered methods over power law graphs, and for both noise models. Similarly to the case of Erdős-Rényi graphs, EigenAlign outperforms other methods in all considered noise levels and network densities. Notably, in noiseless cases, EigenAlign finds true isomorphic mappings across networks without error.

Figure 9 depicts the average running time of these methods over an Erdős-Rényi graph with density $p = 0.4$, and under the noise model I. All methods have been run on the same machine and each experiment has been repeated 10 times. In these experiments, EigenAlign has the second

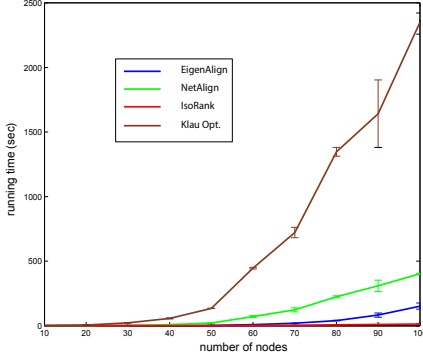


Figure 9: Running time of network alignment methods over Erdős-Rényi graphs.

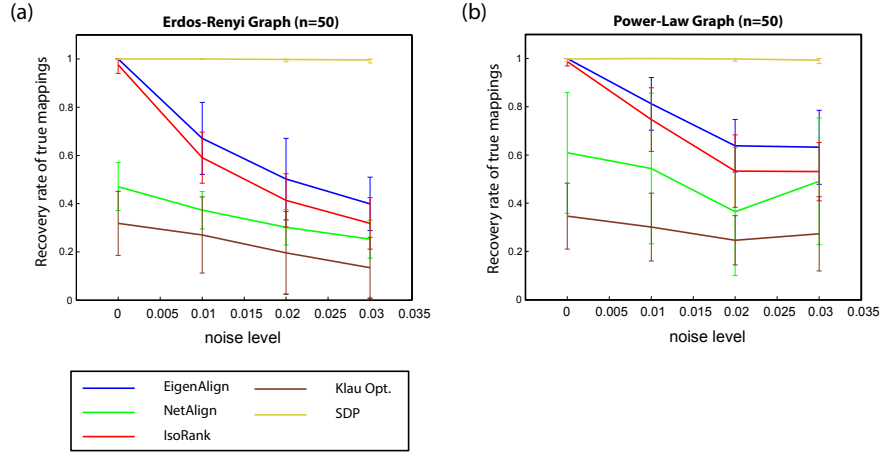


Figure 10: Performance evaluation of network alignment methods over (a) Erdős-Rényi ($p = 0.2$), and power law ($\theta = 3$) graphs, with $n = 50$. The computationally expensive SDP-based method outperforms other methods, while EigenAlign has the second best performance. At each point, simulations have been repeated 20 times.

best runtime, after IsoRank, outperforming NetAlign and Klau relaxation methods. Notably, the running time of Klau optimization method increases drastically as network size grows.

Next, we consider small networks with $n = 50$ nodes so that we are able to include a computationally expensive SDP-based method of [27] in our experiments. Note that, the method proposed in [27] only provides a bound on the value of the underlying QAP objective function and it does not provide a feasible solution. In order to obtain a feasible solution for the network alignment optimization, we use the SDP-based solution in a maximum weight bipartite matching optimization.

Figures 10-a,b illustrate the recovery rate of true mappings obtained by five considered methods over both Erdős-Rényi and power law graphs, under the noise model II. Performance trends under the noise model I is similar. As illustrated in these figures, the computationally expensive SDP-based method outperforms other network alignment methods significantly, while it has the highest running time (Figure 11). Notably, in these experiments, EigenAlign outperforms other methods except the SDP-based one consistent with the cases illustrated in Figures 7 and 8. These results

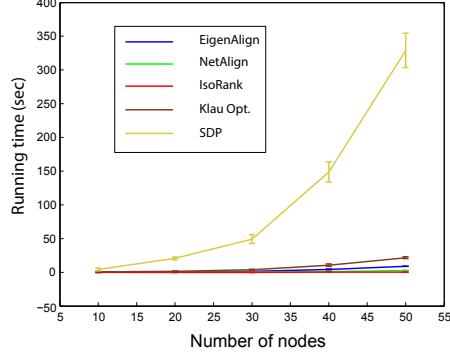


Figure 11: Running time of network alignment methods over Erdős-Rényi graphs with $n = 50$ and $p = 0.2$. The SDP-based method has significantly higher computational complexity compared to other network alignment techniques, which prohibits its use over large graphs. At each point, simulations have been repeated 20 times.

inspired us to propose the EigenAlign+SDP method to both have high recovery rate and low computational complexity (see Section 5).

6.2 Low Rank Alignment of Networks

In this section, we evaluate the performance of LowRank Align algorithm introduced in Section 4. Unlike EigenAlign, LowRank Align uses top k eigenvectors of input graphs according to Optimization (4.14). Here we use $k = 4$ as larger values of k did not have a significant effect on the results. We compare the performance of LowRank Align with EigenAlign, NetAlign [30], IsoRank [3] and an SDP-based network alignment method [27]. Besides these methods, we consider a network alignment solution that projects an optimal orthogonal relaxation of the underlying QAP over permutation matrices according to Theorem 4 and Optimization (4.5) (we refer to this method as OR, for orthogonal relaxation). As we explain in Section 4, there may be exponentially many optimal solutions for orthogonal relaxation of the underlying QAP. We also consider the case where all eigenvectors are oriented to have more positive components than negative ones (we refer to this method as ORP, for orthogonal relaxation with positive orientation of eigenvectors). Moreover, we consider a version of ORP where eigenvectors are scaled with eigenvalues similarly to (4.11) (we refer to this method as ORPS, for ORP with eigenvalue scaling).

Figure 12 shows the recovery rate, the number of inferred matches and mismatches and the mismatch-match ratio for different methods over Erdős-Rényi graphs with $n = 50$ nodes and edge density of $p = 0.2$. Similarly to our results in Section 6.1, the SDP-based network alignment outperforms other methods. However, this method has significantly higher computational complexity compared to other methods which prohibits its use in the alignment of large graphs. As it is illustrated in this figure, LowRank Align outperforms all other methods (except the expensive SDP-based method) in different noise levels. This illustrates that using higher-order eigenvectors in aligning graph structures leads to a tighter approximation of the underlying QAP. Notably, ORPS and ORP both outperform the baseline orthogonal relaxation (OR) method, highlighting the importance of considering eigenvector orientations and scaling in the network alignment optimization described in Section 4. Similar results hold for the alignment of power-law graph structures.

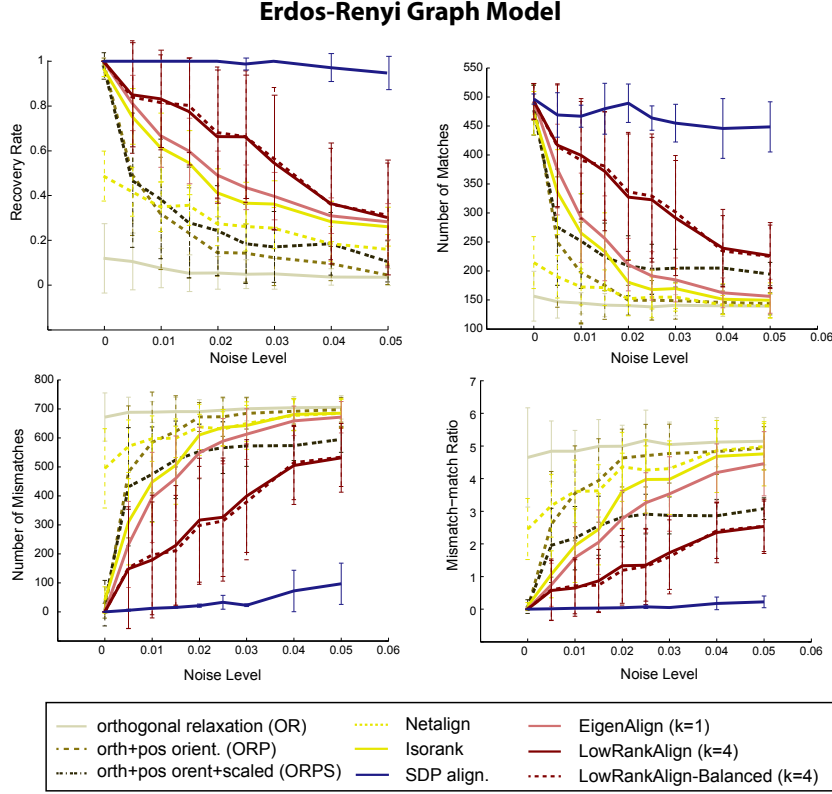


Figure 12: Performance evaluation of different network alignment methods including LowRank Align over Erdős-Rényi graphs with $n = 50$ nodes and edge density of $p = 0.2$. Experiments have been repeated 100 times for all methods except for the SDP-based alignment. For the SDP-based alignment, experiments have been repeated five times owing to its high computational complexity.

Figure 13 shows performance evaluation of different methods over regular graph structures with $n = 50$ nodes and edge density of $p = 0.2$. The alignment of regular graph structures is one of the most difficult network alignment cases because of the homogeneity of node degrees. As illustrated in Figure 13, in this case, LowRank Align outperforms all other methods including the expensive SDP-based network alignment. This illustrates the effectiveness of using higher order eigenvectors in aligning homogenous graph structures.

6.3 Modular Network Structures

We then asses the performance of the proposed EigenAlign+SDP method in Section 5 in aligning networks with modular structures. To be able to compare the performance of the proposed method with the one of the SDP-based method [27], we only consider small modular networks with 50 nodes, having two equal-size modules. As discussed in Section 6.1, the SDP-based method of [27] has high computationally complexity and using it for large networks is not practically feasible. The key idea of the EigenAlign+SDP method is to use the EigenAlign solution to split the large QAP into smaller sub-problems, enabling the use of the SDP-based relaxation method over each

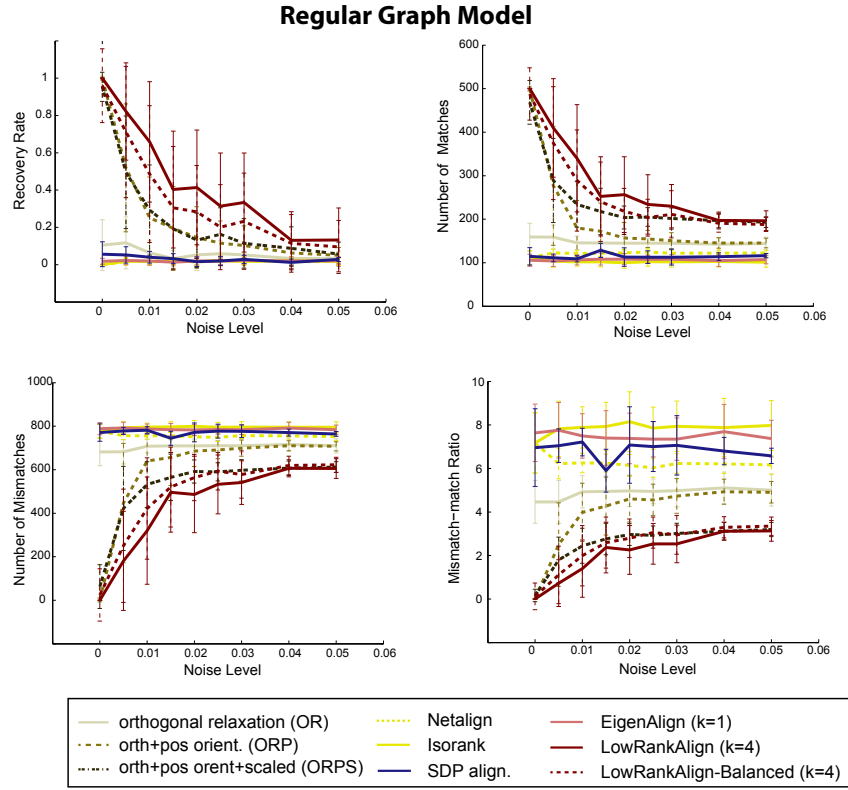


Figure 13: Performance evaluation of different network alignment methods including LowRank Align over regular graphs with $n = 50$ nodes and edge density of $p = 0.2$. Experiments have been repeated 100 times for all methods except for the SDP-based alignment. For the SDP-based alignment, experiments have been repeated five times owing to its high computational complexity.

sub-problem. Moreover, the SDP-based method can be run in parallel over each sub-problem.

Here, we consider network and noise models described in Section 5. In our evaluations, we consider EigenAlign, SDP, and EigenAlign+SDP methods. Moreover, we use the performance evaluation metric introduced in Section 6.1. Figures 14-a,b illustrates the recovery rate of true mappings of different methods, in various noise levels, and for different set of parameters p and q (the density of edges within and across modules, respectively). The average running time of the methods is depicted in Figure 15. As it is illustrated in these figures, while the recovery rate of the EigenAlign+SDP method is close to the one of the SDP-based one, it has significantly lower computational complexity, enabling its use for large complex networks.

7 Inference of Regulatory Networks in Human, Fly and Worm

Having illustrated the efficiency of the proposed network alignment algorithm, both theoretically and through simulations, we wish to use EigenAlign and other network alignment methods to compare the structure of regulatory networks across different species. However, the paucity of com-

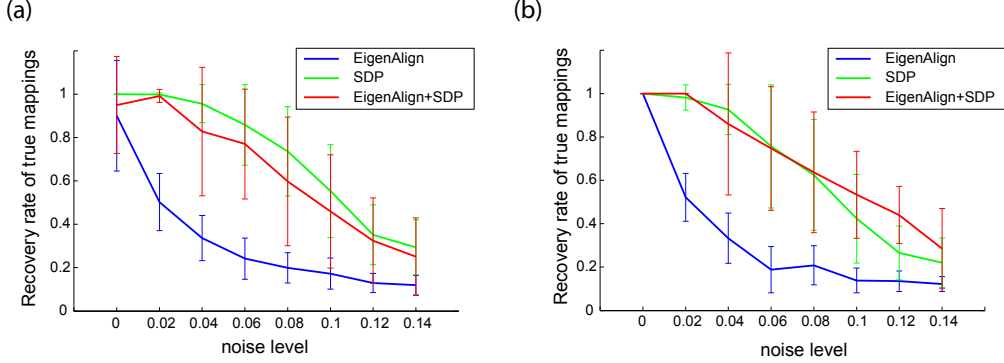


Figure 14: Performance evaluation of network alignment methods over modular network structures with $n = 20$, $m = 2$, $p = 0.2$, and (a) $q = 0.05$, (b) $q = 0.01$. The recovery rate of the EigenAlign+SDP method is close to the one of the SDP-based method, while it has significantly lower computational complexity.

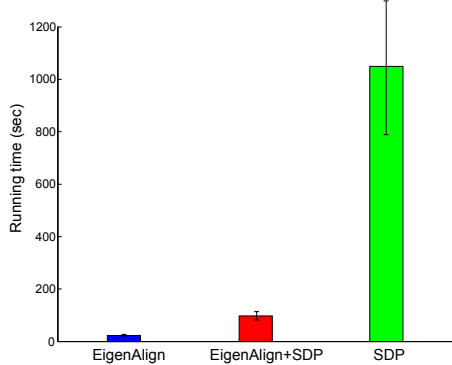


Figure 15: Average running time of network alignment methods over modular network structures with $n = 20$, $m = 2$, $p = 0.2$, and $q = 0.05$. The average running time of the SDP+EigenAlign algorithm is significantly lower than the one of the SDP-based method. Simulations have been repeated 20 times.

hensive catalogs of regulatory genomics datasets has hindered these studies in animal genomes. In this section, we leverage genome-wide functional genomics datasets from ENCODE and modENCODE consortia to infer regulatory networks across human, fly, and worm. In Section 8, we will compare the structure of these inferred networks using EigenAlign and other network alignment techniques.

The temporal and spatial expression of genes is coordinated by a hierarchy of transcription factors (TFs), whose interactions with each other and with their target genes form directed regulatory networks [66]. In addition to individual interactions, the structure of a regulatory network captures a broad systems-level view of regulatory and functional processes, since genes cluster into modules that perform similar functions [67–69]. Accurate inference of these regulatory networks is important both in the recovery and functional characterization of gene modules, and for comparative genomics of regulatory networks across multiple species [70, 71]. This is especially important because animal genomes, as fly, worm, and mouse are routinely used as models for human disease [72, 73].

Here, we infer regulatory networks of human, and model organisms *D. melanogaster* fly, and *C. elegans* worm, three of the most distant and deeply studied metazoan species. To infer regulatory interactions among transcription factors and target genes in each species, we combine genome-wide transcription factor binding profiles, conserved sequence motif instances [74] and gene expression levels [75, 76] for multiple cell types that have been collected by the ENCODE and modENCODE consortia. The main challenge is to integrate these diverse evidence sources of gene regulation in order to infer robust and accurate regulatory interactions for each species.

Ideally, inference of regulatory networks would involve performing extensive all-against-all experiments of chromatin immune-precipitation (ChIP) assays for every known transcription factor in every cell type of an organism, in order to identify all potential targets of TFs, followed by functional assays to verify that a TF-gene interaction is functional [69, 77]. However, the combinatorial number of pairs of TFs and cell types makes this experiment prohibitively expensive, necessitating the use of methods to reduce dimensionality of this problem. Here, we first infer three types of feature-specific regulatory connections based on functional and physical evidences and then integrate them to infer regulatory interactions in each species (Figure 16-a). One feature-specific network is based on using sequence motifs to scan the genome for instances of known binding sites of each TF, and then match predicted binding instances to nearby genes (a motif network). A second approach is to map TFs to genes nearby their ChIP peaks using a window-based approach (a ChIP binding network). The third feature specific network uses gene expression profiles under different conditions in order to find groups of genes that are correlated in expression and therefore likely to function together (an expression-based network).

Previous work [69] has shown that, while ChIP networks are highly informative of true regulatory interactions, the number of experiments that can be carried out is typically very small, yielding a small number of high confidence interactions. Motif networks tend to be less informative than ChIP networks, but yield more coverage of the regulatory network, while co-expression based networks tend to include many false-positive edges and are the least informative [77, 78]. However, integration of these three networks [68, 79–81] into a combined network yield better performance than the individual networks in terms of recovering known regulatory interactions, by predicting interactions that tend to be supported by multiple lines of evidence. Here, we use an integration approach that combines interaction ranks across networks [81]. Inferred regulatory interactions show significant overlap with known interactions in human and fly, indicating the accuracy and robustness of the used inference pipeline. In the following, we explain our network inference framework with more details.

7.1 Inference of feature specific regulatory networks

For each species, we form feature-specific regulatory networks using functional (gene expression profiles) and physical (motif sequences and ChIP peaks) evidences as follows:

Functional association networks. Expression-based networks represent interactions among TFs and target genes which are supported by correlation in gene expression levels across multiple samples [66, 82–84]. There are several methods to infer regulatory networks using gene expression profiles [81]. The input for these algorithms is a gene by condition matrix of expression values. The output of these methods are expression-based regulatory networks. We use the side information of TF lists to remove outgoing edges from target genes (in fact, TF lists are used as inputs to network inference algorithms to enhance their performance by limiting search space of the methods.).

To reduce bias and obtain a single expression-based network for each species, we combine

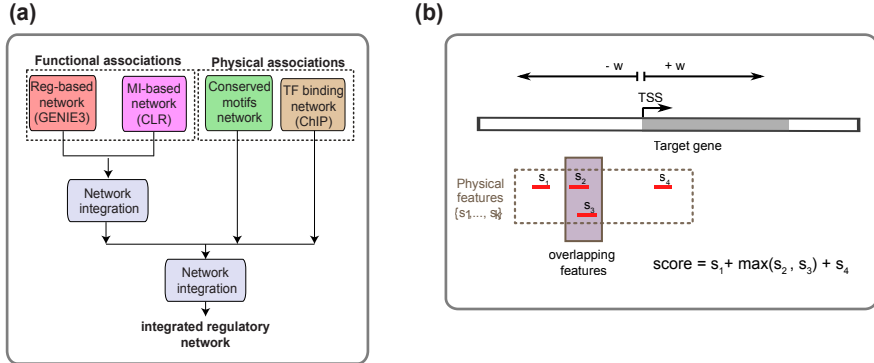


Figure 16: (a) The proposed framework to infer integrative regulatory networks. (b) The proposed framework to infer physical feature-specific regulatory networks.

results of two different expression-based network inference methods (Figure 16-a): one method is CLR [75] (context likelihood of relatedness) which constructs expression networks using mutual information among gene expression profiles along with a correction step to eliminate background correlations. The second method used is GENIE3 [76] (Gene Network Inference with Ensemble of Trees) which is a tree-based ensemble method that decomposes the network inference problem to several feature selection subproblems. In each subproblem, it identifies potential regulators by performing a regression analysis using random forest. GENIE3 has been recognized as the top-performing expression based inference method in the DREAM5 challenge [81].

Table 1 summarizes the number of genes and TFs in expression-based regulatory networks. These numbers refer to genes and TFs that are mapped to Entrez Gene IDs [85], the standard IDs that we use throughout our analysis. As it is illustrated in this table, expression based networks cover most of potential regulatory edges from TFs to targets. Despite a high coverage, however, the quality of inferred expression networks are lower than the one for physical networks [77]. This can be partially owing to indirect effects and transitive interactions in expression-based regulatory networks [81].

Physical association networks. We form two physical regulatory networks for each of the considered species using two types of physical evidences as our inference features: In the first approach, we use conserved occurrences of known sequence motifs [74], while in the second approach, we use experimentally defined TF binding occupancy profiles from ChIP assays of ENCODE and modENCODE [69, 77]. Table 2 shows the number of TFs associated to motifs as well as the number of TFs with genome-wide ChIP profiles in human, fly and worm. TSS coordinates are based on the genome annotations from ENCODE and modENCODE for human and worm, respectively, and the FlyBase genome annotations (FB5.48) for fly.

Each physical feature is assigned to a score: motif sequence features are assigned to conservation scores according to a phylogenetic framework [74], while sequence read density of TFs determines scores of ChIP peaks. Further, two physical features are called overlapping if their corresponding sequences have a minimum overlap of 25% in relation to their lengths (Jaccard Index > 0.25).

Our inference algorithm is based on occurrence of these features (motif sequences or ChIP peaks) within a fixed window size around the transcription start site (TSS) of target genes (Figure 16-b). We use a fixed window of 5kb around the transcription start site (TSS) in human and 1kb

in fly and worm. Then, we apply a max-sum algorithm to assign weights to TF-target interactions in each case: we take the maximum score of overlapping features and sum the scores of non-overlapping ones. In ChIP networks, because read densities are not comparable across different TFs, we normalize TF-target weights for each TF by computing z-scores.

7.2 Inference of integrated regulatory networks

Feature specific networks have certain biases and shortcomings. While Physical networks (motif and ChIP networks) show high quality considering overlap of their interactions with known interactions [77], their coverage of the entire network is pretty low mostly owing to the cost of the experiments. On the other hand, while expression based networks have a larger coverage of regulatory networks compared to physical ones, they include many false-positive edges partially owing to indirect information flows [78]. To overcome these limitations, we therefore integrate these feature-specific regulatory interactions into a single integrated network [68, 79–81] (Figure 16-a).

Suppose there are K input feature-specific regulatory networks, each with n genes and m TFs (only TF nodes can have out-going edges in the network). Let $w_{i,j}^l$ and $w_{i,j}$ represent interaction weights between TF i and target gene j in the input network l and in the integrative network, respectively. We use a rank-based (borda) integration technique to infer integrated networks in considered species. In this approach, integrative weights are computed as follows:

$$w_{i,j} = 1/K \sum_{l=1}^K r_{i,j}^l, \quad (7.1)$$

where $r_{i,j}^l$ represents the rank of interactions $i \rightarrow j$ in the input network l . An edge with the maximum weight is mapped to the rank nm . We also assume non-existent interactions are mapped to rank 0 (if $w_{i,j}^l = 0$, then $r_{i,j}^l = 0$) [81]. Moreover, ties are broken randomly among edges with same weights.

We find that top-ranking integrative interactions in human and fly networks are primarily supported by ChIP and motif evidences, while worm interactions are primarily supported by co-expression edges, consistent with the lower coverage of worm ChIP and motif interactions (Figure 17).

To validate inferred integrated networks, we use known interactions in TRANSFAC [86], REDfly [87] and EdgeDB [88] as human, fly and worm benchmarks, respectively. We assess the quality of various networks by using (a) the area under the receiver operating characteristic curve (AUROC); and (b) the area under the precision recall curve (AUPR), for each benchmark network (Figures 18). Let $TP(k)$ and $FP(k)$ represent the number of true positives and false positives in top k predictions, respectively. Suppose the total number of positives and negatives in the gold standard are represented by P and N , respectively. Then, an ROC curve plots true positive rate vs. false positive rate ($TP(k)/P$ vs. $FP(k)/N$), while a PR curve plots precision ($TP(k)/k$) vs. recall ($TP(k)/P$). A high AUPR value indicates that, top predictions significantly overlap with known interactions, while a high AUROC value indicates the advantage of inferred predictions in discriminating true and false positives compared to random predictions (AUROC of a random predictor is 0.5).

Figure 18 illustrates AUROC and AUPR scores for feature-specific and integrative networks, in different cut-offs, and in all three considered species. Considering the top 5% of interactions in each weighted network as predicted edges, according to AUROC metric, integrative networks outperform

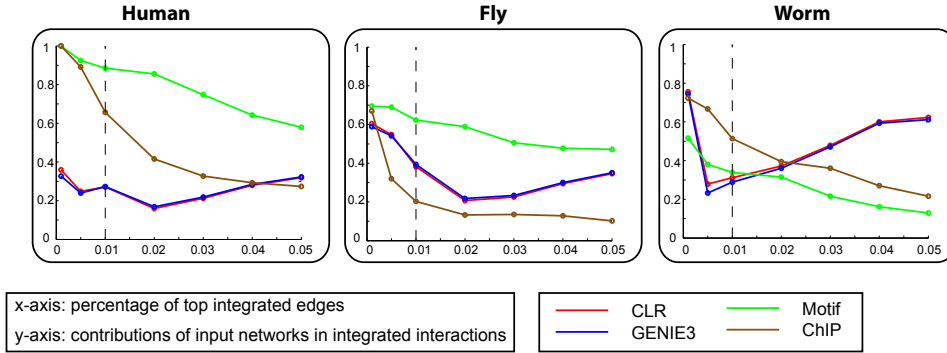


Figure 17: Contributions of input feature-specific networks in integrated interactions.

	Human	Fly	Worm
Genes	19,088	12,897	19,277
TFs	2,757	675	905

Table 1: Number of genes and TFs covered by gene expression data.

	Human	Fly	Worm
Motif network	485	221	30
ChIP network	165	51	88

Table 2: Number of TFs covered by evolutionary conserved motifs and TF binding datasets.

feature-specific networks in all three species. In fact, AUROC values of integrative networks are 0.58 in human, 0.62 in fly, and 0.52 in worm, respectively. AUPR values of integrative networks are 0.019 in human, 0.047 in fly, and 0.037 in worm, respectively. Notably, all methods have low scores over the EdgeDB (worm) benchmark, which can be partially owing to sparse physical networks and/or systematic bias of EdgeDB interactions.

As the cut-off (network density) increases, AUROC values of integrative networks tend to increase while their AUPR scores are decreasing in general. This is because of the fact that, the rate of true positives is lower among medium ranked interactions compared to top ones. Considering both AUROC and AUPR curves for all species, we binarize networks using their top 5% interactions which leads to balanced values of AUROC and AUPR in all inferred networks. This results in $2.6M$ interactions in human, $469k$ in fly and $876k$ in worm. In integrative networks, the median number of targets for each TF is 253 in human, 290 in fly and 640 in worm, with a median of 132 regulators per gene in human, 29 in fly, and 43 in worm.

8 Performance Evaluation Over Gene Networks

Having illustrated the effectiveness of our algorithm both theoretically and through simulations, we apply it to compare gene regulatory networks across human, fly and worm species. We use regulatory networks which we inferred in Section 7 by integrating genome-wide functional and

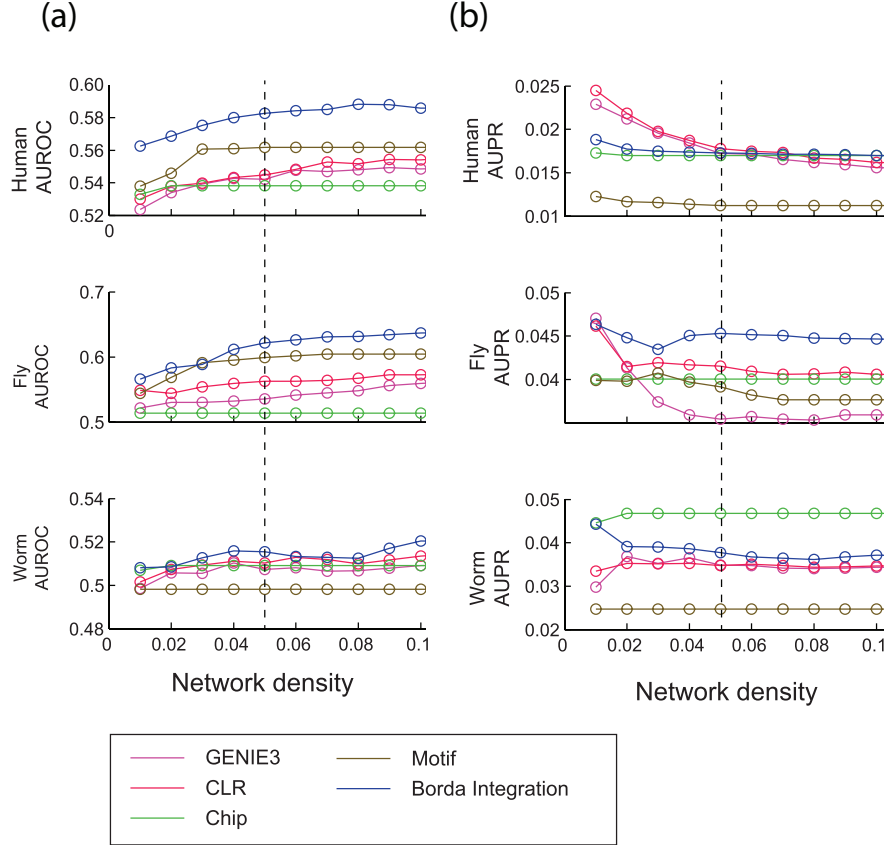


Figure 18: AUROC and AUPR scores of feature-specific and integrated regulatory networks in human, fly and worm species.

physical genomics datasets from ENCODE and modENCODE consortia. Comparative network analysis in evolutionary studies often requires having a one-to-one mapping across genes of two or multiple networks. We use homolog mappings across genes of human, fly and worm provided by the ENCODE and modENCODE consortia [89]. Note that human homologs refer to homologous genes in fly and worm, while fly/worm homologs are defined solely in relation to human. Homolog mappings across species are based on gene sequence similarities over corresponding gene trees [89]. However, since human, fly and worm are distant species and as a result, many gene families have undergone extensive duplications and losses, we observe non-bijective homolog mappings across their genes [89]. For example, one gene in human can be homologous to multiple genes in fly and vice versa (see an example in Figure 19). To infer bijective mappings as a subset of homolog genes across species, we use network alignment methods.

We assess the performance of three network alignment methods (EigenAlign, NetAlign, IsoRank) in comparative analysis across gene regulatory networks of human, fly and worm. We excluded the network alignment method based on Klau optimization [47] from our analysis in this section owing to its high computational complexity, and its low performance over synthetic networks of Section 6. Moreover, as we discussed in Section 6, the SDP-based method of [27] has high-computational complexity which prohibits its use in aligning large regulatory networks. We

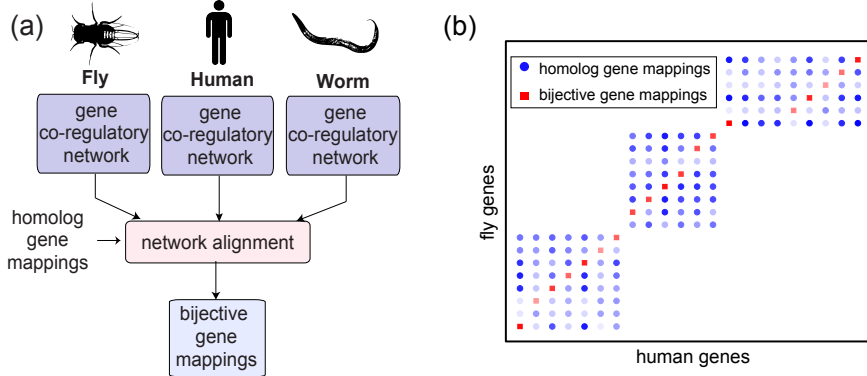


Figure 19: (a) A comparative analysis framework across human, fly and worm regulatory networks. (b) An application example of a network alignment method (EigenAlign) over three gene families across human-fly.

use EigenAlign, IsoRank and NetAlign methods with the setup and parameters similarly to Section 6. Moreover, unlike EigenAlign, IsoRank and NetAlign methods do not take into account the directionality of edges in their network alignment setup. Thus, to have fair performance assessments of considered network alignment methods, we create un-directed co-regulatory networks using inferred regulatory networks of Section 7, by connecting genes when their parent TFs have an overlap larger than 25%. This results in undirected binary networks in human, fly, and worm, with 19, 221, 13, 642, and 19, 296 nodes, and 13.9%, 3.5%, and 4.2% edge densities, respectively.

By application of network alignment methods, we infer bijective mappings across human-fly and human-worm networks. There are numerous mismatched interactions across networks of distal species partially owing to extensive gene functional divergence due to processes such as gene duplication and loss. In this situation, it is critical to consider both matches and mismatches in the network alignment optimization. Unlike existent network alignment algorithms which completely ignore mismatches across networks, EigenAlign considers both matches and mismatches across networks in a balanced way by setting alignment scores according to (6.2). Figures 20-a,b illustrate the number of matched (conserved) and mismatched (error) interactions across human-fly and human-worm networks, inferred using different methods. As it is illustrated in these figures, in both human-fly and human-worm comparisons, EigenAlign significantly outperforms other methods in terms of causing fewer number of mismatches (errors) across networks, while its performance is close to the best one in terms of the number of matches (overlaps). Figure 20-c illustrates the match-mismatch ratio for different network alignment methods, in both human-fly and human-worm comparisons. As it is illustrated in this figure, EigenAlign outperforms other methods significantly indicating that, it finds mappings across networks which maximize the number of matches and minimize the number of mismatches simultaneously. In all cases, the number of conserved interactions is statistically significant ($p - value < 0.01$), suggesting regulatory pathways are conserved between distal species and therefore highlighting their potential role in basic cellular processes. p -values are computed using a rank test by randomly selecting bijective mappings from gene homolog mappings while keeping network structures the same.

We examine enrichment of different biological processes over conserved subgraphs inferred by different alignment methods, across human-fly and human-worm. We expect many basic cellular

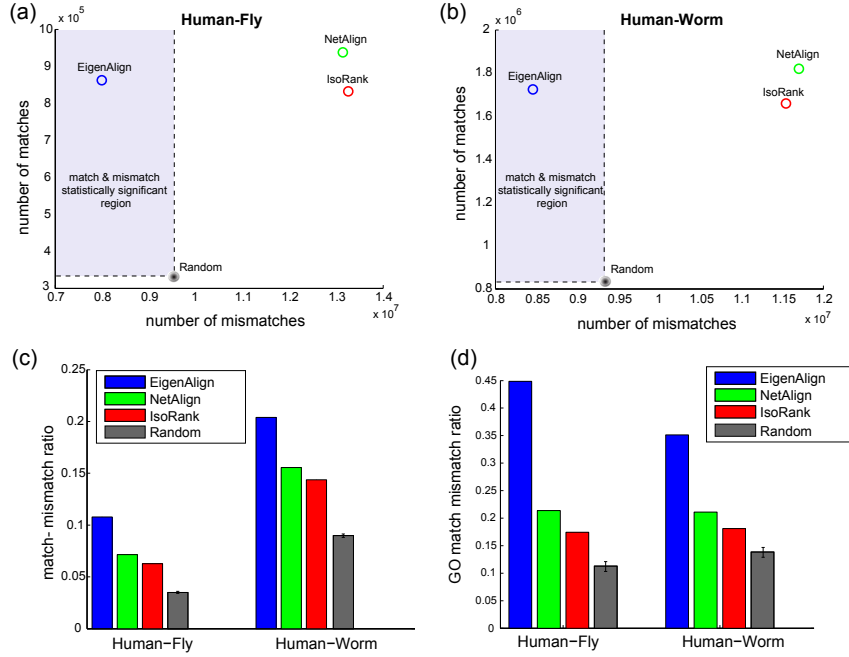


Figure 20: The number of matched and mismatched interactions inferred using different network alignment methods across (a) human-fly and (b) human-worm networks. (c) An average match-mismatch ratio for different network alignment methods, in both human-fly and human-worm comparisons. (d) This panel shows average match-mismatch ratios over pairs of biological processes across both human-fly and human-worm networks. EigenAlign mappings preserve regulatory patterns of biological processes across both human-fly and human-worm networks significantly better than the ones of NetAlign and IsoRank methods.

processes such as transcription elongation, cellular growth, etc to be conserved across these species despite long evolutionary distances. In our comparative analysis, we consider genome ontology (GO) processes that are experimentally verified and have sizes in the range of 100 and 500 genes. We consider pairs of processes across species with more than 50 homolog gene pairs.

Figure 20-d shows average match-mismatch ratios over these pairs of biological processes across both human-fly and human-worm networks. As illustrated in this figure, mappings inferred by EigenAlign preserve regulatory patterns of biological processes significantly better than the ones of NetAlign and IsoRank methods, across both human-fly and human-worm networks. This is consistent with the overall match-mismatch ratio gain of the EigenAlign method across human-fly and human-worm networks, demonstrated in Figure 20-c. Note that the average match-mismatch ratios across GO processes (Figure 20-d) are significantly higher than the ones across entire networks (Figure 20-c). This may indicate that connectivity patterns among genes involved in similar processes are better preserved compared to the rest of the regulatory network. However, note that, this enrichment of GO processes across species may be partially owing to biases in the study of these genes in the literature [90]. Thus, additional experimental validations are required which is beyond the scope of this paper.

Next, we compute p -values for matches and mismatches for each pair of processes using a rank

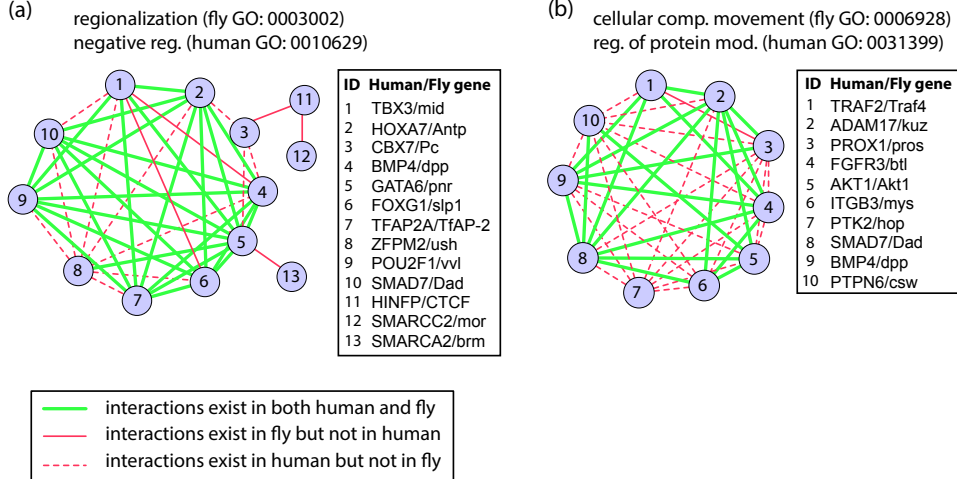


Figure 21: Examples of conserved biological processes (p -values < 0.05) across human and fly inferred by EigenAlign.

test by randomly selecting bijective mappings from gene homolog mappings. Then, we take the worst match/mismatch p -value for each pair and perform Benjamini and Hochberg multiple hypothesis correction [91]. Using EigenAlign mappings, we find five conserved pairs of regulatory processes across human-fly networks (p -values < 0.05) including regionalization/negative regulation of gene expression (Figure 21-a), and cellular component movement/regulation of protein modification process (Figure 21-b). Using NetAlign and IsoRank mappings, no significantly enriched processes across human and fly are found. Moreover, across human and worm, none of the inferred mappings leads to the inference of significantly conserved processes. Similarly to the centrality conservation analysis, this can be partially owe to a large evolutionary distance between human and worm. Finally, we note that, the solution provided by the EigenAlign method can be used in designing future experiments to extend GO catalogs by using gene regulatory networks and cross-species information.

We assess conservation of gene centralities across different networks. Centrality measures over regulatory networks provide useful insights on functional roles of genes in regulatory processes [92–94]. Therefore, comparative analysis of gene centrality measures across species can shed light on how evolution has preserved or changed regulatory patterns and functions across distal species. A suitable alignment should map central nodes in one network to central nodes in the other network (Figure 22-a). Here, we consider three centrality measures: degree centrality, eigen-vector centrality, and the page-rank centrality with the damping factor 0.85. In Figure 22, we illustrate centrality correlation of aligned genes using different network alignment methods, across both human-fly and human-worm networks. As it is illustrated in this figure, the bijective mapping inferred by EigenAlign preserves different node centralities across networks significantly better than other tested methods. That is, EigenAlign is more likely to map central nodes in one network to central nodes in the other network. Finally, we note that, the centrality conservation across human-fly networks is significantly larger than the one across human-worm networks, partially owing to a larger evolutionary distance between human and worm compared to the one between human and fly.

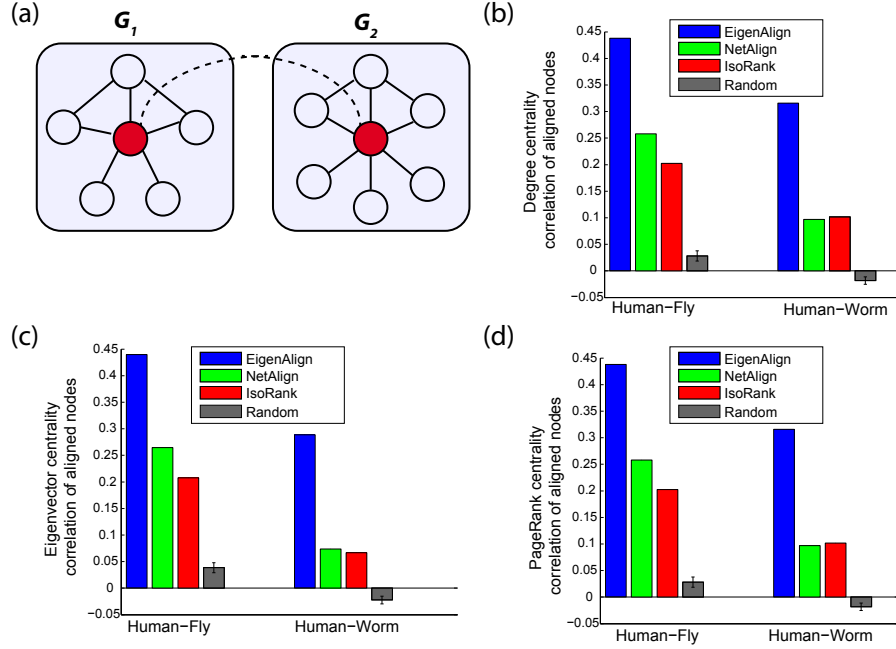


Figure 22: (a) A suitable alignment should map central nodes in one network to central nodes in the other network. Correlation of (b) degree centrality, (c) eigenvector centrality, and (d) page-rank centrality measures of aligned genes using different network alignment methods, in both human-fly and human-worm comparisons.

Note that in the alignment of regulatory networks across human, fly and worm, both EigenAlign and its higher eigenvector extension (LowRank Align) lead to similar solutions, suggesting that in our particular example of aligning regulatory networks of distal species, the leading eigenvectors yield a reasonable approximation of the underlying QAP (Figure 23).

9 User De-anonymization over twitter follower subgraphs

Data anonymization is the process of either encrypting or removing personally identifiable information from a dataset. As more and more personal information is available over social networks such as Facebook and twitter, data anonymization is becoming critical in privacy protection of people [13, 95]. Moreover, because the size and resolution of medical and genetic datasets have increased significantly, serious challenges have arisen with respect to ensuring the privacy of patients and samples [96]. In this circumstance, it is critical to measure the vulnerability of data anonymization methods by aiming to extract personal information from an anonymized dataset to highlight its privacy loopholes.

Here, we examine the power of network alignment techniques in de-anonymizing user IDs using connectivity structures of networks. We consider small subgraphs of the Twitter follower network sampled in years 2008 and 2009. These networks have 53 and 88 nodes, and 58 and 91 edges, respectively (Figure 24-a).

Here, we wish to de-anonymize user IDs in the 2009 network using user IDs in the 2008 network by only knowing a fraction of user IDs in 2009. To do that, we apply different network alignment

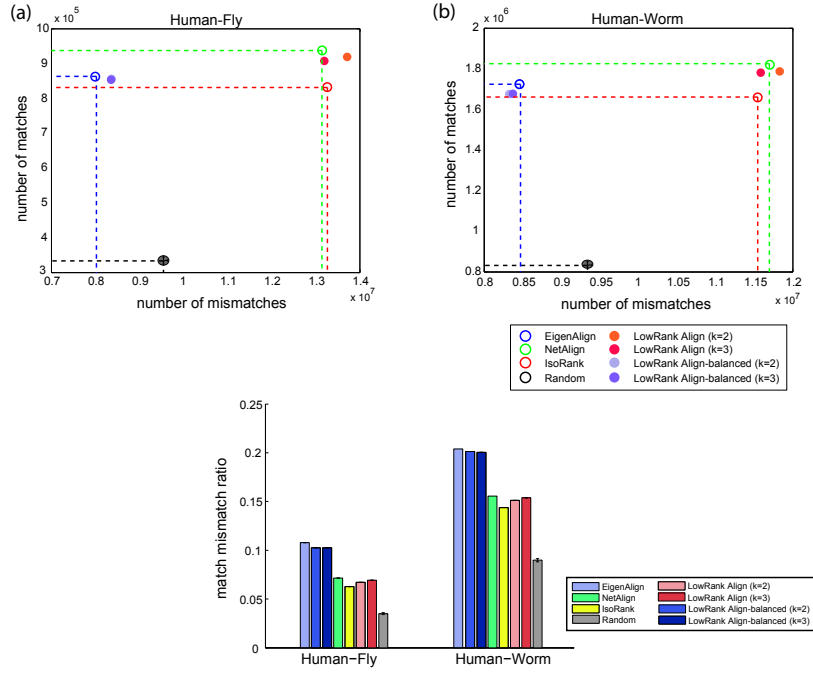


Figure 23: Performance evaluation of different network alignment methods including LowRank Align over co-regulatory networks. EigenAlign and LowRank Align both lead to similar solutions.

methods to infer an alignment across nodes of two networks. Figure 24-b illustrates the fraction of correctly de-anonymized users using different network alignment methods. The EigenAlign algorithm is more efficient than both NetAlign and IsoRank methods in user de-anonymization over these graphs. This application illustrates the extent of personal information that can be retrieved from network structure alone, and raises additional considerations that need to be addressed in different privacy-related applications. Applications of network alignment techniques over the entire twitter graph will require reducing their computational complexity significantly using further relaxations and approximations that we explain in Section 4 (Remark 7).

10 Proofs

In this section, we present proofs of the main results of the paper.

10.1 Proofs of Lemmas 1 and 2

First we prove Lemma 1: Let A be the alignment network of graphs G_1 and G_2 . Suppose \tilde{P} is a permutation matrix where $\rho \triangleq \frac{1}{2n} \|P - \tilde{P}\| > 0$. Let \mathbf{y} and $\tilde{\mathbf{y}}$ be vectorized versions of permutation

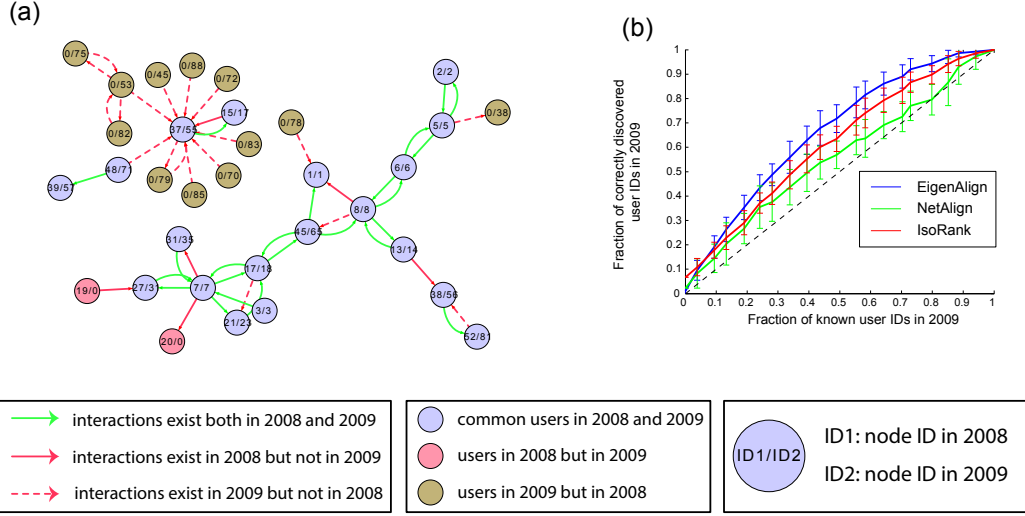


Figure 24: De-anonymization of user IDs over twitter subgraphs. We consider small subgraphs of the twitter follower network sampled in 2008 and 2009 years, with 53 and 88 nodes, and 58 and 91 edges, respectively. Panel (a) illustrates two large components of these networks. Panel (b) illustrates the fraction of correctly de-anonymized users using different network alignment methods. The EigenAlign algorithm is more efficient than both NetAlign and IsoRank methods in user de-anonymization over these graphs.

matrices P and \tilde{P} , respectively. Then, we have,

$$\begin{aligned}
\frac{1}{n^2} \mathbb{E}[\tilde{\mathbf{y}}_2^T A \tilde{\mathbf{y}}_2] &= (1 - \rho)[ps_1 + (1 - p)s_2] + \rho[p^2 s_1 + (1 - p)^2 s_2 + 2p(1 - p)s_3] \\
&\quad < (1 - \rho)[ps_1 + (1 - p)s_2] + \rho[p^2 s_1 + (1 - p)^2 s_2 + p(1 - p)(s_1 + s_2)] \\
&= (1 - \rho)[ps_1 + (1 - p)s_2] + \rho[ps_1 + (1 - p)s_2] \\
&= ps_1 + (1 - p)s_2 \\
&= \frac{1}{n^2} \mathbb{E}[\mathbf{y}_1^T A \mathbf{y}_1].
\end{aligned} \tag{10.1}$$

Now we prove Lemma 2: Similarly to the proof of Lemma 1, let A be the alignment network of graphs G_1 and G_2 and suppose \tilde{P} is a permutation matrix where $\rho \triangleq \frac{1}{2n} \|P - \tilde{P}\| > 0$. Let \mathbf{y} and $\tilde{\mathbf{y}}$ be vectorized versions of permutation matrices P and \tilde{P} , respectively. Define a' and b' as follows:

$$\begin{aligned}
a' &\triangleq p(1 - q)s_1 + (1 - p)(1 - q)s_2 + (pq + (1 - p)q)s_3, \\
b' &\triangleq (p^2(1 - q) + pq(1 - p))s_1 \\
&\quad + ((1 - p)^2(1 - q) + pq(1 - p))s_2 \\
&\quad + (2p(1 - p)(1 - q) + 2p^2q)s_3.
\end{aligned} \tag{10.2}$$

Thus,

$$a' - b' = p(1 - p)(1 - 2q)(s_1 + s_2 - 2s_3) + q(1 - 2p)s_3. \tag{10.3}$$

Because $s_1 > s_2 > s_3$, we have, $s_1 + s_2 - 2s_3 > 0$. Because $0 < p < 1/2$ and $0 \leq q < 1/2$, we have $(1 - 2p) > 0$ and $(1 - 2q) > 0$. Therefore, according to (10.3), $a' > b'$. Thus we have,

$$\frac{1}{n^2} \mathbb{E}[\tilde{\mathbf{y}}^T A \tilde{\mathbf{y}}] = (1 - \rho)a' + \rho b' < a' = \frac{1}{n^2} \mathbb{E}[\mathbf{y}^T A \mathbf{y}].$$

10.2 Proof Of Corollary 1

Without loss of generality and to simplify notations, we assume the permutation matrix P is equal to the identity matrix I , i.e., the isomorphic mapping across G_1 and G_2 is $\{1 \leftrightarrow 1', 2 \leftrightarrow 2', \dots, n \leftrightarrow n'\}$ (otherwise, one can relabel nodes in either G_1 or G_2 to have P equal to the identity matrix). Therefore, $G_1(i, j) = G_2(i', j')$ for all $1 \leq i, j \leq n$. Recall that Y is a vector of length kn which has weights for all possible mappings $(i, j') \in \mathcal{R}$. To simplify notations and without loss of generality, we re-order indices of vector \mathbf{y} as follows:

- The first n indices of \mathbf{y} correspond to correct mappings, i.e., $y(1) = y_{1,1'}, y(2) = y_{2,2'}, \dots, y(n) = y_{n,n'}$.
- The remaining $(k - 1)n$ indices of \mathbf{y} correspond to incorrect mappings. e.g., $y(n + 1) = y_{1,2'}, y(n + 2) = y_{1,3'}, \dots, y(kn) = y_{r,s'} (r \neq s)$.

Therefore, we can write,

$$\mathbf{y} = \begin{bmatrix} \mathbf{y}_1 \\ \mathbf{y}_2 \end{bmatrix},$$

where \mathbf{y}_1 and \mathbf{y}_2 are vectors of length n and $(k - 1)n$, respectively.

We re-order rows and columns of the alignment matrix A accordingly. Define the following notations: $\mathcal{S}_1 = \{1, 2, \dots, n\}$ and $\mathcal{S}_2 = \{n + 1, n + 2, \dots, kn\}$. The alignment matrix A for graphs G_1 and G_2 can be characterized using equation (2.3) as follows:

$$A(t_1, t_2) = \begin{cases} (\alpha + 1)G_1(i, j)G_2(i', j') - G_1(i, j) - G_2(i', j') + 1 + \epsilon, & \text{if } t_1 \sim (i, i'), t_2 \sim (j, j'), \\ & t_1 \text{ and } t_2 \in \mathcal{S}_1, t_1 \neq t_2. \\ (\alpha + 1)G_1(i, j)G_2(r', s') - G_1(i, j) - G_2(r', s') + 1 + \epsilon, & \text{if } t_1 \sim (i, r'), t_2 \sim (j, s'), \\ & t_1 \text{ or } t_2 \in \mathcal{S}_2, t_1 \neq t_2. \\ 1 + \epsilon, & \text{if } t_1 = t_2, \end{cases} \quad (10.4)$$

where notation $t_1 \sim (i, r')$ means that, row (and column) index t_1 of the alignment matrix A corresponds to the mapping (i, r') . Since G_1 and G_2 are isomorphic with permutation matrix $P = I$, we have $G_1(i, j) = G_2(i', j')$. Therefore, equation (10.4) can be written as,

$$A(t_1, t_2) = \begin{cases} (\alpha + 1)G_1(i, j)^2 - 2G_1(i, j) + 1 + \epsilon, & \text{if } t_1 \sim (i, i'), t_2 \sim (j, j'), \\ & t_1 \text{ and } t_2 \in \mathcal{S}_1, t_1 \neq t_2. \\ (\alpha + 1)G_1(i, j)G_1(r, s) - G_1(i, j) - G_1(r, s) + 1 + \epsilon, & \text{if } t_1 \sim (i, r'), t_2 \sim (j, s'), \\ & t_1 \text{ or } t_2 \in \mathcal{S}_2, t_1 \neq t_2. \\ 1 + \epsilon, & \text{if } t_1 = t_2. \end{cases} \quad (10.5)$$

Let \bar{A} be the expected alignment matrix, where $\bar{A}(t_1, t_2) = \mathbb{E}[A(t_1, t_2)]$, the expected value of $A(t_1, t_2)$.

Lemma 3 Let \mathbf{v} be the eigenvector of the expected alignment matrix \bar{A} corresponding to the largest eigenvalue. Suppose

$$\mathbf{v} = \begin{bmatrix} \mathbf{v}_1 \\ \mathbf{v}_2 \end{bmatrix},$$

where \mathbf{v}_1 and \mathbf{v}_2 are vectors of length n and $(k-1)n$, respectively. Then,

$$\begin{aligned} v_{1,1} &= v_{1,2} = \dots = v_{1,n} = v_1^*, \\ v_{2,1} &= v_{2,2} = \dots = v_{2,(k-1)n} = v_2^*, \end{aligned}$$

Moreover, if $n \rightarrow \infty$, then,

$$\frac{v_1^*}{v_2^*} > \beta, \quad (10.6)$$

where $\beta = 1 + \Delta$, and $0 < \Delta < \frac{(\alpha-1)p+1+\epsilon}{(\alpha+1)p^2-2p+1+\epsilon} - 1$.

Proof Since $G_1(i, j)$ is a Bernoulli random variable which is one with probability p , equation (10.5) leads to:

$$\bar{A}(t_1, t_2) = \begin{cases} (\alpha-1)p+1+\epsilon, & \text{if } t_1 \text{ and } t_2 \in \mathcal{S}_1, t_1 \neq t_2, \\ (\alpha+1)p^2-2p+1+\epsilon, & \text{if } t_1 \text{ or } t_2 \in \mathcal{S}_2, t_1 \neq t_2, \\ 1+\epsilon, & \text{if } t_1 = t_2. \end{cases} \quad (10.7)$$

Define $a \triangleq (\alpha-1)p+1+\epsilon$ and $b \triangleq (\alpha+1)p^2-2p+1+\epsilon$.

Since $b\mathbf{v}$ is an eigenvector of \bar{A} , we have,

$$\bar{A}\mathbf{v} = \lambda\mathbf{v}, \quad (10.8)$$

where λ is the corresponding eigenvalue of $b\mathbf{v}$. Therefore,

$$\bar{A}\mathbf{v} = \begin{bmatrix} a\sum_i v_{1,i} + b\sum_j v_{2,j} + (1+\epsilon-a)v_{1,1} \\ \vdots \\ \frac{a\sum_i v_{1,i} + b\sum_j v_{2,j} + (1+\epsilon-a)v_{1,n}}{b\sum_i v_{1,i} + b\sum_j v_{2,j} + (1+\epsilon-a)v_{2,1}} \\ \vdots \\ b\sum_i v_{1,i} + b\sum_j v_{2,j} + (1+\epsilon-a)v_{2,(k-1)n} \end{bmatrix} = \lambda \begin{bmatrix} v_{1,1} \\ \vdots \\ \frac{v_{1,n}}{v_{2,1}} \\ \vdots \\ v_{2,(k-1)n} \end{bmatrix}. \quad (10.9)$$

Therefore,

$$\begin{aligned} a\sum_i v_{1,i} + b\sum_j v_{2,j} &= v_{1,r}(\lambda + a - 1 - \epsilon), & \forall 1 \leq r \leq n, \\ b\sum_i v_{1,i} + b\sum_j v_{2,j} &= v_{2,s}(\lambda + b - 1 - \epsilon), & \forall 1 \leq s \leq (k-1)n. \end{aligned} \quad (10.10)$$

We choose ϵ so that $\lambda + a - 1 - \epsilon \neq 0$ and $\lambda + b - 1 - \epsilon \neq 0$. We will show later in this section that any sufficiently small value of ϵ satisfies these inequalities. Therefore, equation (10.10) leads to,

$$\begin{aligned} v_{1,1} &= v_{1,2} = \dots = v_{1,n} = v_1^*, \\ v_{2,1} &= v_{2,2} = \dots = v_{2,(k-1)n} = v_2^*. \end{aligned} \quad (10.11)$$

Using equations (10.10) and (10.11), we have,

$$\begin{cases} anv_1^* + b(k-1)nv_2^* = v_1^*(\lambda + a - 1 - \epsilon) \\ bnv_1^* + b(k-1)nv_2^* = v_2^*(\lambda + b - 1 - \epsilon). \end{cases} \quad (10.12)$$

We choose ϵ so that $\lambda + b(1-(k-1)n) - 1 - \epsilon \neq 0$. We will show later in this section that any sufficiently small value of ϵ satisfies this inequality. Further, according to PerronFrobenius Theorem 1, $v_{1,i} > 0$ and $v_{2,j} > 0$, for all i and j . Under these conditions, solving equation (10.12) leads to:

$$(\lambda - \lambda_a)(\lambda - \lambda_b) = b^2(k-1)n^2, \quad (10.13)$$

where,

$$\begin{cases} \lambda_a = (n-1)a + 1 + \epsilon, \\ \lambda_b = ((k-1)n-1)b + 1 + \epsilon. \end{cases} \quad (10.14)$$

Equation (10.13) has two solutions for λ . However, since λ is the largest eigenvalue of the expected alignment matrix \bar{A} , we choose the largest of the roots. Note that, since $b^2(k-1)n^2 > 0$, we have $\lambda > \max(\lambda_a, \lambda_b)$. This guarantees conditions that we put on ϵ in the early steps of the proof.

By solving equations (10.13) and (10.14), we have,

$$\lambda = \frac{\lambda_a + \lambda_b + \sqrt{(\lambda_a - \lambda_b)^2 + 4(k-1)b^2n^2}}{2}.$$

First, we show $v_1^* > v_2^*$:

As $n \rightarrow \infty$, equation (10.12) implies,

$$\frac{v_1^*}{v_2^*} = \frac{\lambda}{bn} - k + 1, \quad (10.15)$$

where λ is the largest root of equation (10.13). For sufficiently large n ,

$$\frac{v_1^*}{v_2^*} = \frac{1}{2} \left[\left(\frac{a}{b} - k + 1 \right) + \sqrt{\left(\frac{a}{b} - k + 1 \right)^2 + 4k - 4} \right]. \quad (10.16)$$

If $p \neq 0, 1$, we always have $a > b$. Therefore, there exists $\Delta > 0$ such that $\frac{a}{b} > 1 + \Delta k$. Thus, we have,

$$\frac{a}{b} > 1 + \Delta k > 1 + \Delta \left(1 + \frac{k-1}{1+\Delta} \right) = 1 + \Delta + \frac{\Delta}{\Delta+1} (k-1). \quad (10.17)$$

Using inequality (10.17) in (10.16), we have,

$$\begin{aligned} \frac{v_1^*}{v_2^*} &> \frac{1}{2} \left[\frac{(1+\Delta)^2 - k + 1}{1+\Delta} + \frac{\sqrt{((1+\Delta)^2 - k + 1)^2 + 4(k-1)(1+\Delta)^2}}{1+\Delta} \right] \\ &= 1 + \Delta. \end{aligned} \quad (10.18)$$

This completes the proof of Lemma 3. ■

Remark 8 In Lemma 3, if $kp = c_1$, where $c_1 \ll k$ and $k \gg 1$, choosing $\alpha = c_2 k^2$ results in $\Delta \approx ck$ where $c = \frac{c_1 c_2}{c_1^2 c_2 + 1} > 1$.

If \mathbf{v} is an eigenvector with unit norm, we have:

$$\|\mathbf{v}\| = 1 \Rightarrow nv_1^* + (k-1)nv_2^* = 1. \quad (10.19)$$

By using this equation and Lemma 3, for sufficiently large n , we have:

$$\begin{aligned} v_1^* &= \frac{\beta}{\sqrt{\beta^2 + k}} \frac{1}{\sqrt{n}}, \\ v_2^* &= \frac{1}{\sqrt{\beta^2 + k}} \frac{1}{\sqrt{n}}. \end{aligned} \quad (10.20)$$

Since edges of network G_1 are random, the alignment network is also random matrix. Let Ω be a set of outcomes of edge variables of network G_1 , and let $A(\Omega)$ be the corresponding alignment network. Let $\mathbf{v}(\Omega)$ represent an eigenvector of $A(\Omega)$ with the largest eigenvalue.

Lemma 4 *Let $\mathbf{v}(\Omega)$ be a unit norm eigenvector with the largest eigenvalue of the alignment matrix $A(\Omega)$. Suppose*

$$\mathbf{v}(\Omega) = \begin{bmatrix} \mathbf{v}_1(\Omega) \\ \mathbf{v}_2(\Omega) \end{bmatrix},$$

where $\mathbf{v}_1(\Omega)$ and $\mathbf{v}_2(\Omega)$ are vectors of length n and kn , respectively. Let $\bar{\mathbf{v}} = \mathbb{E}[\mathbf{v}(\Omega)]$. Then,

- (i) For all $1 \leq i \leq n$, $\mathbb{E}[v_{1,i}(\Omega)] = \bar{v}_1$, and $\sigma_{v_{1,i}(\Omega)}^2 = \sigma_1^2$.
- (ii) For all $1 \leq j \leq (k-1)n$, $\mathbb{E}[v_{2,j}(\Omega)] = \bar{v}_2$, and $\sigma_{v_{2,j}(\Omega)}^2 = \sigma_2^2$.
- (iii) Let \mathbf{v} be the eigenvector with the largest eigenvalue of the expected alignment matrix \bar{A} . Then, $\mathbf{v}(\Omega) \cdot \mathbf{v} \geq 1 - \gamma$, where γ is a small positive number, w.h.p.
- (iv) $1 - \gamma \leq \|\bar{\mathbf{v}}\| \leq 1$.
- (v) $\sigma_1^2 \leq \frac{2\gamma}{n}$ and, $\sigma_2^2 \leq \frac{2\gamma}{(k-1)n}$.
- (vi) If $v_1^*/v_2^* = \beta$, for sufficiently large n and w.h.p., $\bar{v}_1 = \frac{a_1}{\sqrt{n}}$ and $\bar{v}_2 = \frac{a_2}{\sqrt{n}}$, where $a_1 > a_2$ and,

$$\begin{aligned} a_1 &\approx \frac{\beta(1-\gamma)}{\sqrt{\beta^2 + k - 1}}, \\ a_2 &\approx \frac{(1-\gamma)}{\sqrt{\beta^2 + k - 1}}. \end{aligned} \quad (10.21)$$

Proof Owing to symmetry of the problem, for all $1 \leq i \leq n$, random variables $v_{1,i}(\Omega)$ have the same probability distribution. Therefore, they have the same mean and variance. The same argument holds for random variables $v_{2,j}(\Omega)$ for all $1 \leq j \leq (k-1)n$. This proves parts (i) and (ii).

To prove part (iii), first we show that, with high probability and for sufficiently large n , $\|E\| \triangleq \|A(\Omega) - \bar{A}\| < \delta n$, where δ is a small positive number, and $\|\cdot\|$ is the spectral norm operator. Since \bar{A} and $A(\Omega)$ have the same diagonal elements, all diagonal elements of E are zero.

Theorem 9 (Gershgorin Circle Theorem) Let E be a complex matrix with entries $e_{i,j}$. Let $R_i = \sum_{j \neq i} |e_{i,j}|$ be the sum of absolute values of the off-diagonal entries in the row i . Let $D(e_{i,i}, R_i)$ be the closed disc centered at $e_{i,i}$ with radius R_i . Every eigenvalue of E lies within at least one of the Gershgorin discs $D(e_{ii}, R_i)$.

Proof See reference [54]. ■

We use Gershgorin Circle Theorem to show that, $\|E\| < \delta n$ for sufficiently large n , w.h.p. First, we show that, for sufficiently large n and w.h.p., $R_i < \delta n$, where δ is a small positive number. To simplify notations, we write R_t for different t as follows:

If $i \leq n$, then,

$$\begin{aligned} R_t &= \sum_{i=2}^n (\alpha + 1) G_i^2 - 2G_i + 1 + \sum_{(i,j) \in \mathcal{B}} (\alpha + 1) G_i G_j - G_i - G_j + 1 \\ &\quad - (n-1)((\alpha + 1)p - 2p + 1) - (k-1)n((\alpha + 1)p^2 - 2p + 1), \end{aligned} \quad (10.22)$$

where G_i is an iid Bernoulli variable with $Pr[G_i = 1] = p$, and $\mathcal{B} = \mathcal{R} - \{(i, i') : 1 \leq i \leq n\}$. Similarly, if $n < t \leq kn$, we can write,

$$R_t = \sum_{(i,j) \in \mathcal{B}} ((\alpha + 1) G_i G_j - G_i - G_j + 1) - (k-1)n((\alpha + 1)p^2 - 2p + 1). \quad (10.23)$$

Using Chernoff bound, for sufficiently large n , for a given $\delta_1 > 0$, there exists $\epsilon_1 > 0$ so that,

$$\begin{aligned} Pr\left[\left|\frac{1}{n} \sum_{i=1}^n G_i - p\right| > \delta_1\right] &\leq e^{-n\epsilon_1}, \\ Pr\left[\left|\frac{1}{n} \sum_{i=1}^n G_i^2 - p\right| > \delta_1\right] &\leq e^{-n\epsilon_1}, \\ Pr\left[\left|\frac{1}{(k-1)n} \sum_{(i,j) \in \mathcal{B}} G_i G_j - p^2\right| > \delta_1\right] &\leq e^{-n\epsilon_1}. \end{aligned} \quad (10.24)$$

Proposition 3 Let U_1 and U_2 be two random variables such that,

$$\begin{aligned} Pr[U_1 \in (-\delta_1, \delta_1)] &> 1 - e^{-n\epsilon_1}, \\ Pr[U_2 \in (-\delta_2, \delta_2)] &> 1 - e^{-n\epsilon_2}. \end{aligned}$$

Then, w.h.p.,

$$\begin{aligned} Pr[U_1 + U_2 \geq \delta_1 + \delta_2] &\leq e^{-n \min(\epsilon_1, \epsilon_2)}, \\ Pr[U_1 U_2 \geq \delta_1 \delta_2] &\leq e^{-n \min(\epsilon_1, \epsilon_2)}. \end{aligned}$$

Proof Let T be a random variable representing the event $U_1 \in (-\delta_1, \delta_1)$, and T^c be its complement. Then,

$$\begin{aligned} Pr[U_1 + U_2 \geq \delta_1 + \delta_2] &= Pr[U_1 + U_2 \geq \delta_1 + \delta_2 | T] Pr[T] \\ &\quad + Pr[U_1 + U_2 \geq \delta_1 + \delta_2 | T^c] Pr[T^c] \\ &\leq Pr[U_2 \geq \delta_2] + Pr[T^c] \\ &\leq e^{-n \min(\epsilon_1, \epsilon_2)}. \end{aligned}$$

A similar argument can be made for the case of $U_1 U_2$. This completes the proof of Proposition 3. \blacksquare

According to equations (10.22) and (10.23), for all $1 \leq t \leq kn$, $E[R_t] = 0$. Using Proposition 3 and equation (10.24), there exists $\delta > 0$ such that, $|R_t| \leq \delta n$ for sufficiently large n , w.h.p. Thus, using Gershgorin circle Theorem 9, the maximum eigenvalue of matrix E is smaller than δn , for sufficiently large n , w.h.p., which indicates that $\|E\| \leq \delta n$, for sufficiently large n , w.h.p.

Theorem 10 (Wedin Sin Theorem) *Let \mathbf{v} and $\mathbf{v}(\Omega)$ be eigenvectors of matrices \bar{A} and $A(\Omega)$ corresponding to their largest eigenvalues, respectively. Let λ_1 and λ_2 be the largest and second largest eigenvalues of matrix \bar{A} . Then, there exists a positive constant μ such that,*

$$|\sin \angle(\mathbf{v}, \mathbf{v}(\Omega))| \leq \mu \frac{\|A - A(\Omega)\|}{\lambda_1 - \lambda_2}. \quad (10.25)$$

Proof See reference [53]. \blacksquare

According to equation (10.10), as $n \rightarrow \infty$, the two largest eigenvalues of the matrix \bar{A} are the roots of equation (10.13) because other eigenvalues are equal to $-a + 1 + \epsilon$ or $-b + 1 + \epsilon$. Solving equation (10.13) for sufficiently large n , we have,

$$\begin{aligned} |\lambda_1 - \lambda_2| &= \sqrt{(\lambda_a - \lambda_b)^2 + 4(k-1)b^2n^2} \\ &= nb \sqrt{\left(\frac{a}{b} - k + 1\right)^2 + 4(k-1)} \\ &> nb \sqrt{\left(1 + \Delta \frac{k-1}{1+\Delta}\right) + 4(k-1)} \\ &= \frac{b(\beta^2 + k-1)}{\beta} n. \end{aligned} \quad (10.26)$$

Therefore, using equation (10.26) in Wedin sin Theorem 10, for any small positive δ , we have,

$$|\sin \angle(\mathbf{v}, \mathbf{v}(\Omega))| \leq \frac{\mu \beta}{b(\beta^2 + k-1)} \delta. \quad (10.27)$$

This completes the proof of part (iii).

To prove part (iv), first we use Jensen's inequality. Since norm is a convex function, we have,

$$\|\bar{\mathbf{v}}\| = \|\mathbb{E}[\mathbf{v}(\Omega)]\| \leq \mathbb{E}[\|\mathbf{v}(\Omega)\|] = 1. \quad (10.28)$$

From part (iii), we have,

$$\mathbf{v}(\Omega) \cdot \mathbf{v} \geq 1 - \gamma \Rightarrow \bar{\mathbf{v}} \cdot \mathbf{v} \geq 1 - \gamma. \quad (10.29)$$

Then, using Cauchy Schwarz inequality, we have,

$$\|\bar{\mathbf{v}}\| = \|\bar{\mathbf{v}}\| \|\mathbf{v}\| \geq \bar{\mathbf{v}} \cdot \mathbf{v} \geq 1 - \gamma. \quad (10.30)$$

This completes the proof of part (iv).

To prove part (v), we can write,

$$\begin{aligned}\mathbb{E}[\|\mathbf{v}(\Omega) - \bar{\mathbf{v}}\|^2] &= \mathbb{E}[1 + \|\bar{\mathbf{v}}\|^2 - 2\mathbf{v}(\Omega) \cdot \bar{\mathbf{v}}] = 1 - \|\bar{\mathbf{v}}\|^2 \\ &\leq 1 - (1 - \gamma)^2 = \gamma(2 - \gamma) \leq 2\gamma.\end{aligned}\quad (10.31)$$

On the other hand,

$$\mathbb{E}[\|\mathbf{v}(\Omega) - \bar{\mathbf{v}}\|^2] = n\sigma_1^2 + (k-1)n\sigma_2^2. \quad (10.32)$$

Therefore,

$$\begin{aligned}n\sigma_1^2 \leq 2\gamma &\Rightarrow \sigma_1^2 \leq \frac{2\gamma}{n}, \\ (k-1)n\sigma_2^2 \leq 2\gamma &\Rightarrow \sigma_2^2 \leq \frac{2\gamma}{(k-1)n}.\end{aligned}\quad (10.33)$$

This completes the proof of part (v).

To prove part (vi), we assume that in the worst case, vectors \mathbf{v} and $\bar{\mathbf{v}}$ has inner product value of $1 - \gamma$. Therefore, using part (iii) and (iv), we have,

$$\begin{cases} nv_1^* \bar{\mathbf{v}}_1 + (k-1)nv_2^* \bar{\mathbf{v}}_2 = 1 - \gamma, \\ n\bar{\mathbf{v}}_1^2 + (k-1)n\bar{\mathbf{v}}_2^2 = c, \end{cases} \quad (10.34)$$

where $1 - \gamma \leq c = \|\bar{\mathbf{v}}\| \leq 1$. Solving equation (10.34) using equation (10.20) for sufficiently large n , we have,

$$\begin{aligned}a_1 &= \frac{\beta(1 - \gamma) + \sqrt{(k-1)(c - (\gamma - 1)^2)}}{\sqrt{\beta^2 + k - 1}}, \\ a_2 &= \frac{(1 - \gamma)\sqrt{k - 1} - \beta\sqrt{c - (\gamma - 1)^2}}{\sqrt{(k-1)(\beta^2 + k - 1)}}.\end{aligned}\quad (10.35)$$

Choosing δ sufficiently small and n sufficiently large, equation (10.35) leads to equation (10.34). This completes the proof of part (vi). \blacksquare

Now, we have all technology to prove Theorem 1. Recall notations $\mathcal{S}_1 = \{1, 2, \dots, n\}$ and $\mathcal{S}_2 = \{n+1, n+2, \dots, kn\}$. Let $\mathcal{S}_1(m) \subseteq \mathcal{S}_1$ and $\mathcal{S}_2(m) \subseteq \mathcal{S}_2$ where $|\mathcal{S}_1(m)| = |\mathcal{S}_2(m)| = m$. Define following variables:

$$\begin{aligned}U_1 &\triangleq \frac{1}{n} \sum_{i \in \mathcal{S}_1} v_i(\Omega), \\ U_2 &\triangleq \frac{1}{n} \left[\sum_{i \in \mathcal{S}_1(n-m)} v_i(\Omega) + \sum_{j \in \mathcal{S}_2(m)} v_j(\Omega) \right].\end{aligned}\quad (10.36)$$

Let $\rho = m/n \neq 0$. According to Lemma 4, $\mathbb{E}[U_1] = \bar{\mathbf{v}}_1$ and $\mathbb{E}[U_2] = (1 - \rho)\bar{\mathbf{v}}_1 + \rho\bar{\mathbf{v}}_2$. Moreover, $\sigma_{U_1}^2 \leq \sigma_1^2$ and $\sigma_{U_2}^2 \leq (1 - \rho)\sigma_1^2 + \rho\sigma_2^2 < \sigma_1^2$. Define,

$$d \triangleq \frac{|\mathbb{E}[U_1] - \mathbb{E}[U_2]|}{2} = \frac{c_1(1 - \gamma)}{\sqrt{n}}, \quad (10.37)$$

where $c_1 = \frac{\rho\Delta}{2\sqrt{(1+\Delta)^2+k-1}}$.

Using Chebyshev's inequality, we have,

$$\begin{aligned} \Pr[U_1 \leq \mathbb{E}[U_1] - d] &\leq \frac{2}{c_1^2} \frac{\gamma}{(1-\gamma)^2} \leq c_2\gamma = \epsilon_1, \\ \Pr[U_2 \geq \mathbb{E}[U_2] + d] &\leq \frac{2}{c_1^2} \frac{\gamma}{(1-\gamma)^2} \leq c_2\gamma = \epsilon_1. \end{aligned} \quad (10.38)$$

Therefore,

$$\Pr[U_1 < U_2] < \epsilon_1, \quad (10.39)$$

where ϵ_1 can be arbitrarily small for sufficiently large n . This completes the proof of Theorem 1.

10.3 Proof of Theorem 2

Without loss of generality and similarly to the proof of Theorem 1, let $P = I$. Let A be the alignment network of graphs G_1 and G_2 defined according to equation (2.3). Similarly to the proof of Theorem 1, re-order row (and column) indices of matrix A so that the first n indices correspond to the true mappings $\{(i, i') : i \in \mathcal{V}_1, i' \in \mathcal{V}_2\}$. Define the expected alignment network \bar{A} as $\bar{A}(t_1, t_2) = \mathbb{E}[A(t_1, t_2)]$, where t_1 and t_2 are two possible mappings across networks. Recall notations $\mathcal{S}_1 = \{1, 2, \dots, n\}$ and $\mathcal{S}_2 = \{n+1, n+2, \dots, kn\}$.

First, we consider the noise model I (3.8):

Define,

$$\begin{aligned} a' &\triangleq p(1-p_e)(\alpha + \epsilon) + (1-p)(1-p_e)(1+\epsilon) + (pp_e + (1-p)p_e)\epsilon \\ b' &\triangleq (p^2(1-p_e) + pp_e(1-p))(\alpha + \epsilon) \\ &\quad + ((1-p)^2(1-p_e) + pp_e(1-p))(1+\epsilon) \\ &\quad + (2p(1-p)(1-p_e) + 2p^2p_e)\epsilon. \end{aligned} \quad (10.40)$$

Since $G_1(i, j)$ and $Q(i, j)$ are Bernoulli random variables with parameters p and p_e , respectively, the expected alignment network can be simplified as follows:

$$\bar{A}(t_1, t_2) = \begin{cases} a', & \text{if } t_1 \text{ and } t_2 \in \mathcal{S}_1, t_1 \neq t_2, \\ b', & \text{if } t_1 \text{ or } t_2 \in \mathcal{S}_2, t_1 \neq t_2, \\ 1 + \epsilon, & \text{if } t_1 = t_2. \end{cases} \quad (10.41)$$

We have,

$$a' - b' = (\alpha + 1)(2p_e - 1)p(p - 1) + p_e(1 - 2p)\epsilon. \quad (10.42)$$

Thus, if $p \neq 0, 1$ and $p_e < 1/2$, for small enough ϵ , $a' > b' > 0$. Therefore, there exists a positive Δ such that $\frac{a'}{b'} = 1 + \Delta$. The rest of the proof is similar to the one of Theorem 1.

The proof for the noise model II of (3.9) is similar. To simplify notation and illustrate the main idea, here we assume ϵ is sufficiently small with negligible effects.

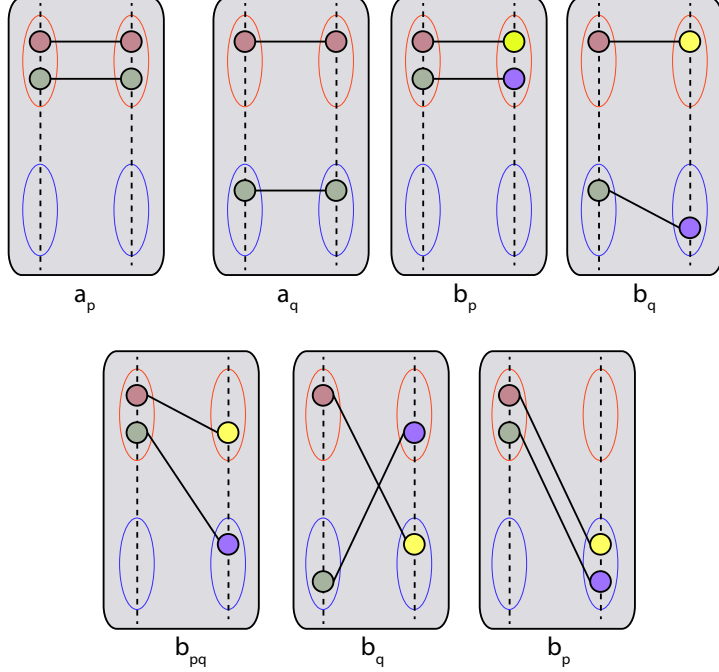


Figure 25: Expected alignment scores of different mapping combinations. Ellipses with the same color represent corresponding modules across two networks. Nodes with the same color represent true mappings across two networks.

Define,

$$\begin{aligned} a'' &\triangleq p(1 - p_e)(\alpha) + (1 - p)(1 - p_{e_2}) = 1 - p(1 + \alpha(p_e - 1) + p_e) \\ b'' &\triangleq p^2(1 - p_e)\alpha + (1 - p)^2(1 - p_{e_2}) + 2p(1 - p)p_{e_2}(1 + \alpha) \\ &= 1 - p(2 + p_e) + p^2(1 + \alpha + 2p_e). \end{aligned} \quad (10.43)$$

The expected alignment network in this case is:

$$\bar{A}(t_1, t_2) = \begin{cases} a'', & \text{if } t_1 \text{ and } t_2 \in \mathcal{S}_1, t_1 \neq t_2, \\ b'', & \text{if } t_1 \text{ or } t_2 \in \mathcal{S}_2, t_1 \neq t_2, \\ 1 + \epsilon, & \text{if } t_1 = t_2. \end{cases} \quad (10.44)$$

Moreover, we have,

$$a'' - b'' = p((1 - p - p_e)(1 + \alpha) + p_e(1 - 2p)). \quad (10.45)$$

If $p < 1/2$ and $p_e < 1/2$, then $a'' - b'' > 0$. The rest of the proof is similar to the previous case.

10.4 Proof Of Theorem 3

By writing Taylor's expansion of $\text{Tr}(G_1 X G_2 X^T)$ around the point X_0 , we have,

$$\text{Tr}(G_1 X G_2 X^T) = \text{Tr}(G_1 X_0 G_2 X_0^T) + 2\text{Tr}(G_1 X_0 G_2 (X - X_0)^T) + \text{Tr}(G_1 (X - X_0) G_2 (X - X_0)^T). \quad (10.46)$$

Let $\Delta \triangleq X - X_0$. Thus, we have,

$$f(X) = \tilde{f}(X) + \text{Tr}(G_1 \Delta G_2 \Delta^T). \quad (10.47)$$

Let $\sigma_i(G)$ be the i -th largest singular value of matrix G .

Theorem 11 (Von Neumann's trace inequality) *Suppose A and B are two $n \times n$ complex matrices. We have,*

$$|\text{Tr}(AB)| \leq \sum_{i=1}^n \sigma_i(A) \sigma_i(B). \quad (10.48)$$

Using Theorem 11, we have,

$$|\text{Tr}(G_1 \Delta G_2 \Delta^T)| \leq \sum_{i=1}^n \sigma_i(G_1 \Delta) \sigma_i(G_1 \Delta^T). \quad (10.49)$$

Moreover, using Allahverdiev's characterization of singular values, we have,

$$\begin{aligned} \sigma_i(G_1 \Delta) &\leq \min\{\sigma_k(G_1) \sigma_{i+1-k}(\Delta) : 1 \leq k \leq i\}, \\ &\leq \sigma_i(G_1) \sigma_1(\Delta). \end{aligned} \quad (10.50)$$

Moreover,

$$\begin{aligned} \sigma_i(G_1 \Delta) &\geq \max\{\sigma_k(G_1) \sigma_{n+i-k}(\Delta) : i \leq k \leq n\}, \\ &\geq \sigma_i(G_1) \sigma_n(\Delta). \end{aligned} \quad (10.51)$$

Moreover, since $\|\Delta\|_2 \leq \epsilon$, we have $|\sigma_i(\Delta)| \leq \epsilon$, for $1 \leq i \leq n$. Using (10.50) and (10.51), we have,

$$|\sigma_i(G_1 \Delta)| \leq \epsilon \sigma_i(G_1). \quad (10.52)$$

Similarly, we have,

$$|\sigma_i(G_2 \Delta^T)| \leq \epsilon \sigma_i(G_2). \quad (10.53)$$

Thus, using (10.49) and (10.53), we have,

$$|\text{Tr}(G_1 \Delta G_2 \Delta^T)| \leq \epsilon^2 \sum_{i=1}^n \sigma_i(G_1) \sigma_i(G_2). \quad (10.54)$$

Using (10.47) and (10.54), we have,

$$|f(X) - \tilde{f}(X)| \leq \epsilon^2 \sum_{i=1}^n \sigma_i(G_1) \sigma_i(G_2). \quad (10.55)$$

Moreover, since X^* and X_{lin}^* are optimal solutions of optimizations (4.2) and (4.6), respectively, we have,

$$\begin{aligned} f(X^*) &\leq \tilde{f}(X^*) + \epsilon^2 \sum_{i=1}^n \sigma_i(G_1) \sigma_i(G_2) \\ &\leq \tilde{f}(X_{lin}^*) + \epsilon^2 \sum_{i=1}^n \sigma_i(G_1) \sigma_i(G_2) \\ f(X^*) &\geq f(X_{lin}^*) \geq \tilde{f}(X_{lin}^*) - \epsilon^2 \sum_{i=1}^n \sigma_i(G_1) \sigma_i(G_2). \end{aligned} \quad (10.56)$$

This completes the proof.

10.5 Proof of Theorem 5

Without loss of generality, let $P = I$ in (3.11). Let A be the alignment network of graphs G_1 and G_2 defined according to (2.3). G_1 and G_2 are stochastic block networks with m modules, each with n nodes. Modules of G_1 are represented by $\{V_1^1, V_1^2, \dots, V_1^m\}$ where $V_1^a = \{i_a^1, i_a^2, \dots, i_a^n\}$. Similarly, modules of G_2 are represented by $\{V_2^1, V_2^2, \dots, V_2^m\}$ where $V_2^a = \{j_a^1, j_a^2, \dots, j_a^n\}$. The alignment network A has n^2m^2 nodes. We re-order row (and column) indices of matrix A so that the first mn^2 indices are within module mappings:

$$(i_1^1, j_1^1), (i_1^2, j_1^2), \dots, (i_1^n, j_1^n), (i_1^1, j_1^2), (i_1^1, j_1^3), \dots, (i_1^n, j_1^{n-1}).$$

The remaining $(m^2 - m)n^2$ indices correspond to across module mappings:

$$(i_1^1, j_2^1), (i_1^1, j_2^2), \dots, (i_m^n, j_{m-1}^{n-1}), (i_m^n, j_{m-1}^n).$$

Define,

$$\begin{aligned} a_p &\triangleq (\alpha - 1)p + 1, \\ b_p &\triangleq (\alpha + 1)p^2 - 2p + 1, \\ a_q &\triangleq (\alpha - 1)q + 1, \\ b_q &\triangleq (\alpha + 1)q^2 - 2q + 1, \\ b_{pq} &\triangleq \alpha pq + (1 - p)(1 - q). \end{aligned} \tag{10.57}$$

To form the expected alignment network \bar{A} , we consider seven types of mapping-pairs illustrated in Figure 25. Thus, the expected network alignment matrix has the following structure:

$$\bar{A} = \left[\begin{array}{cccc|ccc} A_1 & A_2 & A_2 & \cdots & A_2 & A_3 & \cdots & A_3 \\ A_2 & A_1 & A_2 & \cdots & A_2 & & & \\ \vdots & & \ddots & & \vdots & & \ddots & \vdots \\ A_2 & & \cdots & & A_1 & A_3 & \cdots & A_3 \\ \hline A_3 & & \cdots & & A_3 & A_4 & A_5 & A_5 & \cdots & A_5 \\ & & & & & A_5 & A_4 & A_5 & \cdots & A_5 \\ \vdots & & \ddots & & \vdots & \vdots & & \ddots & & \vdots \\ A_3 & & \cdots & & A_3 & A_5 & & \cdots & & A_4 \end{array} \right], \tag{10.58}$$

where the upper and lower blocks have mn^2 and $(m^2 - m)n^2$ rows, respectively. A_i is a matrix of

size $n^2 \times n^2$, defined as follows:

$$A_1 = \left[\begin{array}{ccc|ccc} a_p & \cdots & a_p & b_p & \cdots & b_p \\ \vdots & \ddots & \vdots & \vdots & \ddots & \vdots \\ a_p & \cdots & a_p & b_p & \cdots & b_p \\ \hline b_p & \cdots & b_p & b_p & \cdots & b_p \\ \vdots & \ddots & \vdots & \vdots & \ddots & \vdots \\ b_p & \cdots & b_p & b_p & \cdots & b_p \end{array} \right], \quad (10.59)$$

$$A_2 = \left[\begin{array}{ccc|ccc} a_q & \cdots & a_q & b_q & \cdots & b_q \\ \vdots & \ddots & \vdots & \vdots & \ddots & \vdots \\ a_q & \cdots & a_q & b_q & \cdots & b_q \\ \hline b_q & \cdots & b_q & b_q & \cdots & b_q \\ \vdots & \ddots & \vdots & \vdots & \ddots & \vdots \\ b_q & \cdots & b_q & b_q & \cdots & b_q \end{array} \right],$$

$$A_3 = b_{pq} \mathbb{1}_{n^2},$$

$$A_4 = b_p \mathbb{1}_{n^2},$$

$$A_5 = b_q \mathbb{1}_{n^2},$$

where $\mathbb{1}_{n^2}$ is a $n^2 \times n^2$ matrix whose elements are ones.

Suppose v is the leading eigenvector of the expected alignment matrix \bar{A} . We wish to show that,

$$v(i) > v(j), \quad \forall 1 \leq i \leq mn^2, \forall mn^2 < j \leq m^2n^2. \quad (10.60)$$

Lemma 5 *Let A be a positive matrix. If one or any number of entries of row i are increased and all the other rows remain fixed, and if the i -th entry of the Perron vector is held a fixed constant equal to 1, then the remaining entries of the Perron vector strictly decrease.*

Proof See a proof in [97]. ■

Define matrix B as follows:

$$B = \left[\begin{array}{ccccc|ccccc} B_1 & B_2 & B_2 & \cdots & B_2 & B_3 & & \cdots & B_3 \\ B_2 & B_1 & B_2 & \cdots & B_2 & & & & \\ \vdots & \ddots & & \vdots & & \vdots & \ddots & & \vdots \\ B_2 & & \cdots & B_1 & & B_3 & & \cdots & B_3 \\ \hline B_3 & & \cdots & B_3 & | & B_1 & B_2 & B_2 & \cdots & B_2 \\ & & & & | & B_2 & B_1 & B_2 & \cdots & B_2 \\ & & & & | & \vdots & & \ddots & & \vdots \\ & & & & | & B_3 & & \cdots & B_1 \end{array} \right], \quad (10.61)$$

where,

$$B_1 = b_p \mathbb{1}_{n^2}, \quad (10.62)$$

$$B_2 = b_q \mathbb{1}_{n^2},$$

$$B_3 = b_{pq} \mathbb{1}_{n^2}.$$

Because $a_p > b_p$ and $a_q > b_q$, using Lemma 5, it is sufficient to show (10.60) for the matrix B . Suppose v_B is the leading eigenvector of the matrix B . We wish to show,

$$v_B(i) > v_B(j), \quad \forall 1 \leq i \leq mn^2, \forall mn^2 < j \leq m^2n^2. \quad (10.63)$$

Note that,

$$B = \mathbb{1}_{n^2} \otimes C, \quad (10.64)$$

where C is a $m^2 \times m^2$ matrix with a structure illustrated as follows:

$$C = \left[\begin{array}{cc|cc|cc} b_p & b_q & b_q & \cdots & b_q & b_{pq} & \cdots & b_{pq} \\ b_q & b_p & b_q & \cdots & b_q & \vdots & \ddots & \vdots \\ \vdots & \ddots & \vdots & & \vdots & & \ddots & \vdots \\ \hline b_q & \cdots & b_p & & b_{pq} & \cdots & b_{pq} \\ b_{pq} & \cdots & b_{pq} & & b_p & b_q & b_q & \cdots & b_q \\ & & & & b_q & b_p & b_q & \cdots & b_q \\ \vdots & \ddots & \vdots & & \vdots & & \ddots & \vdots \\ b_{pq} & \cdots & b_{pq} & & b_q & \cdots & b_p \end{array} \right]. \quad (10.65)$$

Let v_C be the leading eigenvector of the matrix C . Using the property of Kronecker products, we have,

$$v_B = \mathbb{1}_{n^2} \otimes v_C. \quad (10.66)$$

Therefore, to show (10.60) and (10.63), it is sufficient to show that,

$$v_C(i) > v_C(j), \quad \forall 1 \leq i \leq m, \forall m < j \leq m^2. \quad (10.67)$$

Lemma 6 Consider the matrix

$$X = \left[\begin{array}{cc|cc|cc} c & b & b & \cdots & b & a & \cdots & a \\ b & c & b & \cdots & b & \vdots & \ddots & \vdots \\ \vdots & \ddots & \vdots & & \vdots & & \ddots & \vdots \\ \hline b & \cdots & c & & a & \cdots & a \\ a & \cdots & a & & c & b & b & \cdots & b \\ & & & & b & c & b & \cdots & b \\ \vdots & \ddots & \vdots & & \vdots & & \ddots & \vdots \\ a & \cdots & a & & b & \cdots & c \end{array} \right], \quad (10.68)$$

where the size of the top and bottom blocks are n_1 and n_2 , respectively. Let v^* be the leading eigenvector of X . Then, if $a > b > 0$, $c > 0$, and $n_2 > n_1$, we have,

$$v^*(i) > v^*(j), \quad \forall 1 \leq i \leq n_1, \forall n_1 < j \leq n_1 + n_2. \quad (10.69)$$

Proof Suppose v is an eigenvector of the matrix X with the corresponding eigenvalue λ . Owing to the symmetric structure of the matrix X , we have,

$$\begin{cases} v(1) = \dots = v(n_1) \triangleq v_1, \\ v(n_1 + 1) = \dots = v(n_1 + n_2) \triangleq v_2. \end{cases} \quad (10.70)$$

Using (10.70) in the eigen decomposition equality, we have,

$$\begin{cases} cv_1 + (n_1 - 1)bv_1 + n_2av_2 = \lambda v_1 \\ n_1av_1 + cv_2 + (n_2 - 1)bv_2 = \lambda v_2. \end{cases} \quad (10.71)$$

Thus, we have,

$$(\lambda' - \lambda_1)(\lambda' - \lambda_2) = n_1n_2a^2, \quad (10.72)$$

where,

$$\begin{cases} \lambda' = \lambda - c, \\ \lambda_1 = (n_1 - 1)b, \\ \lambda_2 = (n_2 - 1)b. \end{cases} \quad (10.73)$$

Let λ^* be the largest root of (10.72), which corresponds to the leading eigenvector of the matrix v^* . To prove the lemma, it is sufficient to show that,

$$\lambda^* > n_1a + (n_2 - 1)b. \quad (10.74)$$

This is true if $a > b$ and $n_2 > n_1$. To show this, we need to show,

$$\lambda^* = \frac{\lambda_1 + \lambda_2 + \sqrt{(\lambda_1 - \lambda_2)^2 + 4n_1n_2a^2}}{2} > n_1a + (n_2 - 1)b, \quad (10.75)$$

which is true under the conditions of the lemma. This completes the proof. \blacksquare

If $p > q$ and $\alpha > 1/q - 1$, we have $b_{pq} > b_q$. Thus, Lemma 6 leads to (10.67). This completes the proof.

10.6 Proof of Theorem 6

We use the same setup considered in the proof of Theorem 5 to form the expected alignment network. Considering $0 < p_e^2 \ll 1$ and $0 < p_{e_2}^2 \ll 1$, expected scores of different mapping-pairs illustrated in Figure 25 can be approximated as follows:

$$\begin{aligned} a_p &\simeq p(1 - p_e)\alpha, \\ b_p &\simeq p^2(1 - p_e)^2\alpha + 2p(1 - p)p_{e_2}\alpha, \\ a_q &\simeq q(1 - p_e)\alpha, \\ b_q &\simeq q^2(1 - p_e)^2\alpha + 2q(1 - q)p_{e_2}\alpha, \\ b_{pq} &\simeq pq(1 - p_e)^2\alpha + p(1 - q)p_{e_2}\alpha + (1 - p)qp_e\alpha. \end{aligned} \quad (10.76)$$

The proof is similar to the one of Theorem 5. To use Lemma 5, we need to have,

$$\begin{cases} a_p > b_p, \\ a_q > b_q, \end{cases} \quad (10.77)$$

which results in following conditions:

$$\begin{aligned} p &< \frac{1 - pp_e}{1 + p_e^2}, \\ q &< \frac{1 - pp_e}{1 + p_e^2}. \end{aligned} \quad (10.78)$$

Because $p_e^2 \ll 1$, we then have,

$$\begin{aligned} p &< \frac{1}{1 + p_e}, \\ q &< \frac{1}{1 + p_e}. \end{aligned} \quad (10.79)$$

To use Lemma 6, we need to have $b_{pq} > b_q$. Using (10.76), we have:

$$b_{pq} - b_q = (1 - p)q(p - q) + p_e \underbrace{(p^2(1 + 2q) - 6pq + q(1 + 2q))}_{\text{polynomial I}}. \quad (10.80)$$

To show the non-negativity of the right-hand side of (10.80), it is sufficient to show the non-negativity of polynomial I. This polynomial has two roots at

$$p_{\text{roots}} = \frac{6q \pm \sqrt{-4q(4q-1)(q-1)}}{2(1+2q)}. \quad (10.81)$$

If $0 < q \leq 1/4$,

$$-4q(4q-1)(q-1) < 0. \quad (10.82)$$

Because the value of the polynomial I at $p = 0$ is positive, if $0 < q \leq 1/4$, the polynomial is always non-negative. If $q > 1/4$, we need to have,

$$p \leq \frac{6q - \sqrt{4q(4q-1)(1-q)}}{2(1+2q)}, \quad (10.83)$$

which guarantees the non-negativity of polynomial I. The rest of the proof is similar to the one of Theorem 5.

10.7 Proof of Theorem 7

We use the same setup considered in the proof of Theorem 5 to form the expected alignment network. Suppose $S(P)$ and $S(\tilde{P})$ correspond to the expected objective function of the network alignment optimization 2.5 using permutation matrices P and \tilde{P} , respectively, where,

$$\frac{1}{nm} \|P - \tilde{P}\| > 0. \quad (10.84)$$

We wish to show that, $S(P) > S(\tilde{P})$. We have,

$$\begin{aligned} S(P) &= mn^2 a_p + (m^2 - m)n^2 a_q \\ &> (mn)^2 a_q \end{aligned} \quad (10.85)$$

where a_p and a_q are defined according to (10.57). Under conditions of Theorem 5, we have $b_p > b_{pq} > b_q$ according to (10.57). Thus,

$$S(\tilde{P}) \leq (mn)^2 b_p. \quad (10.86)$$

Using (10.85) and (10.86), we need to show that $a_q > b_p$. We have,

$$b_p - a_q = (\alpha + 1)p^2 - 2p - (\alpha - 1)q. \quad (10.87)$$

This polynomial have two roots at

$$p_{roots} = \frac{1 \pm \sqrt{1 + (\alpha^2 - 1)q}}{\alpha + 1}. \quad (10.88)$$

Because $\alpha > 1$, the minimum root is always negative. Moreover, at $p = 0$, the polynomial value is negative. Thus, (10.87) is negative if

$$0 < p \leq \frac{1 + \sqrt{1 + (\alpha^2 - 1)q}}{1 + \alpha}. \quad (10.89)$$

This completes the proof.

10.8 Proof of Theorem 8

We use the same setup considered in the proof of Theorem 5 to form the expected alignment network. Similarly to the proof of Theorem 7, we need to show $a_q > b_p$ according to (10.76). We have,

$$a_q - b_p = \alpha(q(1 - p_e) - p^2(1 + p_e^2)) \quad (10.90)$$

which is positive if

$$p^2 \leq \frac{q(1 - p_e)}{1 + p_e^2}. \quad (10.91)$$

This completes the proof.

11 Conclusion and Future Directions

In this paper, we made a principled connection between spectral network alignment techniques and relaxations of the network alignment optimization (quadratic assignment problem). Using such connection, we proposed a network alignment algorithm which employs an orthogonal relaxation of the underlying QAP in a maximum weight bipartite matching optimization. Our method simplifies, in a principled way, the network alignment optimization to simultaneous alignment of eigenvectors of (transformations of) adjacency graphs scaled by corresponding eigenvalues. Our framework also provides a theoretical justification for other existing heuristic spectral network alignment methods.

Our proposed framework advances existing network alignment methods not only in algorithmic aspects, but also in qualitative terms of the network alignment objective function. Our formulation considers both matched and mismatched interactions in its optimization and therefore, it is effective

in aligning networks even with low similarity. This is critical in applications where networks have low similarities such as comparative analysis of biological networks of distal species. This idea can also be adapted to existing network alignment packages.

For Erdős-Renyi graphs graphs, we proved that the proposed algorithm is asymptotically optimal with high probability, under some general conditions. Through simulations, we compared the performance of our algorithm with the one of existing network alignment methods based on belief propagation (NetAlign), spectral decomposition (IsoRank), Lagrange relaxation (Klau optimization), and a SDP-based method. Our simulations illustrated the effectiveness of our proposed algorithm in aligning various network structures such as Erdős-Renyi, power law, regular, and stochastic block structures, under different noise models.

For modular graph structure, we proposed a framework that uses spectral network alignment to split the large network alignment optimization into small subproblems. This enables the use of computationally expensive, but tight, semidefinite programming relaxations over each subproblem. This hybrid method has high performance similar to SDP, with significantly less computational complexity. Designing other SDP-based network alignment methods with low computational complexity for various network models remains a promising direction for future work. Moreover, in the our network alignment framework one can use other relaxations of QAP (for example by considering the alignment matrix in the intersection of the sets of orthogonal and stochastic matrices) to obtain tighter bounds.

Here we considered two real-data applications. We applied our proposed network alignment algorithm to compare gene regulatory networks across human, fly and worm species which we inferred by integrating genome-wide functional and physical genomics datasets from ENCODE and modENCODE consortia. Our method inferred conserved regulatory interactions across these species despite large evolutionary distances spanned. Moreover, we found strong conservation of centrally-connected genes and biological pathways, especially for human-fly comparisons. In a second application, we used network alignment in user de-anonymization over twitter follower subgraphs sampled in two different years. This application illustrates the extent of personal information that can be retrieved from network structures, and raises additional considerations that need to be addressed in different privacy-related applications.

12 Author Contributions and Acknowledgements

This study was designed by S. Feizi, G. Quon and M. Kellis. S. Feizi initiated, developed and analyzed the methods, and performed the experiments. G. Quon and M. Kellis contributed to the inference and comparative analysis of regulatory networks across species. M. Medard and A. Jadbabaie contributed to analysis of the methods, characterizing performance guarantees, and comparison with other optimization techniques. M. Mendoza contributed to the inference of regulatory networks and processing of expression datasets. The manuscript was written by S. Feizi, and commented on by all the authors.

Authors thank ENCODE and modENCODE consortia for collecting and providing genome-wide functional genomics datasets. We thank FONTOM5 consortium for providing initial TF lists. We thank Przemyslaw Grabowicz for providing the twitter follower subgraphs. Authors acknowledge funding from Coding Instead of Splitting (6927164) and AFOSR Complex Networks program and ONR Basic research challenge program on decentralized and online optimization. Mariana Recamonde-Mendoza acknowledges the CAPES Foundation/Brazil (Bolsista CAPES -

References

- [1] R. Sharan and T. Ideker, “Modeling cellular machinery through biological network comparison,” *Nature biotechnology*, vol. 24, no. 4, pp. 427–433, 2006.
- [2] J. A. Bondy and U. S. R. Murty, *Graph theory with applications*. Macmillan London, 1976, vol. 6.
- [3] R. Singh, J. Xu, and B. Berger, “Global alignment of multiple protein interaction networks with application to functional orthology detection,” *Proceedings of the National Academy of Sciences*, vol. 105, no. 35, pp. 12 763–12 768, 2008.
- [4] C.-S. Liao, K. Lu, M. Baym, R. Singh, and B. Berger, “Isorankn: spectral methods for global alignment of multiple protein networks,” *Bioinformatics*, vol. 25, no. 12, pp. i253–i258, 2009.
- [5] J. Flannick, A. Novak, B. S. Srinivasan, H. H. McAdams, and S. Batzoglou, “Graemlin: general and robust alignment of multiple large interaction networks,” *Genome research*, vol. 16, no. 9, pp. 1169–1181, 2006.
- [6] M. Zaslavskiy, F. Bach, and J.-P. Vert, “Global alignment of protein–protein interaction networks by graph matching methods,” *Bioinformatics*, vol. 25, no. 12, pp. i259–1267, 2009.
- [7] B. P. Kelley, B. Yuan, F. Lewitter, R. Sharan, B. R. Stockwell, and T. Ideker, “Pathblast: a tool for alignment of protein interaction networks,” *Nucleic acids research*, vol. 32, no. suppl 2, pp. W83–W88, 2004.
- [8] M. Kalaev, M. Smoot, T. Ideker, and R. Sharan, “Networkblast: comparative analysis of protein networks,” *Bioinformatics*, vol. 24, no. 4, pp. 594–596, 2008.
- [9] D. Conte, P. Foggia, C. Sansone, and M. Vento, “Thirty years of graph matching in pattern recognition,” *International journal of pattern recognition and artificial intelligence*, vol. 18, no. 03, pp. 265–298, 2004.
- [10] C. Schellewald and C. Schnörr, “Probabilistic subgraph matching based on convex relaxation,” in *Energy minimization methods in computer vision and pattern recognition*. Springer, 2005, pp. 171–186.
- [11] S. Lacoste-Julien, B. Taskar, D. Klein, and M. I. Jordan, “Word alignment via quadratic assignment,” in *Proceedings of the main conference on Human Language Technology Conference of the North American Chapter of the Association of Computational Linguistics*. Association for Computational Linguistics, 2006, pp. 112–119.
- [12] S. Melnik, H. Garcia-Molina, and E. Rahm, “Similarity flooding: A versatile graph matching algorithm and its application to schema matching,” in *Data Engineering, 2002. Proceedings. 18th International Conference on*. IEEE, 2002, pp. 117–128.
- [13] A. Narayanan and V. Shmatikov, “De-anonymizing social networks,” in *Security and Privacy, 2009 30th IEEE Symposium on*. IEEE, 2009, pp. 173–187.

- [14] R. E. Burkard, *Quadratic assignment problems*. Springer, 2013.
- [15] K. Makarychev, R. Manokaran, and M. Sviridenko, “Maximum quadratic assignment problem: Reduction from maximum label cover and lp-based approximation algorithm,” in *Automata, Languages and Programming*. Springer, 2010, pp. 594–604.
- [16] M. Bazaraa and O. Kirca, “A branch-and-bound-based heuristic for solving the quadratic assignment problem,” *Naval research logistics quarterly*, vol. 30, no. 2, pp. 287–304, 1983.
- [17] M. S. Bazaraa and H. D. Sherali, “On the use of exact and heuristic cutting plane methods for the quadratic assignment problem,” *Journal of the Operational Research Society*, pp. 991–1003, 1982.
- [18] E. L. Lawler, “The quadratic assignment problem,” *Management science*, vol. 9, no. 4, pp. 586–599, 1963.
- [19] L. Kaufman and F. Broeckx, “An algorithm for the quadratic assignment problem using bender’s decomposition,” *European Journal of Operational Research*, vol. 2, no. 3, pp. 207–211, 1978.
- [20] A. Frieze and J. Yadegar, “On the quadratic assignment problem,” *Discrete applied mathematics*, vol. 5, no. 1, pp. 89–98, 1983.
- [21] W. P. Adams and T. A. Johnson, “Improved linear programming-based lower bounds for the quadratic assignment problem,” *DIMACS series in discrete mathematics and theoretical computer science*, vol. 16, pp. 43–75, 1994.
- [22] G. Finke, R. E. Burkard, and F. Rendl, “Quadratic assignment problems,” *North-Holland Mathematics Studies*, vol. 132, pp. 61–82, 1987.
- [23] S. Hadley, F. Rendl, and H. Wolkowicz, “A new lower bound via projection for the quadratic assignment problem,” *Mathematics of Operations Research*, vol. 17, no. 3, pp. 727–739, 1992.
- [24] K. Anstreicher and H. Wolkowicz, “On lagrangian relaxation of quadratic matrix constraints,” *SIAM Journal on Matrix Analysis and Applications*, vol. 22, no. 1, pp. 41–55, 2000.
- [25] K. M. Anstreicher and N. W. Brixius, “Solving quadratic assignment problems using convex quadratic programming relaxations,” *Optimization Methods and Software*, vol. 16, no. 1-4, pp. 49–68, 2001.
- [26] Q. Zhao, S. E. Karisch, F. Rendl, and H. Wolkowicz, “Semidefinite programming relaxations for the quadratic assignment problem,” *Journal of Combinatorial Optimization*, vol. 2, no. 1, pp. 71–109, 1998.
- [27] J. Peng, H. Mittelmann, and X. Li, “A new relaxation framework for quadratic assignment problems based on matrix splitting,” *Mathematical Programming Computation*, vol. 2, no. 1, pp. 59–77, 2010.
- [28] J. T. Vogelstein, J. M. Conroy, V. Lyzinski, L. J. Podrazik, S. G. Kratzer, E. T. Harley, D. E. Fishkind, R. J. Vogelstein, and C. E. Priebe, “Fast approximate quadratic programming for large (brain) graph matching,” *arXiv preprint arXiv:1112.5507*, 2011.

[29] M. Kolář, J. Meier, V. Mustonen, M. Lässig, and J. Berg, “Graphaligment: Bayesian pairwise alignment of biological networks,” *BMC systems biology*, vol. 6, no. 1, p. 144, 2012.

[30] M. Bayati, D. F. Gleich, A. Saberi, and Y. Wang, “Message-passing algorithms for sparse network alignment,” *ACM Transactions on Knowledge Discovery from Data (TKDD)*, vol. 7, no. 1, p. 3, 2013.

[31] M. Leordeanu and M. Hebert, “A spectral technique for correspondence problems using pairwise constraints,” in *Computer Vision, 2005. ICCV 2005. Tenth IEEE International Conference on*, vol. 2. IEEE, 2005, pp. 1482–1489.

[32] M. Carcassoni and E. R. Hancock, “Alignment using spectral clusters.” in *BMVC*, 2002, pp. 1–10.

[33] E. Kazemi, H. S Hamed, and M. Grossglauser, “Growing a graph matching from a handful of seeds,” in *Proceedings of the Vldb Endowment International Conference on Very Large Data Bases*, vol. 8, no. EPFL-ARTICLE-207759, 2015.

[34] C. Clark and J. Kalita, “A multiobjective memetic algorithm for ppi network alignment,” *Bioinformatics*, p. btv063, 2015.

[35] N. Malod-Dognin and N. Pržulj, “L-graal: Lagrangian graphlet-based network aligner,” *Bioinformatics*, p. btv130, 2015.

[36] E. M. Loiola, N. M. M. de Abreu, P. O. Boaventura-Netto, P. Hahn, and T. Querido, “A survey for the quadratic assignment problem,” *European Journal of Operational Research*, vol. 176, no. 2, pp. 657–690, 2007.

[37] M. E. Newman, “Modularity and community structure in networks,” *Proceedings of the National Academy of Sciences*, vol. 103, no. 23, pp. 8577–8582, 2006.

[38] D. L. Sussman, M. Tang, D. E. Fishkind, and C. E. Priebe, “A consistent adjacency spectral embedding for stochastic blockmodel graphs,” *Journal of the American Statistical Association*, vol. 107, no. 499, pp. 1119–1128, 2012.

[39] T. Qin and K. Rohe, “Regularized spectral clustering under the degree-corrected stochastic blockmodel,” in *Advances in Neural Information Processing Systems*, 2013, pp. 3120–3128.

[40] A. Athreya, V. Lyzinski, D. J. Marchette, C. E. Priebe, D. L. Sussman, and M. Tang, “A central limit theorem for scaled eigenvectors of random dot product graphs,” *arXiv preprint arXiv:1305.7388*, 2013.

[41] A. Saade, F. Krzakala, and L. Zdeborová, “Spectral clustering of graphs with the bethe hessian,” in *Advances in Neural Information Processing Systems*, 2014, pp. 406–414.

[42] P. Erdős and A. Rényi, “On the strength of connectedness of a random graph,” *Acta Mathematica Hungarica*, vol. 12, no. 1, pp. 261–267, 1961.

[43] T. Czajka and G. Pandurangan, “Improved random graph isomorphism,” *Journal of Discrete Algorithms*, vol. 6, no. 1, pp. 85–92, 2008.

- [44] W. Ali and C. M. Deane, “Functionally guided alignment of protein interaction networks for module detection,” *Bioinformatics*, vol. 25, no. 23, pp. 3166–3173, 2009.
- [45] M. E. Newman, “Communities, modules and large-scale structure in networks,” *Nature Physics*, vol. 8, no. 1, pp. 25–31, 2012.
- [46] E. Segal, M. Shapira, A. Regev, D. Pe’er, D. Botstein, D. Koller, and N. Friedman, “Module networks: identifying regulatory modules and their condition-specific regulators from gene expression data,” *Nature genetics*, vol. 34, no. 2, pp. 166–176, 2003.
- [47] G. W. Klau, “A new graph-based method for pairwise global network alignment,” *BMC bioinformatics*, vol. 10, no. Suppl 1, p. S59, 2009.
- [48] P. Schweitzer, “Problems of unknown complexity: graph isomorphism and ramsey theoretic numbers,” Ph.D. dissertation, Saarbrucken, Univ., Diss., 2009, 2009.
- [49] L. Babai and L. Kucera, “Canonical labelling of graphs in linear average time,” in *Foundations of Computer Science, 1979., 20th Annual Symposium on.* IEEE, 1979, pp. 39–46.
- [50] L. Babai, P. Erdős, and S. M. Selkow, “Random graph isomorphism,” *SIAM Journal on Computing*, vol. 9, no. 3, pp. 628–635, 1980.
- [51] D. B. West *et al.*, *Introduction to graph theory*. Prentice hall Upper Saddle River, 2001, vol. 2.
- [52] J. Kuczynski and H. Wozniakowski, “Estimating the largest eigenvalue by the power and lanczos algorithms with a random start,” *SIAM journal on matrix analysis and applications*, vol. 13, no. 4, pp. 1094–1122, 1992.
- [53] P.-A. Wedin, “Perturbation bounds in connection with singular value decomposition,” *Informationsbehandling (BIT)*, vol. 12, pp. 99–111, 1972.
- [54] E. W. Weisstein, “Gershgorin circle theorem,” 2003.
- [55] S. Umeyama, “An eigendecomposition approach to weighted graph matching problems,” *Pattern Analysis and Machine Intelligence, IEEE Transactions on*, vol. 10, no. 5, pp. 695–703, 1988.
- [56] S. Tu and J. Wang, “Practical first order methods for large scale semidefinite programming,” 2014.
- [57] S. Burer and R. D. Monteiro, “A nonlinear programming algorithm for solving semidefinite programs via low-rank factorization,” *Mathematical Programming*, vol. 95, no. 2, pp. 329–357, 2003.
- [58] Z. Wen, D. Goldfarb, S. Ma, and K. Scheinberg, “Row by row methods for semidefinite programming,” *Industrial Engineering*, pp. 1–21, 2009.
- [59] C. Helmberg and F. Rendl, “A spectral bundle method for semidefinite programming,” *SIAM Journal on Optimization*, vol. 10, no. 3, pp. 673–696, 2000.
- [60] J. Renegar, “Efficient first-order methods for linear programming and semidefinite programming,” *arXiv preprint arXiv:1409.5832*, 2014.

[61] G. Evanno, S. Regnaut, and J. Goudet, “Detecting the number of clusters of individuals using the software structure: a simulation study,” *Molecular ecology*, vol. 14, no. 8, pp. 2611–2620, 2005.

[62] G. W. Milligan and M. C. Cooper, “An examination of procedures for determining the number of clusters in a data set,” *Psychometrika*, vol. 50, no. 2, pp. 159–179, 1985.

[63] A. Bobbio and K. S. Trivedi, “An aggregation technique for the transient analysis of stiff markov chains,” *Computers, IEEE Transactions on*, vol. 100, no. 9, pp. 803–814, 1986.

[64] W. Aiello, F. Chung, and L. Lu, “A random graph model for power law graphs,” *Experimental Mathematics*, vol. 10, no. 1, pp. 53–66, 2001.

[65] R. Kohavi *et al.*, “A study of cross-validation and bootstrap for accuracy estimation and model selection,” in *IJCAI*, vol. 14, no. 2, 1995, pp. 1137–1145.

[66] R. De Smet and K. Marchal, “Advantages and limitations of current network inference methods,” *Nature Reviews Microbiology*, vol. 8, no. 10, pp. 717–729, 2010.

[67] E. Segal, M. Shapira, A. Regev, D. Pe’er, D. Botstein, D. Koller, and N. Friedman, “Module networks: identifying regulatory modules and their condition-specific regulators from gene expression data,” *Nature genetics*, vol. 34, no. 2, pp. 166–176, 2003.

[68] Z. Bar-Joseph, G. K. Gerber, T. I. Lee, N. J. Rinaldi, J. Y. Yoo, F. Robert, D. B. Gordon, E. Fraenkel, T. S. Jaakkola, R. A. Young *et al.*, “Computational discovery of gene modules and regulatory networks,” *Nature biotechnology*, vol. 21, no. 11, pp. 1337–1342, 2003.

[69] D. Marbach, S. Roy, F. Ay, P. E. Meyer, R. Candeias, T. Kahveci, C. A. Bristow, and M. Kellis, “Predictive regulatory models in drosophila melanogaster by integrative inference of transcriptional networks,” *Genome research*, vol. 22, no. 7, pp. 1334–1349, 2012.

[70] R. Sharan and T. Ideker, “Modeling cellular machinery through biological network comparison,” *Nature biotechnology*, vol. 24, no. 4, pp. 427–433, 2006.

[71] S. A. McCarroll, C. T. Murphy, S. Zou, S. D. Pletcher, C.-S. Chin, Y. N. Jan, C. Kenyon, C. I. Bargmann, and H. Li, “Comparing genomic expression patterns across species identifies shared transcriptional profile in aging,” *Nature genetics*, vol. 36, no. 2, pp. 197–204, 2004.

[72] J. O. Woods, U. M. Singh-Blom, J. M. Laurent, K. L. McGary, and E. M. Marcotte, “Prediction of gene–phenotype associations in humans, mice, and plants using phenologs,” *BMC bioinformatics*, vol. 14, no. 1, p. 203, 2013.

[73] V. R. Chintapalli, J. Wang, and J. A. Dow, “Using flyatlas to identify better drosophila melanogaster models of human disease,” *Nature genetics*, vol. 39, no. 6, pp. 715–720, 2007.

[74] P. Kheradpour, A. Stark, S. Roy, and M. Kellis, “Reliable prediction of regulator targets using 12 drosophila genomes,” *Genome research*, vol. 17, no. 12, pp. 1919–1931, 2007.

[75] J. J. Faith, B. Hayete, J. T. Thaden, I. Mogno, J. Wierzbowski, G. Cottarel, S. Kasif, J. J. Collins, and T. S. Gardner, “Large-scale mapping and validation of escherichia coli transcriptional regulation from a compendium of expression profiles,” *PLoS biology*, vol. 5, no. 1, p. e8, 2007.

[76] A. Irrthum, L. Wehenkel, P. Geurts *et al.*, “Inferring regulatory networks from expression data using tree-based methods,” *PLoS one*, vol. 5, no. 9, p. e12776, 2010.

[77] S. Roy, J. Ernst, P. V. Kharchenko, P. Kheradpour, N. Negre, M. L. Eaton, J. M. Landolin, C. A. Bristow, L. Ma, M. F. Lin *et al.*, “Identification of functional elements and regulatory circuits by drosophila modencode,” *Science*, vol. 330, no. 6012, pp. 1787–1797, 2010.

[78] S. Feizi, D. Marbach, M. Médard, and M. Kellis, “Network deconvolution as a general method to distinguish direct dependencies in networks,” *Nature biotechnology*, 2013.

[79] D. J. Reiss, N. S. Baliga, and R. Bonneau, “Integrated biclustering of heterogeneous genome-wide datasets for the inference of global regulatory networks,” *BMC bioinformatics*, vol. 7, no. 1, p. 280, 2006.

[80] A. Greenfield, A. Madar, H. Ostrer, and R. Bonneau, “Dream4: Combining genetic and dynamic information to identify biological networks and dynamical models,” *PLoS one*, vol. 5, no. 10, p. e13397, 2010.

[81] D. Marbach, J. C. Costello, R. Küffner, N. M. Vega, R. J. Prill, D. M. Camacho, K. R. Allison, M. Kellis, J. J. Collins, G. Stolovitzky *et al.*, “Wisdom of crowds for robust gene network inference,” *Nature methods*, vol. 9, no. 8, pp. 796–804, 2012.

[82] D. Marbach, R. J. Prill, T. Schaffter, C. Mattiussi, D. Floreano, and G. Stolovitzky, “Revealing strengths and weaknesses of methods for gene network inference,” *Proceedings of the National Academy of Sciences*, vol. 107, no. 14, pp. 6286–6291, 2010.

[83] R. Bonneau, D. J. Reiss, P. Shannon, M. Facciotti, L. Hood, N. S. Baliga, and V. Thorsson, “The inferelator: an algorithm for learning parsimonious regulatory networks from systems-biology data sets de novo,” *Genome biology*, vol. 7, no. 5, p. R36, 2006.

[84] N. Friedman, M. Linial, I. Nachman, and D. Pe’er, “Using bayesian networks to analyze expression data,” *Journal of computational biology*, vol. 7, no. 3-4, pp. 601–620, 2000.

[85] D. Maglott, J. Ostell, K. D. Pruitt, and T. Tatusova, “Entrez gene: gene-centered information at ncbi,” *Nucleic acids research*, vol. 33, no. suppl 1, pp. D54–D58, 2005.

[86] E. Wingender, X. Chen, R. Hehl, H. Karas, I. Liebich, V. Matys, T. Meinhardt, M. Prüß, I. Reuter, and F. Schacherer, “Transfac: an integrated system for gene expression regulation,” *Nucleic acids research*, vol. 28, no. 1, pp. 316–319, 2000.

[87] S. M. Gallo, D. T. Gerrard, D. Miner, M. Simich, B. Des Soye, C. M. Bergman, and M. S. Halfon, “Redfly v3. 0: toward a comprehensive database of transcriptional regulatory elements in drosophila,” *Nucleic acids research*, vol. 39, no. suppl 1, pp. D118–D123, 2011.

[88] M. I. Barrasa, P. Vaglio, F. Cavasino, L. Jacotot, and A. J. Walhout, “Edgedb: a transcription factor-dna interaction database for the analysis of c. elegans differential gene expression,” *BMC genomics*, vol. 8, no. 1, p. 21, 2007.

[89] A. P. Boyle, C. L. Araya, C. Brdlik, P. Cayting, C. Cheng, Y. Cheng, K. Gardner, L. W. Hillier, J. Janette, L. Jiang *et al.*, “Comparative analysis of regulatory information and circuits across distant species,” *Nature*, vol. 512, no. 7515, pp. 453–456, 2014.

- [90] P. D. Thomas, V. Wood, C. J. Mungall, S. E. Lewis, J. A. Blake, G. O. Consortium *et al.*, “On the use of gene ontology annotations to assess functional similarity among orthologs and paralogs: a short report,” *PLoS computational biology*, vol. 8, no. 2, p. e1002386, 2012.
- [91] Y. Benjamini and Y. Hochberg, “Controlling the false discovery rate: a practical and powerful approach to multiple testing,” *Journal of the Royal Statistical Society. Series B (Methodological)*, pp. 289–300, 1995.
- [92] L. d. F. Costa, F. A. Rodrigues, G. Travieso, and P. R. Villas Boas, “Characterization of complex networks: A survey of measurements,” *Advances in Physics*, vol. 56, no. 1, pp. 167–242, 2007.
- [93] L. C. Freeman, “A set of measures of centrality based on betweenness,” *Sociometry*, pp. 35–41, 1977.
- [94] M. P. Joy, A. Brock, D. E. Ingber, and S. Huang, “High-betweenness proteins in the yeast protein interaction network,” *BioMed Research International*, vol. 2005, no. 2, pp. 96–103, 2005.
- [95] B. Zhou, J. Pei, and W. Luk, “A brief survey on anonymization techniques for privacy preserving publishing of social network data,” *ACM SIGKDD Explorations Newsletter*, vol. 10, no. 2, pp. 12–22, 2008.
- [96] M. F. Schwartz, A. R. Brecher, J. Whyte, and M. G. Klein, “A patient registry for cognitive rehabilitation research: a strategy for balancing patients privacy rights with researchers need for access,” *Archives of physical medicine and rehabilitation*, vol. 86, no. 9, pp. 1807–1814, 2005.
- [97] E. Deutsch and M. Neumann, “On the first and second order derivatives of the perron vector,” *Linear algebra and its applications*, vol. 71, pp. 57–76, 1985.